Alma Mater Studiorum – Università di Bologna

Dipartimento di Medicina Specialistica, Diagnostica e Sperimentale

DOTTORATO DI RICERCA IN

ONCOLOGIA, EMATOLOGIA E PATOLOGIA

Ciclo XXX

Settore Concorsuale: 06/A2 – Patologia Generale e Patologia Clinica

Settore Scientifico Disciplinare: MED/04 – Patologia Generale

MAMMARY CARCINOMA AND ANGIOGENESIS: STUDY OF THE ROLE OF HER2 IN RELATION TO TUMOR ANGIOGENESIS PROCESS AND TO THE SENSITIVITY TO ANTI-TUMORAL DRUGS

Presentata da:

Tania Balboni

Coordinatore Dottorato

Prof. Pier-Luigi Lollini

Supervisore

Prof. Pier-Luigi Lollini

Co-supervisore

Dott.ssa Arianna Palladini

Esame finale anno 2018

Contents

Abstract

The 28% of female patients with cancer disease in Italy is affected by mammary carcinoma. Moreover, breast cancer is the first most frequent cause of cancer death among Italian women. About 15-20% of human mammary carcinomas overexpress the proto-oncogene HER2, a tyrosine kinase receptor that belongs to EGFR family. HER2-positive tumors are more aggressive, and the prognosis of the patients is worse.

HER2 is known to be involved in tumor angiogenesis, through the increase of the expression of VEGF, COX-2 and HIF-α. In patients, the simultaneous expression of HER2 and VEGF correlates with a poorer prognosis. HER2 has also been linked to vasculogenic mimicry, that is the formation of perfused blood vessels by tumor cells.

Despite the correlation between HER2 expression and tumor angiogenesis, anti-angiogenesis drugs, such as bevacizumab, sunitinib and pazopanib, failed to reach sufficient efficacy in patients to be approved for HER2-positive breast cancer.

About half of HER2-positive breast cancer presents an alternative splicing isoform called Δ16 because of the lack of exon 16. The absence of 48 amino acids in the juxtamembrane region changes the conformational structure of the receptor, causing the formation of more stable homodimers. This greater capability of homodimerization confers higher signaling activity that leads to higher invasivity *in vitro* and higher tumorigenicity *in vivo*. Moreover, the presence of Δ16 has been linked to reduced sensitivity to trastuzumab *in vitro*, but not *in vivo*.

In Δ16-transgenic mice (Δ16-HER2 mice), the spontaneous development of mammary tumors occurs much earlier than in HER2-transgenic mice (FVBhuHER2 mice). A double-transgenic mouse model that bear both isoforms of HER2 (F1 mice) was recently developed, in which the spontaneous carcinogenesis occurs as early as in Δ16-HER2 model.

The three above-mentioned mouse models have been studied at the Laboratory of Immunology and Biology of Metastases directed by Prof. Pier-Luigi Lollini (Department of Experimental, Diagnostic and Specialty Medicine, University of Bologna, Italy), where this project has been carried out. In the tumors developed on these models, angiogenesis seems to occur in different ways. In FVBhuHER2 mice, tumors display a reddish and hemorrhagic aspect with a soft texture. Δ16-HER2 tumors, on the other hand, are often pale and solid. In F1 tumors, both characteristics

can be present. In this way, HER2 and Δ16 seem to drive different angiogenic phenotypes.

Therefore, the aim of this thesis was to better analyze the role of the two isoforms in determining different patterns of vascularization, especially in the light of the fact that the role of the splice isoform Δ16 in angiogenesis has never been investigated so far. The different vascularization has been put in relation to the different effects of anti-angiogenic and anti-HER2 drugs. This study has been performed through histological, functional and molecular analysis of the tumors of FVBhuHER2, Δ16-HER2 and F1 female mice, in relation to the expression of the full-length HER2 and Δ16. Furthermore, cell lines derived from these tumors have been used to study angiogenesis *in vitro*.

The analysis of the vascularization in F1 tumors, in which one isoform or both can be expressed, revealed that the presence of full-length HER2 is crucial for the establishment of the FVBhuHER2-like phenotype, that is with few large vessels. When only Δ16 is expressed, the vascular pattern with numerous small vessels, that is typical of Δ16-HER2 tumors, is present.

The dominant role of full-length HER2 in tumor angiogenesis has been confirmed in a dynamic *in vivo* model of modulation of the expression of this isoform. In two Mouse-Derived Isograft (MDI) models, fluctuations of the levels of expression of HER2 determined the acquisition of different vascular patterns: when the levels of HER2 rose, the vessels decreased in number and were larger, and when the levels of HER2 decreased, the vessels became more and smaller.

The differences between the vascular patterns sustained by the two isoforms not only involved phenotypic aspects, but they also differed from the functional, molecular and therapeutic point of view. In particular, the vasculature with few large vessels typical of HER2-expressing tumors was less permeable to drugs, as it has been proved by the evaluation of the accumulation of doxorubicin and trastuzumab by flow cytometry. Moreover, FVBhuHER2 tumors were less sensitive to anti-angiogenic drugs such as sunitinib and pazopanib than Δ16-HER2 tumors. Sunitinib and pazopanib had an effect on Δ16-HER2 tumors both through an anti-angiogenic mechanism by

reducing the number of vessels inside treated tumors, and through an anti-tumoral effect by blocking cell proliferation, as proved by *in vitro* studies.

A molecular profile with a higher number of genes related to sprouting angiogenesis was found in FVBhuHER2 tumors, suggesting that this process might be more actively induced and likely less coordinated than in Δ16-HER2 tumors.

A less regular angiogenesis may explain these characteristics in FVBhuHER2 tumors. A higher presence of $CD44^{+}$ $CD24^{-/low}$ cells has been found in a FVBhuHER2-derived cell line. Studies reported in literature have linked the presence of stem cell populations within tumors with vasculogenic mimicry. Vasculogenic mimicry has been also associated with the capability of forming tubes on Matrigel. This ability was found higher in HER2-expressing cell lines, while Δ16-expressing ones were not able to form any tube. The tube formation ability was affected by sunitinib *in vitro* through the decrease of tube formation activity.

Sunitinib was also effective on triple-negative breast cancer, both *in vitro* and *in vivo*.

In conclusion, HER2 isoforms have been found to have a crucial role in tumor angiogenesis. The dominant behavior of full-length HER2 affects the regularity of the vascular pattern, determining a vasculature that is less permeable to drugs and therefore less sensitive to anti-angiogenic and targeted agents. A molecular profile with more genes involved in sprouting angiogenesis suggests the need to further study the role of full-length HER2 in tumor vascularization, to find new targets to improve the pharmacological response to therapies.

Introduction

1. Angiogenesis

The structure of complex organisms such as vertebrates requires an adequate supply of oxygen and nutrients to tissues. This supply is guaranteed by an extended network of blood vessels throughout the entire body (Adair and Montani, 2010).

The mechanisms by which blood vessels can be created are multiple. During early embryonic development, *de novo* blood vessels form by a process called vasculogenesis that consists in the formation of endothelium from mesoderm cell precursors, called angioblasts (Risau and Flamme, 1995). Vasculogenesis does not take place after birth in physiological conditions. On the contrary, angiogenesis (from the Greek word *Angêion*, meaning vessel) consists in the growth of vessels from pre-existing vasculature and can occur both in uterus and after birth (Adair and Montani, 2010). Angiogenesis can also occur in pathological conditions such as cancer, but the vessels that form in this context are aberrant and bloody supply is not uniform.

The key trigger of angiogenesis is the need of oxygen in hypoxic tissues. Hypoxia results in the increase of Reactive Oxygen Species (ROS) that triggers the production of Hypoxia Inducible Factor α (HIF-α), which in turn causes the secretion of Vascular Endothelial Growth Factor-A (VEGF-A). The increase of VEGF-A levels breaks the balance between stimulating and inhibiting molecules and results in the so-called angiogenic switch (Adair and Montani, 2010).

The most important proangiogenic factors belong to VEGF, Angiopoietin, Platelet-Derived Growth Factor (PDGF) and Fibroblast Growth Factor (FGF) families. Other molecules can be involved, such as Transforming Growth factor β (TGF-β), Hepatocyte Growth Factor (HGF), Insulin-like Growth Factor (IGF), Interleukin 8 (IL-8), Placental Growth Factor (PlGF), and many others (Carmeliet and Jain, 2000).

Among the inhibiting molecules, the most relevant ones are Trombospondin-1 and 2 and the statins, such as Angiostatin, Endostatin and Vasostatin (Carmeliet and Jain, 2000).

1.1 Physiological angiogenesis

The two main physiological mechanisms of angiogenesis are called sprouting angiogenesis and intussusceptive angiogenesis, depending on the way vessels form (picture 1). Sprouting angiogenesis forms blood vessels starting from sprouts of endothelial cells to provide vessel-free tissues with vasculature. On the other hand, intussusceptive angiogenesis occurs to expand the existing vascular network through a splitting process.

In physiologic conditions, angiogenesis is a well-coordinated process, but that often results in a complex network of vessels, in which some of them are 'useless'. Remodeling of vasculature occurs to prune the redundant vessels and to mature the remaining ones.

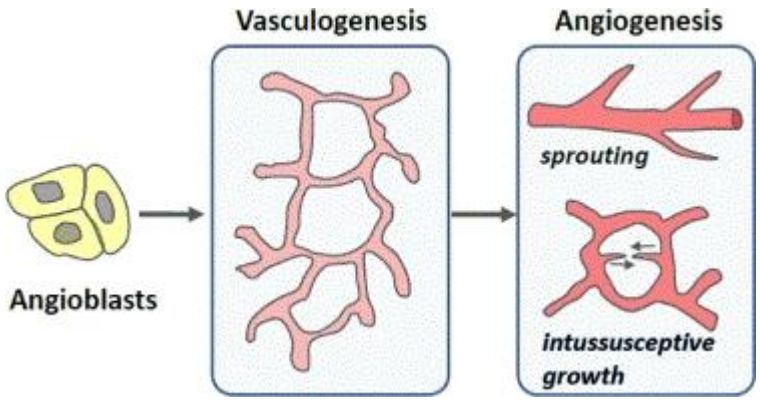

Picture 1. Basic types of primary vascular growth. Redrawn after Carmeliet and Collen, 2000 (Adair and Montani, 2010).

1.1.1 Sprouting angiogenesis

Sprouting angiogenesis is a quite known mechanism since it was discovered about 200 years ago (Adair and Montani, 2010). The term "sprouting" derives from the sprouts of endothelial cells that originate from a pre-existing vessel. These sprouts grow in response to an increasing gradient of VEGF-A, that is secreted by hypoxic cells (picture 2a). Hypoxic cells also secrete Angiopoietin-2 (Ang2), which detaches pericytes from endothelium thanks to its bond to its receptor Tie2.

Endothelial cells that are exposed to high concentrations of VEGF-A are selected to become tip cells (picture 2b). A tip cell is an endothelial cell that guides the

formation of new vessels and is morphologically characterized by cellular processes called filopodia.

Delta-like ligand 4 (Dll4)-Notch pathway is essential for tip cell selection. Dll4 expression is induced on cells exposed to VEGF. Dll4 binds to Notch receptor on neighbouring cells causing its proteolytic cleavage. In this way, cleaved Notch intracellular domain (NICD) goes to the nucleus to decrease Vascular Endothelial Growth Factor Receptor 2 (VEGFR2) and Neuropilin 1 (Nrp1) expression, that are essential for tip cell phenotype. On the other hand, NICD increases Vascular Endothelial Growth Factor Receptor 1 (VEGFR1) expression, which traps VEGF making the neighbouring cells less responsive to it (Welti *et al.*, 2013). The cells with VEGF-induced expression of Dll4 and VEGFR2 gain the motility and the morphological characteristics of the tip cells, while the cells in which Notch signaling is activated and are less responsive to VEGF-A become stalk cells (Carmeliet *et al.*, 2009).

The sprouting angiogenesis process starts with the enzymatic degradation of capillary basement membrane thanks to matrix metalloproteinases secreted by filopodia on tip cells. Filopodia are also enriched with VEGFR2, which allow tip cells to sense the increasing gradient of VEGF and to lead the sprout (picture 2c). The contraction of actin filaments allows filopodia to invade tissues towards the higher concentration of VEGF.

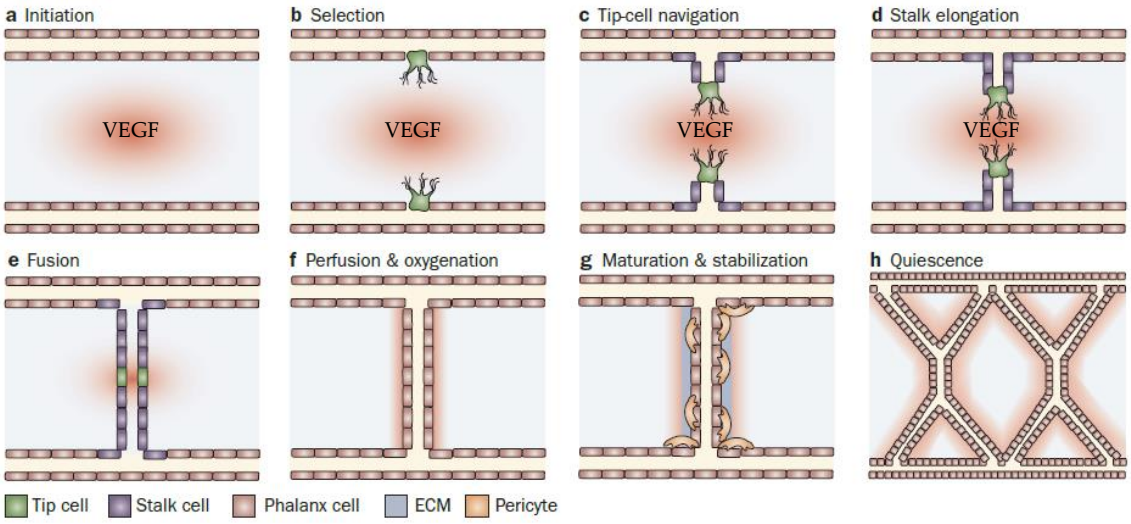

Picture 2. Formation of new vessel branches through sprouting angiogenesis (modified from Carmeliet *et al.*, 2009).

Behind tip cells, stalk cells proliferate to elongate the nascent sprout (picture 2d). Meanwhile, vacuoles inside of them grow and converge to create the lumen of the vessel. When two tip cells from different sprouts meet, they fuse to connect the newborn vessels (picture 2e) and create a lumen in which oxygenated blood can flow (picture 2f).

Finally, newborn vessels are surrounded by pericytes and extracellular matrix (picture 2g), and endothelial cells assume a quiescent "phalanx" phenotype (picture 2h).

1.1.2 Intussusceptive angiogenesis

Intussusceptive angiogenesis consists in the formation of a vascular wall into the lumen of pre-existing vessels and for this reason it is also called splitting angiogenesis.

In comparison with sprouting angiogenesis, intussusceptive angiogenesis is a faster and more efficient process because it is not based on cell migration and proliferation, but on the formation of transcapillary tissue pillars that split the vessel into two (Risau, 1997).

It occurs to divide large vessels into smaller ones to create bifurcations in arteries or veins, or to prune inefficient vessels. It seems to be mostly determined by shear stress, which is the force applied by blood flow on endothelial cells (Mentzer and Konerding, 2014).

The process begins with the protrusion of opposing endothelial cells into the capillary lumen until they touch each other and establish cell-to-cell junctions. The endothelial bilayer and basement membranes are perforated centrally to permit the entrance of growth factors and the migration of fibroblasts and pericytes. These cells finally produce collagen and other components of ECM in order to form the tissue pillar (Mentzer and Konerding, 2014).

1.1.3 Remodeling

The vascular network that results from sprouting or intussusceptive angiogenesis is often enriched in redundant and poorly perfused vessels that need to be eliminated.

The process with which useless vessels regress to form a mature and more functional vascular plexus is known as remodeling.

Very little is known about this process so far. It is known that one of the leading causes of remodeling is shear stress, which is the force that blood flow applies on endothelium walls. Flow can promote the maturation of the endothelium through the proliferation of endothelial cells, the reorganization of the junctions between them and the deposition of extracellular matrix. In this sense, high blood flow leads to maturation, whereas poor perfusion promotes vessel regression (Carmeliet, 2003).

Recent studies on mouse retinas showed that endothelial cells adapt their morphology, patterns of gene activity and polarity (i.e. the relative position of the nucleus and the Golgi) in response to shear stress. In particular, endothelial cells change their polarity in order to polarize against blood flow and to counteract its action (Franco *et al.*, 2015).

As said, remodeling essentially consists in vascular regression, which does not occur by apoptosis but by active migration of endothelial cells to neighbouring vessels (Franco *et al.*, 2015). In particular, endothelial cells migrate from vascular segments with low or oscillatory flow to high-flow ones nearby. As a conclusion, low-flow branches regress and high-flow ones are stabilized.

Recent studies have demonstrated that remodeling in mouse retinas is negatively regulated by non-canonical Wnt signaling, a pathway that is known to be involved in the establishment of planar cell polarity (Franco *et al.*, 2016). The loss of this pathway causes enhanced sensitivity to lower shear stress and therefore in earlier vascular regression and accelerated remodeling.

1.2 Tumor angiogenesis

The ability of forming new blood vessels is one of the ten hallmarks of cancer, in addition to sustaining proliferative signaling, evading growth suppressors, resisting cell death, enabling replicative immortality, activating invasion and metastases, genome instability and mutations, avoiding immune destruction, tumor-promoting inflammation and deregulating cellular energetics (Hanahan and Weinberg, 2011).

The first observation about how tumors and angiogenesis are strictly correlated was made in early 1900s (Goldmann, 1907), but the first scientist that hypothesized that tumors are dependent on blood supply was Judah Folkman in 1971. He observed that when tumors reach 2-3 mm in diameter, endothelial cells activate and proliferate to form new capillaries. This phenomenon can be explained by the fact that below that dimension, gases and nutrients can be distributed by diffusion. If blood supply is not provided, masses cannot grow further (Folkman, 1971).

The formation of blood vessels in the tumor context can occur by the active recruitment of angioblasts from the bone marrow or by co-opting the existing vasculature (Carmeliet and Jain, 2000). In the first case, the tumor is completely avascular and forms *de novo* blood vessels by vasculogenesis. In the second case, it co-opts the host vascular network, but the co-opted vessels start soon to regress as a mechanism of defense. As a consequence, the tumor mass is deprived of oxygen, it becomes hypoxic and produces VEGF, forming its own vasculature by sprouting or intussusceptive angiogenesis (Yancopoulos *et al.*, 2000).

Now it is widely known that angiogenesis starts when the 'angiogenic switch' occurs, that is when pro-angiogenic signals exceed anti-angiogenic ones (picture 3; Bouck *et al.*, 1996). These signals can be molecular (e.g. members of VEGF and Angiopoietin families), mechanical (e.g. pressure from proliferating cells), metabolic (e.g. low pO_2), genetic (e.g. loss or gain of function of molecules involved in angiogenesis) or immune/inflammatory factors (Carmeliet and Jain, 2000).

In comparison with physiological angiogenesis, the expression of molecules that stimulate or inhibit the formation of new vessels is not well-coordinated in tumors. This leads to the growth of abnormal vessels, which may lack pericytes and have fenestrations. They can also have tumor cells among endothelial cells creating 'mosaic vessels', or there even can be vessels made by cancer cells (the so-called vasculogenic mimicry). They can have too many branches or shunts, or be tortuous or with uneven diameters. The structure can be so abnormal that the definition of arteries, capillaries and veins can be tricky (Lagenkamp and Molema, 2009). The presence of structural abnormalities and malformations leads to chaotic and variable blood flow that impairs oxygen and nutrient supply. Therefore, there are often areas of hypoxia and necrosis

within the tumor that may select more malignant and metastatic cells. Moreover, hypoxic tissues produce HIF-α that stimulates the production of VEGF, with the consequent inducement of the formation of new vessels.

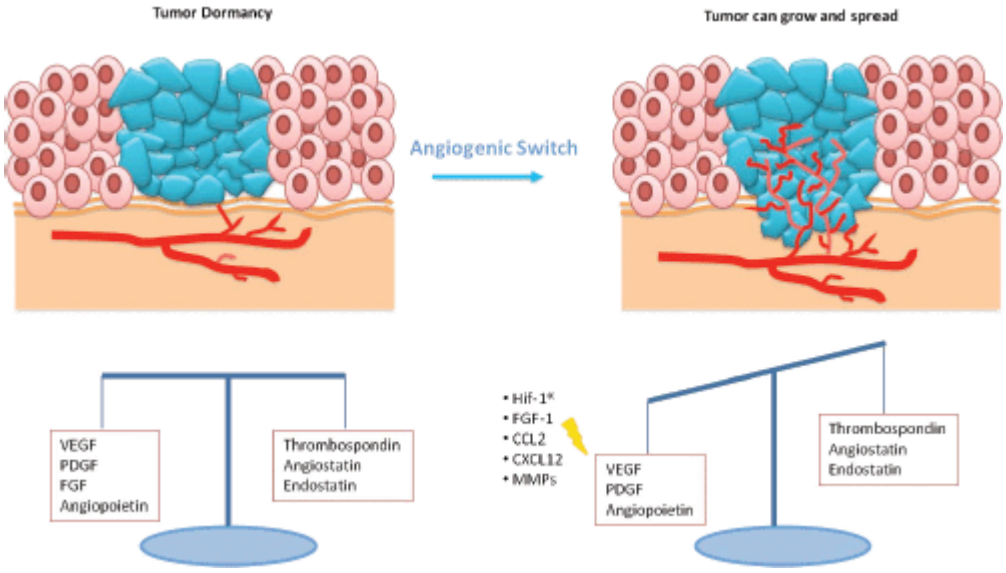

Picture 3. Schematic representation of angiogenic switch, which occurs when proangiogenic signals exceed antiangiogenic ones. When angiogenic switch occurs and new vessels are formed, dormant tumors start to proliferate and eventually may spread to other tissues (Gelao *et al.*, 2013).

The ultrastructure of tumor vessels is also affected. In fact, they may present fenestrations, transcellular holes or vesicles that affect permeability. Abnormalities like these can result in hemorrhages and higher interstitial fluid pressure, which eventually limit perfusion (Carmeliet and Jain, 2011). Moreover, the base membrane may be discontinuous or absent, and endothelial cells may have an irregular shape and/or grow one on each other. All of these aspects have a great impact on vascular functionality and structure: tumor vessels are usually much leakier than normal vasculature and their permeability is considerably higher, even if these characteristics may vary between tumor type and after treatment (Carmeliet and Jain, 2000).

The abnormal vascular structures found in tumors show high heterogeneity (table I). Six different types of tumor vessels have been identified. Four of the six vessel types (mother vessels, capillaries, glomeruloid microvascular proliferations, and vascular malformations) are formed by angiogenesis, starting from preexisting normal vessels, usually venules and capillaries. The two remaining ones (feeder arteries and draining veins) develop from a process called arterio-venogenesis. This mechanism is

poorly understood, but it is known to involve the remodeling of preexisting arteries and veins (Nagy *et al.*, 2010).

Process involved	Vessel type	Vessel properties
Angiogenesis	Mother vessels (MV)	Large, thin-walled, hyperpermeable, lightly fenestrated pericyte-poor sinusoids that are engorged with red blood cells.
	Capillaries	Formed from MV by a process that involves intra-luminal bridging and intussusception.
	Glomeruloid microvascular proliferations (GMP)	Poorly organized vascular structures that resemble renal glomeruli macroscopically. GMP are comprised of endothelial cells and pericytes with minimal vascular lumens and reduplicated basement membranes.
	Vascular malformations (VM)	Mother vessels that have acquired an often-asymmetric coat of smooth muscle cells and/or fibrous connective tissue.
Arterio-venogenesis	Feeder arteries (FA)	Enlarged, often tortuous arteries and veins that are derived from preexisting arteries and veins. They extend radially from the tumor mass, supplying and draining the angiogenic vessels within.
	Draining veins (DV)	

Table I. Classification of tumor vessels (Nagy and Dvorak, 2012).

From the molecular point of view, many proangiogenic factors are overexpressed in tumors. The first to be discovered was the fibroblast growth factor (FGF), but the most ubiquitous is VEGF-A. The other family members of VEGF-A (VEGF-B, VEGF-C and VEGF-D) are also present in tumors, as well as PlGF and Angiopoietins (Bergers and Benjamin, 2003). The abundance of angiogenesis-stimulating factors enhances the formation of new blood vessels.

Many molecular mechanisms are involved in tumor angiogenesis. VEGF and angiopoietin family members have a predominant role. In particular, VEGF is the main driver of the formation of new vessels and it is often overexpressed, causing an abundance of vessel sprouts. On the other hand, the high expression of Angiopoietin 2 (Ang2), which has a negative effect on vessel stability, causes failure in blood vessel maturation and integrity (Yancopoulos *et al.*, 2000).

The impaired balance of proangiogenic and inhibiting factors leads to up- or downregulation of adhesion molecules. For instance, they are upregulated by VEGF

and tumor-necrosis factor-α (TNF-α), whereas their presence decreases thanks to basic fibroblast growth factor (bFGF) and transforming growth factor-β1 (TGF-β1). The irregularity of distribution and expression of adhesion molecules, in addition to a chaotic blood flow, can lead to an impaired interaction with leukocytes on endothelium walls, causing a lower immune response (Jain *et al.*, 1996).

Irregular angiogenesis can also lead to the formation of blood vessels by tumor cells without the participation of endothelial cells. This phenomenon has been called vasculogenic mimicry (VM). It was first observed in melanoma, both *in vivo* and *in vitro*. In human invasive uveal melanoma specimens, vascular channel networks negative for endothelial markers were observed. These channels were absent in poorly invasive melanomas. Highly invasive melanomas conserved the ability to form vascular-like channels *in vitro*, in absence of endothelial cells or fibroblasts and without the addition of soluble growth factors such as bFGF, TGF-β, VEGF, PDGF. Moreover, the presence of these structures correlated with a poorer prognosis (Maniotis *et al.*, 1999).

Vascular networks made of tumor cells stain negative for endothelial cell markers (such as Factor VIII-related antigen, *Ulex*, CD31, CD34, and KDR) but are positive for the staining of the periodic acid-Schiff (PAS) reagent, that dyes the basement membrane (Folberg *et al.*, 2000). Interestingly, it has been observed that in melanoma these channels were rich in laminin, collagens IV and VI, and heparin sulfate proteoglycans, and contained plasma and red blood cells, indicating a perfusion (Kirschmann *et al.*, 2012). Other characteristics that define VM are the presence of cancer cells that line the channels rather than endothelial cells, the expression of a stem cell-like phenotype, the presence of ECM remodeling, and the connection of the network with the tumor microcirculation system (Qiao *et al.*, 2015).

VM has been found in other tumor types, such as sarcomas (Ewing, mesothelial, synovial, osteosarcoma, alveolar rhabdomyosarcoma), carcinomas (breast, ovary, lung, prostate, bladder, kidney) and brain tumors (gliomas, glioblastoma, astrocytoma) (Kirschmann *et al.*, 2012).

Many molecular pathways have been associated with VM. One of them is linked to VE-cadherin, a transmembrane glycoprotein usually expressed by endothelial cells

that promotes homotypic cell-cell interactions. It also regulates EphA2 (erythropoietin-producing hepatocellular carcinoma-A2) activity by mediating its ability to become phosphorylated through interactions with its ligand Ephrin-A1 (Kirschmann *et al.*, 2012). VEGF-A is important to sustain VM and to promote cell plasticity. Through its binding to the receptor VEGFR1 and the activation of the PI3K-Akt cascade, it is thought to mediate endothelial cell differentiation and organization into vascular tubes. In melanoma cells, VM seems to be triggered by the synergic action of VEGFR1/VEGF-A/PI3K/PKCα and integrin-signaling pathways (Cheng *et al.*, 2003).

In breast cancer cells, high expression of COX-2 (cyclo-oxygenase 2) correlates with the presence of VM networks (Kirschmann *et al.*, 2012). COX-2 induces the release of VEGF and activates the endothelial cells through the production of eicosanoids (Gately, 2000).

In general, cell plasticity is important for the establishment of VM. Many studies have reported that VM is linked with stemness and epithelial-mesenchymal transition (EMT) (Qiao *et al.*, 2015; Liu *et al.*, 2016). The presence of cancer stem cells (CSCs) has been linked with VM in many tumor types, such as leukemia, oral squamous cell carcinoma, melanoma, glioblastoma (Qiao *et al.*, 2015).

Since CSCs have been linked to drug resistance and CSCs induce VM, the presence of VM may affect the response to anti-cancer treatments. Indeed, anti-angiogenic drugs reduce the tumor vasculature and increase hypoxia, forcing the CSCs to differentiate into endothelial-like cells and forming VM. Therefore, drugs targeting VM and EMT have to be studied to overcome recurrence and drug resistance (Liu *et al.*, 2016).

2. *Mammary carcinoma*

Breast cancer is the most frequent type of cancer that affects women. Every year, about 50,000 patients are diagnosed with breast cancer in Italy, representing the 28% of all female tumors. It is also the first leading cause of cancer death in women in Italy, killing about 12,000 patients every year (AIOM, 2017).

Breast cancer cannot be considered as a unique disease, but as a heterogeneous group of many subtypes with different characteristics from the molecular, histological and clinical point of view (Dawson *et al.*, 2013). These differences between subtypes must be taken into account for the choice of the proper therapy and to establish the correct prognosis.

From the histopathological point of view, the majority (about 70-80%) of breast cancers is classified as invasive ductal carcinomas. The remaining ones can be described as lobular, tubular, medullary or metaplastic carcinomas (Ellis, 2003). Tumor grade assessment, based on the level of differentiation and on the proliferative index (Ki67 score) of the mass, is also implemented to define the biologic characteristics of the tumor and to predict the clinical behavior.

Immunohistochemical techniques (IHC) are also used to classify mammary carcinomas based on their expression of the hormone receptors (HR, that are the estrogen receptor and the progesterone receptor) and of the Human Epidermal growth factor Receptor 2 (HER2, see paragraph §2.1). Therefore, there can be many possibilities: triple-positive (HR+/HER2+), luminal A, luminal B, HER2+, HR+/HER2-, HER2+/HR-, triple-negative (HER2-/HR-).

Another way to classify breast cancer is based on the PAM50 assay, a Real Time qPCR-based test that analyzes the expression of 50 genes and identifies four main gene expression signatures. Overlapping the results from the ICH-based classification with the one based on the PAM50 assay, four subtypes can be identified, even if some discordance is present (table II): luminal A, luminal B, basal-like and HER2-enriched (Prat *et al.*, 2015).

IHC-based group	**N**	**PAM50 intrinsic subtype distribution**			
		Luminal A	**Luminal B**	**HER2-enriched**	**Basal-like**
HR+/HER2-	4295	60.3%	31.9%	6.6%	1.2%
Luminal A	637	62.2%	27.0%	10.2%	0.6%
Luminal B	317	34.1%	51.1%	11.0%	3.8%
HER2+	831	17.6%	26.8%	44.6%	11.0%
HER2+/HR+	182	33.0%	46.2%	18.7%	2.2%
HER2+/HR-	168	19.0%	4.2%	66.1%	10.7%
TNBC	868	1.6%	3.2%	9.1%	86.1%

Table II. Distribution of the PAM50 intrinsic subtypes within the pathology-based groups (Prat *et al.*, 2015).

The luminal subtypes represent the vast majority of mammary carcinomas (about 75% of all breast cancers), and are characterized by the expression of estrogen (ER) and/or progesterone (PR) receptors, and the lack of HER2 overexpression (Yersal and Barutca, 2014). Compared to the other subtypes, they also have the best prognosis, due to their sensitivity to the chemotherapy and also to the hormone therapy, including tamoxifen and the aromatase inhibitors (Tang *et al.*, 2016). The main difference between the luminal A and luminal B subtypes lies in the different proliferative index: in fact, Ki67 positivity is higher in luminal B breast cancers (>14%). They also differ in the response to therapies: luminal A subtype is usually more responsive to endocrine treatments, whereas luminal B one responds better to chemotherapy (Tang *et al.*, 2016). This difference is probably due to the fact that luminal B tumors usually have a lower expression of PR (Prat *et al.*, 2015). The relapse rate is usually higher in patients with luminal B subtype (Yersal and Barutca, 2014), often due to the presence of a higher number of mutations (Prat *et al.*, 2015).

The basal-like subtype is the most aggressive subtype, and represents the 10-15% of all breast cancers. It is also called triple-negative, because it lacks the expression of HER2 and of both hormone receptors. For this reason, it is not eligible for targeted therapy. Usually, basal-like carcinomas are treated with taxanes, anthracyclines, platinum-based chemotherapy and poly ADP ribose polymerase (PARP) inhibitors. The risk of primary or secondary resistance and of recurrence is very high, and the level of aggressiveness of this subtype is also more elevated than in the other subtypes. These tumors usually have a high expression of proliferation-related genes and keratins, which are mostly expressed by the basal layer of the skin. They also present a high number of mutations across the genome (Prat *et al.*, 2015). For these reasons, the prognosis is usually poorer (Tang *et al.*, 2016). Among the basal-like subtype, some breast cancers can be classified as claudin-low. This subtype includes those triple-negative carcinomas that have a low expression of tight junction proteins and of cell-to-cell adhesion molecules (such as claudins, occludin and E-cadherin), and show epithelial-mesenchymal transition and stem cell features. The clinical outcome is also poor, like other basal-like cancers (Yersal and Barutca, 2014).

The HER2-enriched subtype represents about 15-20% of all breast cancers and is characterized by the overexpression of the receptor HER2. It is characterized by the highest number of mutations across the genome (Prat *et al.*, 2015). According to the American Society of Clinical Oncology (ASCO) and the College of American Pathologists (CAP) guidelines, the standardized test to determine if HER2 is overexpressed is the Hercep Test™ and is based on IHC. This overexpression is usually due to the amplification of the gene that can be detected by FISH (Fluorescence *In Situ* Hybridization).

The Hercep Test™ provides a score of positivity ranging from 0 to +3. The score 0 defines a negative sample; a score +1 corresponds to a negative sample with a barely perceptible positivity with incomplete membrane staining in less than 10% of the tumor cells; a +2 sample is classified as weakly positive, with moderate complete membrane staining in more than 10% of the cells; finally, a +3 sample displays a strong and complete membrane staining in more than 10% of the tumor cells. Samples classified as 2+ also undergo the FISH analysis to detect the amplification of the gene (Dako Hercep Test™ Manual). The amplification of the HER2 gene is classified as positive if the HER2 copy number is higher than 4 or the HER2/centromere of chromosome 17 ratio is higher than 2 (Wolff *et al.*, 2013).

Compared to luminal subtypes, the abundance of HER2 confers higher aggressiveness to the tumor, but lower than basal-like subtype. Usually HER2-positive breast cancers have high proliferative index. 75% have a high histological and nuclear grade. Moreover, they often have p53 mutations, and about half of them are positive for ER, even if they generally express low ER levels (Yersal and Barutca, 2014). Despite their intrinsic malignity, the prognosis has been improved by the introduction of HER2-targeted drugs such as trastuzumab in clinical practice (see paragraph §2.3.1).

2.1 HER2

The proto-oncogene HER2, also known as ErbB2, is a tyrosine kinase (TK) receptor that belongs to the ErbB family. Its gene is localized on chromosome 17 (17q12) and encodes for a 185 kD protein that has three main domains: an extracellular domain (composed by two ligand-binding domains and two cysteine-rich regions), a

transmembrane domain and an intracellular domain (that includes a carboxy-terminal tail rich in tyrosine residues, and a tyrosine-kinase domain).

Like the other TK receptors, in absence of the ligand the receptors of ErbB family are in a monomeric form and in a close and inactive conformational status, in which the two cysteine-rich regions are in contact with each other and with the carboxy-terminal tail that keeps the tyrosine-kinase domain inactivated. The binding with the ligand causes the opening of the monomer and the separation of the two cysteine-rich regions. One of the latter is called dimerization arm, because it gets in contact with the dimerization arm of another monomer. The dimerization of the two receptors changes the conformational structure of the receptor and causes the extrusion of the carboxy-terminal tail. Consequently, the activation of the tyrosine-kinase domain triggers the trans-phosphorylation of the tyrosine residues on the carboxy-terminal tail of the other monomer. The phosphorylated tyrosine residues can be bound by numerous molecules involved in many intracellular signaling pathways, including survival, proliferation and invasivity (Burgess *et al.*, 2003).

Unlike the other members of the ErbB family (i.e. Epidermal Growth Factor Receptor – EGFR, HER3 and HER4), HER2 does not have a known ligand, and it is always in a constitutively open conformation (Cho *et al.*, 2003). Therefore, there is no need of the binding with a ligand to trigger signaling cascades.

The role of HER2 on human physiology lies in the correct formation of the cardiac trabeculae and of the cranial neural crest during embryonic development (Lee *et al.*, 1995). After birth, it is important for the early stages of the mammary morphogenesis: conditional knock-out murine models for HER2 showed defects in the elongation and the ramification of the mammary ducts, but with little impact on the capability to lactate (Andrechek *et al.*, 2005).

The overexpression of this receptor in tumors was discovered in 1985 by Axel Ullrich at Genentech, CA, USA (Coussens *et al.*, 1985). HER2 was found to have strong molecular analogies with EGFR and the same chromosomal location of the rat oncogene *neu*, that had been previously associated with glioblastoma (Schechter *et al.*, 1984). In 1989, Slamon and colleagues observed that HER2 was overexpressed in 25-

30% of human mammary carcinomas and it was also implicated in the pathogenesis of human ovarian cancers (Slamon *et al.*, 1989).

HER2 was later found to be overexpressed in other cancer types: 6-35% of non-small cell lung cancers (Mar *et al.*, 2015), 6-29.5% of gastric carcinomas (Boku, 2014), 2-66% of ovarian cancers (Hodeib *et al.*, 2015), 11% of esophageal carcinomas (Zhang *et al.*, 2016), 35.5% of salivary duct carcinomas (Ettl *et al.*, 2012), 17-33% of uterine cancers (Diver *et al.*, 2015), 14% colon cancers (Drecoll *et al.*, 2014) and 28-85% of bladder carcinomas (Zhao *et al.*, 2015).

HER2 can form homodimers, but preferentially forms heterodimers with the other members of the ErbB family or with different receptors. Several pathways can be activated according to the heterodimer that is formed (Moasser, 2007). As schematically represented in picture 4, these pathways lead to enhanced proliferation, cell motility, higher invasivity, resistance to apoptosis and angiogenesis (Arteaga *et al.*, 2011).

In general, the overexpression of HER2 changes the composition of dimers between HER family members. The number of HER2-containing dimers and HER2 homodimers increases, deregulating cell polarity and cell adhesion and causing prolonged signaling activity that can evade signal attenuation mechanisms. As a result, the potency of signaling is much higher in HER2-positive tumors (Moasser, 2007).

Higher survival and proliferation are the major effects of the signaling of HER2. These effects are driven by the activation of PI3K (Phosphatidyl-Inositol 3 Kinase)-Akt and Ras-Raf-MAPK (Mitogen-Activated Protein Kinase) pathways. Proliferation and survival are also the consequences of the deregulation of the G1/S checkpoint in the cell cycle through the increase of cyclin D1, cyclin E and cdk6 (cyclin-dependent kinase 6) and the degradation of $p27^{kip1}$, a cyclin-cdk complex inhibitor (Moasser, 2007).

The heterodimers formed by HER2 and HER3 are very stable and active from the transductional point of view. Like HER2, HER3 is a functionally incomplete receptor, because it lacks the binding site for ATP in its catalytic domain. Therefore, HER3 is functionally inactive and needs to heterodimerize to trigger signaling cascades (Berger *et al.*, 2004). The formation of HER2-HER3 heterodimers causes the enhancement of survival and cell proliferation, through the activation of Erk that is activated through

the Ras-Raf pathway. This leads to the activation of numerous nuclear targets, including Elk1, PEA3, Sp1, AP1 and c-Myc. Another signaling pathway activated by the dimer HER2-HER3 is the PI3K-Akt cascade, that leads to higher anti-apoptotic signals and enhanced survival due to the inhibition of proapoptotic molecules such as Bad, GSK3 and the transcription factor FKHR-L1. Moreover, the activation of PLCγ and JAK-STAT pathways promotes cell proliferation through the activation of cyclin D1 (Citri *et al.*, 2003).

On the other hand, EGFR-HER2 dimers lead to the activation of MAPK and PI3K pathways, resulting in higher invasivity and in the deregulation of cell cycle. Moreover, these dimers are very stable, and their formation blocks the internalization and the degradation of EGFR that is normally activated by the binding of the ligand and the homodimerization. In this way, the proliferative and pro-invasive stimuli due to the dimerization between HER2 and EGFR last more (Moasser, 2007).

HER2 homodimers interact with the Par3-Par6-aPKC-CDC42 complex, causing its disruption that leads to the delocalization of proteins involved in cell polarity and adhesion, such as gp135, ZO-1 (*Zonula Occludens* 1) and E-cadherin (Aranda *et al.*, 2006; Moasser, 2007).

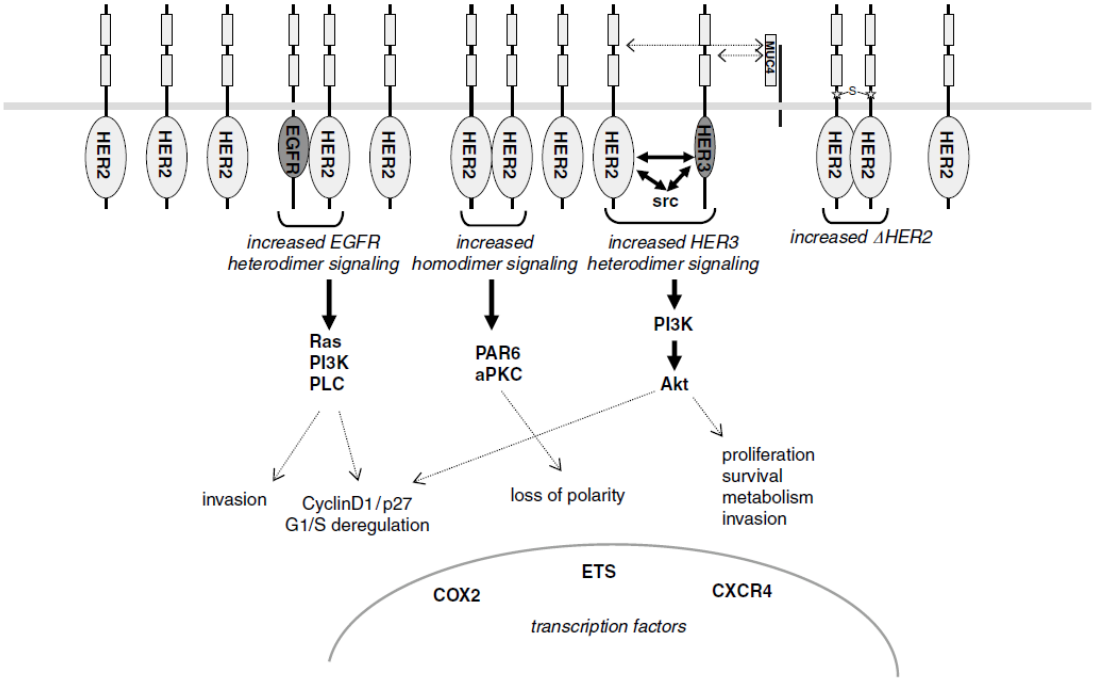

Picture 4. Schematic representation of the signaling pathways activated by the HER family members, according to the dimers formed (Moasser, 2007).

2.1.1 HER2 isoforms: Δ16

Many molecular alterations of HER2 have been identified both in human proto-oncogene HER2 and in rat *neu*. The origin of these alterations may be due to somatic mutations or post-transcriptional or post-translational modifications. In *neu*, somatic mutations are prevalent, whereas in human breast cancer mutations on HER2 gene are extremely rare. In fact, the alterations of human HER2 are mostly caused by modifications of the transcript or by proteolytic cleavage of the protein (Moasser, 2007; Arribas *et al.*, 2011).

One of the most important variant of HER2 is the alternative splicing isoform Δ16. Its name is due to the in-frame deletion of exon 16 (picture 5). This splice isoform, which is exclusively present in tumors, represents about the 8.6-9.9% of the total transcript of HER2 (Castiglioni *et al.*, 2006; Mitra *et al.*, 2009). It is present in 52% of HER2-positive mammary carcinomas and in 89% of locally disseminated ones (Mitra *et al.*, 2009).

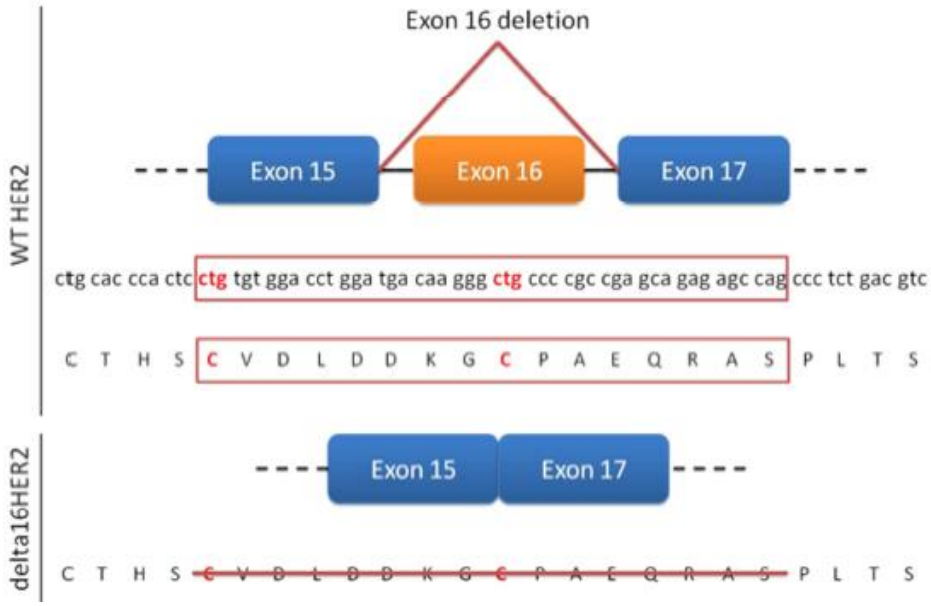

Picture 5. Schematic representation of the Δ16 (referred as delta16HER2) alternative splice form of the human HER2 gene with an in-frame deletion of exon 16 (Ghedini *et al.*, 2013).

Δ16 was first discovered by Kwong and Hung in cancer cell lines in 1998. They found a splicing variant of HER2 lacking 48 bp coding for 16 amino acids, which were localized in the juxtamembrane region of the receptor. This variant showed enhanced

ligand-independent signaling activity and higher transforming capability than those of HER2 (Kwong and Hung, 1998; Siegel *et al.*, 1999).

The lack of exon 16 causes the removal of two cysteines disrupting two disulfide bonds and changing the conformational structure of the receptor (picture 5). In this way, two cysteine residues are left unpaired and, therefore, they are free to form intermolecular bonds. The dimers that form in this way are mainly homodimers and they are more stable, more active and more numerous compared to the full-length isoform (Mitra *et al.*, 2009).

Overall, the Ras-Raf-MAPK and PI3K-Akt signaling pathways are more activated by Δ16 than full-length HER2, leading to higher invasivity and migration *in vitro* (Mitra *et al.*, 2009; Alajati *et al.*, 2013). Moreover, Alajati and colleagues found that Src kinase is more activated and co-localized with Δ16 in Δ16-transfected MCF-7 cells, whereas Src is inactive and localized in the perinuclear region in HER2-transfected MCF-7 cells (Alajati *et al.*, 2013).

Δ16 also shows higher invasivity and tumorigenicity *in vivo*. When transfected with Δ16, different cell lines (HEK293, NIH 3T3, MCF-10A) showed a higher incidence of tumors formed when injected in mice, in comparison with full-length HER2 (Castiglioni *et al.*, 2006; Alajati *et al.*, 2013). Alajati and colleagues also proved that the metastatic burden to the lungs is higher when injecting Δ16-transfected MCF-7 cells intravenously or orthotopically rather than HER2-transfected ones (Alajati *et al.*, 2013).

At the beginning, the isoform Δ16 had been linked to trastuzumab resistance *in vitro*, due to a decreased binding to this antibody (Castiglioni *et al.*, 2006; Mitra *et al.*, 2009). Mitra and colleagues analyzed the activation of the PI3K suppressor PTEN (Phosphatase and TENsin homolog), and they found that it is dephosphorylated and therefore activated in HER2-transfected MCF-7 cells treated with trastuzumab. The activation of PTEN caused a 50%-decrease in the proliferation rate in these cells, due to the cytostatic effect of the drug. In Δ16-trasfected cells, instead, PTEN was phosphorylated and therefore inactive, and the proliferation rate and the ability of forming colonies were unaltered in comparison with untreated cells (Mitra *et al.*, 2009).

However, three groups of researchers have recently proved that Δ16-positive tumors are sensitive to trastuzumab *in vivo.* In particular, Alajati and colleagues

observed that the tumors derived from the *in vivo* injection of the cell line MCF-10A, previously transfected with Δ16, were sensitive to this drug in terms of inhibition of tumor growth and of cell proliferation (Alajati *et al.*, 2013). A study performed by the Laboratory of Immunology and Biology of Metastases (University of Bologna, Italy), where this thesis was developed, and the Istituto Nazionale dei Tumori (Milan, Italy), also demonstrated that patients with HER2-positive breast cancers responded better to trastuzumab if their tumors co-expressed activated Δ16 homodimers and phosphorylated Src, showing a functional relationship between them. This result confirmed what they observed in tumors of Δ16-transgenic mice, in which Δ16 was optimally activated through the activation of Src (Castagnoli *et al.*, 2014). In a very recent article by the team of researchers at the Laboratory of Immunology and Biology of Metastases, trastuzumab was effective in preventing or delaying the tumor onset in Δ16-transgenic mice. Moreover, Δ16-expressing cells resulted sensitive to trastuzumab in 3D-culture, while HER2-expressing ones showed resistance (Palladini *et al.*, 2017).

A strict correlation between Δ16-driven aggressiveness and stemness was recently found: cancer cell lines derived from spontaneous mammary tumors of Δ16-transgenic mice had higher expression of Notch, Wnt and epithelial-mesenchymal transition-related genes, compared to cell lines derived from tumors of full-length HER2-transgenic mice. Moreover, the stem-like population of $CD29^{high}/CD24^{+}/Sca\text{-}1^{low}$ cells was more abundant and they showed greater *in vivo* ability to engraftment in serial dilution conditions (Castagnoli *et al.*, 2017).

Δ16 has been recently linked to *de novo* resistance to the TKI inhibitor lapatinib and acquired resistance to the selective Src inhibitor saracatinib, but Δ16-driven breast carcinogenesis can be completely suppressed by the irreversible small molecule pan-HER inhibitor dacomitinib (Tilio *et al.*, 2016).

2.2 HER2 and tumor angiogenesis

HER2 has an active role in tumor angiogenesis. Preclinical and clinical studies have pointed out that the activation of HER2 leads to an increase of pro-angiogenesis factors (Alameddine *et al.*, 2013).

In a cohort study that involved 611 patients with HER2-positive breast carcinoma, a positive association between HER2 and VEGF expression was observed. Moreover, the simultaneous expression of HER2 and VEGF correlates with a poorer prognosis (Konecny *et al.*, 2004).

Alameddine and colleagues have discovered that cell lines that overexpress HER2 had a high expression of VEGF, COX-2 and HIF-α. VEGF was more elevated when HER2 dimerizes with EGFR or HER3 (Alameddine *et al.*, 2013).

The increase in expression of pro-angiogenic factors is mediated by the activation of PI3K-Akt and MEK-ERK pathways (picture 6). Downstream, the activation of mammalian target of rapamycin (mTOR) leads to the activation of the p70S6k kinase, which promotes the translation of the VEGF (picture 6.I) and HIF (picture 6.II) mRNAs (Klos *et al.*, 2006). On the other hand, the activation of MAPK pathway promotes the transcription of the VEGF gene (picture 6.III).

The third angiogenesis-related target of the activation of HER2 is COX-2 (Moasser, 2007; Alameddine *et al.*, 2013). Through receptor-mediated endocytosis, HER2 is internalized and translocated into the nucleus where, thanks to its kinase activity, directly bonds and activates the COX-2 promoter (picture 6.IV).

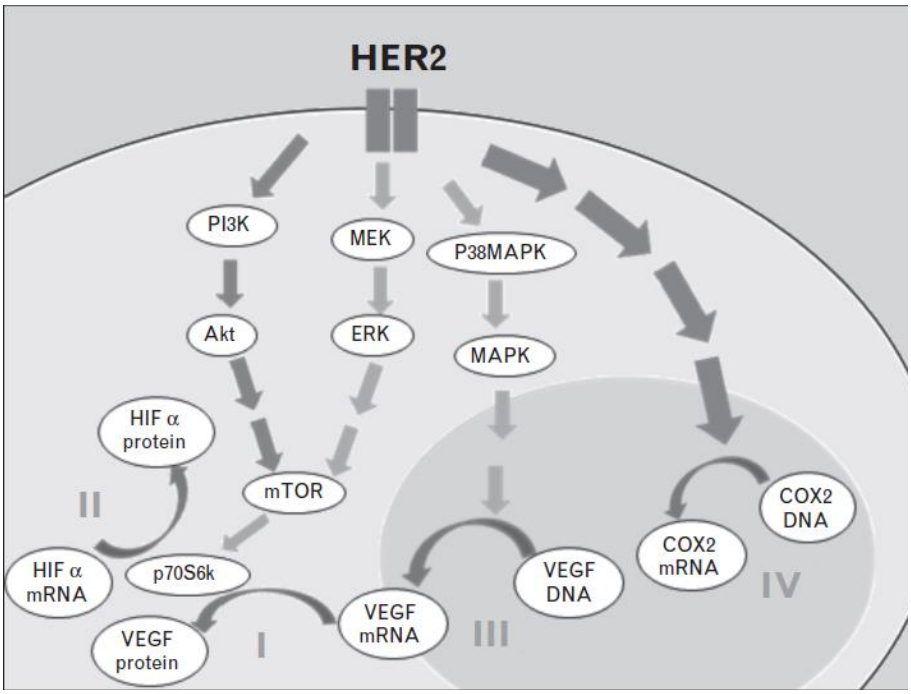

Picture 6. Angiogenesis-related pathways activated by HER2 (Alameddine *et al.*, 2013): induction of VEGF (I) and HIF-α (II) translation through PI3K/Akt and MEK/ERK pathways; induction of VEGF transcription through MAPK pathway (III); direct induction of COX-2 transcription through receptor-mediated endocytosis (IV).

HER2 has been also linked to vasculogenic mimicry. Liu and colleagues observed this phenomenon in invasive breast cancer specimens, defined as CD31-negative/PAS-positive vessel-like structures with or without red blood cells inside. According to their observations, vasculogenic mimicry was more present in HER2-positive samples. Moreover, the number of vascular-like channels was more abundant in 3+ HER2-positive carcinomas compared to 2+ or 0/+1 samples. A positive correlation between HER2 and vasculogenic mimicry was confirmed *in vitro* by comparing the number of vessel-like structures formed by MCF-7 cells transfected with HER2 and seeded on Matrigel: this number was higher compared to parental cells (Liu *et al.*, 2013).

2.3 Anti-HER2 targeted drugs in mammary carcinoma

As said, the overexpression of HER2 confers higher malignity and increased aggressiveness to the tumor. However, the prognosis of the patients affected by HER2-positive breast cancer has been improved thanks to anti-HER2 targeted drugs, both in terms of disease- or progression-free survival (DFS and PFS respectively) and overall survival (OS) (Gu *et al.*, 2016).

All carcinomas that are scored 3+ or 2+ but positive for HER2 amplification by FISH test are eligible for targeted therapy against HER2 (Wolff *et al.*, 2013).

2.3.1 Trastuzumab

The standard therapy is based on trastuzumab (Herceptin®, Genentech), a humanized monoclonal antibody that binds the juxtamembrane region of HER2. This drug has been approved by FDA (Food and Drug Administration) in 1998 for metastatic HER2-positive breast carcinoma and in 2006 for early stage HER2-positive breast carcinoma, both in adjuvant and neo-adjuvant settings (Tagliabue *et al.*, 2011).

In adjuvant setting, trastuzumab is administered after chemotherapy, or in association with taxanes after doxorubicin and cyclophosphamide-based therapy, or in association with carboplatin and docetaxel (Arteaga *et al.*, 2011).

In neo-adjuvant setting, trastuzumab is administered in association with chemotherapy for patients with locally advanced breast cancer or early stage breast

carcinoma. For patients with metastatic HER2-positive breast cancer, trastuzumab is administered alone or associated with paclitaxel or docetaxel (Arteaga *et al.*, 2011).

The major problem regarding the safety of trastuzumab is cardiotoxicity, but all adverse effects are usually treatable and largely reversible (Arteaga *et al.*, 2011).

The mechanisms of action of trastuzumab are many (picture 7), with a cytostatic or a cytotoxic effect. The mechanisms with a cytostatic effect are the inhibition of receptor dimerization, the inhibition of HER2 extracellular domain proteolytic cleavage and the consequent inhibition of activated p95-truncated HER2 receptor and the inhibition of tumor angiogenesis. On the other hand, the cytotoxic effects involve the antibody-dependent cell-mediated cytotoxicity (ADCC) and the inhibition of DNA repair (Tagliabue *et al.*, 2011).

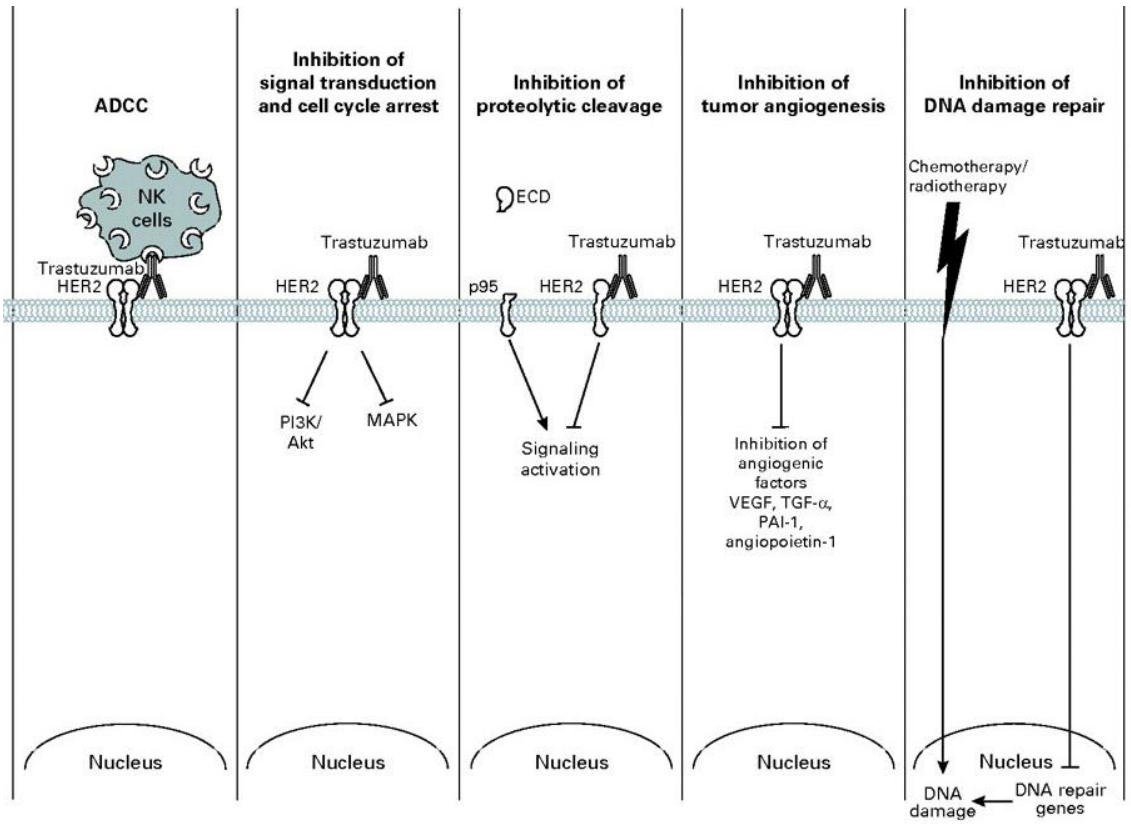

Picture 7. Mechanisms of action of trastuzumab (modified from Spector and Blackwell, 2009).

Trastuzumab binds the domain IV of HER2 (Parakh *et al.*, 2017), causing the inhibition of dimerization by steric hindrance. If HER2 cannot dimerize, the signal pathways downstream are not activated, affecting proliferation. Cell cycle arrest in G1 phase is also induced, because HER2 is not able to downregulate the cyclin-dependent

kinase inhibitor $p27^{Kip1}$ anymore. Apoptosis can also be induced through the upregulation of p53 (Spector and Blackwell, 2009).

The binding of trastuzumab also inhibits the cleavage of the extracellular domain (ECD) of HER2, preventing the formation of the truncated form p95, that has been linked to higher malignity and a poorer prognosis (Arribas *et al.*, 2011). This ECD-lacking isoform is more active because it can homodimerize in a more stable way thanks to five cysteine residues that can form disulphide bonds between two different molecules. p95 homodimers activate numerous signaling pathways (MAPK, Akt, Src and PLCγ) that increase the expression of pro-metastatic proteins such as MMP1, Angiopoietin-like 4, MET, CD44, PLAUR, EphA2, ITGA2, ITGFB, TGF-α and interleukin-11 (Pedersen *et al.*, 2009).

Tumor angiogenesis is inhibited too, causing hypoxia to the tumor. *In vitro*, the treatment with this antibody leads to a decreased expression of VEGF, Angiopoietin-1, TGF-α and PAI-1 (Plasminogen Activator Inhibitor 1), and an increased expression of the anti-angiogenic factor TSP-1 (Thrombospondin 1) (Izumi *et al.*, 2002).

In addition to the previous ones, another cytostatic mechanism of action of trastuzumab involves the internalization and the consequent downregulation of HER2, through c-Cbl-mediated ubiquitination. However, this process seems to occur only after a prolonged exposure to trastuzumab (Baselga *et al.*, 2001).

Among the cytotoxic effects, the ADCC is the most relevant one. This mechanism does not depend only on the drug, but also involves the immune system of the patient. It consists in the interaction between the Fc portion of trastuzumab and the FcγRIIIA receptors on NK cells, macrophages and dendritic cells. The binding activates these cells, which will finally mediate the tumor cell death or involve $CD8^+$ cytotoxic T cells (Kohrt *et al.*, 2012).

Besides ADCC, other immunologic mechanisms are involved in the therapeutic response to trastuzumab: complement-dependent cytotoxicity; antibody-dependent cellular phagocytosis (phagocytosis of monoclonal antibody-opsonized debris of target cells through receptors for the Fc portion of IgG of dendritic cells and macrophages); immune complex (monoclonal antibody and tumor antigen) uptake by antigen-presenting cells (APCs); induction of a cross-talk among immune cells, including

natural killer cells and dendritic cells; induction of production of immunomodulatory cytokines (i.e. type I and type II interferons); induction of cross-presentation of tumor antigens by APCs and helper $CD4^+$ T cells to cytotoxic $CD8^+$ T cells, leading to priming of specific adaptive immune response such as tumor antigen-specific T lymphocyte response (Bianchini and Gianni, 2014). In general, in patients the major effects seem to be mediated by immunologic mechanisms.

Finally, trastuzumab can interfere with the mechanisms of DNA repair through the inhibition of p21/WAF1, a protein involved in the cellular response to genomic damage (Spector and Blackwell, 2009).

2.3.2 Mechanisms of resistance to trastuzumab

Primary and secondary resistance to trastuzumab is one of the major problem in the clinical setting, affecting about 70% of patients with HER2-positive breast cancer (Parakh *et al.*, 2017). The molecular mechanisms that have been proposed to explain drug resistance to trastuzumab are several.

The first one concerns the modification of the target itself. If HER2 is altered, the drug binding might be compromised. In this case, the mutations involve the binding domain. One example is the p95 fragments that lack the extracellular domain but can activate the pathways downstream (Rexer and Arteaga, 2012).

The binding site may not be accessible due to the steric hindrance mediated by membrane-associated glycoproteins such as MUC4, that co-localizes with HER2 when overexpressed. The cleaved form of MUC1 has been also found to have a role in masking the binding site of trastuzumab. However, the cleaved form of MUC1 can also homodimerize and activate proliferation and survival signaling pathways (Rexer and Arteaga, 2012).

The ligand-dependent formation of heterodimers may be enhanced through the overexpression of EGFR and/or HER3, or of one of their ligands. This is consistent with the data regarding the inability of trastuzumab of preventing the ligand-dependent heterodimerization of HER2 (Rexer and Arteaga, 2012).

Trastuzumab action can also be bypassed through the overexpression of molecular partners that do not belong to HER family, such as IGF1R or Met, that can

activate alternative pathways leading to increased proliferation and survival. The formation of IGF1R-HER2 dimers can potently activate PI3K/Akt pathway, whereas the dimerization with Met leads to the inhibition of the cell cycle inhibitor $p27^{kip1}$ (Arteaga *et al.*, 2011; Puglisi *et al.*, 2012).

The activation of EphA2 has been linked to trastuzumab resistance too. *In vitro* studies have demonstrated that overexpression of this receptor confers resistance to trastuzumab, and the treatment with EphA2 blocking antibody restores sensitivity to the drug (Rexer and Arteaga, 2012).

The trastuzumab-mediated inhibition of HER2 may have no effect if one of the downstream molecules is mutated to be constitutively activated. One example can be point mutation on the *PIK3CA* gene, which encodes the catalytic subunit p110α of PI3K, or on the gene of mTOR. Point mutations that inactivate PTEN have also been observed (Arteaga *et al.*, 2011; Puglisi *et al.*, 2012).

A special mention goes to Src, which has been associated with overexpression of HER2 and trastuzumab resistance in breast cancer cell lines. The overactivation of Src has also been observed in patients whose tumors gained resistance to trastuzumab (Zhang *et al.*, 2011). However, Castagnoli and colleagues found that the presence of Δ16 in tumors with activated Src confers higher sensitivity to trastuzumab (Castagnoli *et al.*, 2014).

In some cases, a downregulation of HER2 can be observed. In a clinical study reported by Mittendorf and colleagues, 8 patients with HER2-positive breast cancer out of 25 did not show a complete pathological response after the treatment with trastuzumab, due to the loss of HER2 overexpression (Mittendorf *et al.*, 2009).

Other mechanisms involve the alteration of proteins which have a role in regulating apoptosis or the cell cycle, such as the upregulation of cyclin E or the downregulation of $p27^{kip1}$ (Rimawi *et al.*, 2015). Moreover, elevated levels of the anti-apoptotic proteins survivin and Mcl-1 have been found in HER2-overexpressing cell lines that are resistant to trastuzumab (Valabrega *et al.*, 2011).

As said, the major effect exerted by trastuzumab is mediated by the immune system of the patient through ADCC. Therefore, alterations in host factors with immunomodulatory functions can determine trastuzumab resistance. For example,

defects in FcγRIII or in the functionality of NK or macrophages are associated with poor response to trastuzumab in clinical and preclinical studies (Rexer and Arteaga, 2012). Other immunological mechanisms of escape have been proposed, including the increase MHC class I expression on tumor cells by type I interferons and interferon γ, which can diminish the effect of NK cells by engaging inhibitory receptors, and impair cytotoxic T lymphocyte functions by non-classic MHC class I molecules (e.g., HLA-G). Type I interferons and interferon γ, in addition to the upregulation of oncogenic pathways, can also promote increased expression of PD-L1 protein in tumor cells, which inhibits activated T cells. The expression of PD-L1 and the costimulatory molecules CD80 and CD86 on dendritic cells may lead to the inhibition of the adaptive immune response. Moreover, T-cell-mediated immune responses can be decreased by the tumor-dependent downregulation of MHC class I molecules (Bianchini and Gianni, 2014).

Many strategies to overcome trastuzumab resistance have been proposed. Trastuzumab can be associated with hormone therapy, chemotherapy or other targeted drugs, such as lapatinib (a TKI that blocks the catalytic domain of EGFR and HER2), pertuzumab (a monoclonal antibody which binds another site on HER2 extracellular domain) or PI3K/Akt inhibitors. Another strategy consists in the modification of the trastuzumab itself, like trastuzumab-DM1, which is trastuzumab conjugated with a cytotoxic compound that blocks microtubule polymerization that is released in the cytoplasm when the drug is internalized into the cell (Rexer and Arteaga, 2012).

2.3.3 Breast Cancer Stem Cells

Another possible explanation about the mechanisms that drive drug resistance concerns the existence of a sub-population among cancer cells which is intrinsically resistant to treatments and can regenerate the tumor mass. These cells have stem-like properties, such as self-renewal and the ability to differentiate into several cellular types with reduced proliferative and differentiative potential. For these reasons, this population has been defined as Cancer Stem Cells (CSCs) (Korkaya and Wicha, 2013).

The CSCs are present in many human tumor types, including breast cancer. The Breast Cancer Stem Cells (BCSCs) have been defined as cells with high expression of

CD44 and low or absent expression of CD24, as well as without displaying mammary lineage markers, such as CD2, CD3, CD10, CD16, CD18, CD31, CD64 and CD140b (Al-Hajj *et al.*, 2003).

The $CD44^+$ $CD24^{-/low}$ Lineage $(Lin)^-$ cells have a very elevated proliferative ability and were initially named as Cancer Initiating Cells, because just one hundred of these cells were able to engraft and grow as a tumor mass, when ten thousand of unselected cells failed. Even if they represent a very small portion of the tumor (11-35% of the Lin^- cells), their number is sufficient to generate a neoplastic mass (Al-Hajj *et al.*, 2003).

Li and colleagues observed that this population is more present in HER2-positive breast cancers than in HER2-negative ones (10% versus 4.7%), suggesting a possible role of HER2 in sustaining the stemness of cancer cells. Moreover, the $CD44^+$ $CD24^{-/low}$ Lin^- cells showed drug resistance to chemotherapy (Li *et al.*, 2008). In their study, 31 patients with HER2-negative breast cancer were treated with docetaxel or doxorubicin and cyclophosphamide, whereas 21 patients with HER2-positive mammary carcinoma were treated with lapatinib, because previous studies had suggested a possible role of EGFR in maintaining the self-renewal ability in mammospheres (Farnie *et al.*, 2007). Before and after the treatment, a biopsy from each patient has been collected and analyzed for the presence of $CD44^+$ $CD24^{-/low}$ Lin^- cells and for the ability of forming mammospheres *in vitro*. In HER2-negative breast cancer, both the percentage of BCSCs and the ability of forming mammospheres increased after the treatment with chemotherapy. On the contrary, a decrease in those parameters has been observed in HER2-positive biopsies after the treatment with lapatinib, even if not statistically significant (Li *et al.*, 2008).

HER2 has a fundamental role in BCSCs (Korkaya and Wicha, 2013). Ithimakin and colleagues observed that the $CD44^+$ $CD24^{-/low}$ Lin^- cells of bone metastases, originated from primary tumors classified as HER2-negative breast cancer, actually expressed HER2 with a mechanism that was not dependent on gene amplification. These cells expressed RANK, which binds to its ligand that is present in bone microenvironment and activated molecular pathways finally leading to HER2 increased expression (Ithimakin *et al.*, 2013). Moreover, HER2 expression in BCSCs is

also mediated by the interaction with several molecules, including CXCR1 and Notch (Korkaya and Wicha, 2013).

HER2 expression might be important for the maintenance of the self-renewal ability, through the activation of the β-catenin signaling pathway and the inhibition of PTEN, which activates PI3K/Akt pathway (Korkaya *et al.*, 2009).

In mouse models of breast cancers, other stem cell markers have been identified, such as Sca-1, CD29, Thy1.1 and Nanog (Arigoni *et al.*, 2013; Castagnoli *et al.*, 2017).

2.4 Anti-angiogenic therapies in mammary carcinoma

Since the ten hallmarks of cancer include tumor angiogenesis, inhibiting the formation of new blood vessels inside the tumor is a possible therapeutic approach that can be considered in addition to targeted and conventional strategies.

As previously said, it must be considered that tumor angiogenesis is not an efficient and homogeneous process. There can be hypoxic regions that enhance genomic instability, and hyperpermeability that interferes with the distribution of the drugs. Thus, normalizing the tumor vasculature may also be a valid strategy to improve therapeutic response: this approach is the so-called Jain's concept (Goel *et al.*, 2011).

Indeed, Willet and colleagues analyzed biopsies from rectal carcinoma patients treated with a single injection of bevacizumab, a monoclonal antibody that targets VEGF. They observed a reduction in tumor perfusion, in vascular volume, in the microvascular density, in interstitial fluid pressure and in the number of viable circulating endothelial and progenitor cells, whereas the fraction of vessels with pericyte coverage was increased (Willett *et al.*, 2004).

Since VEGF is the main molecular driver of physiological and pathological angiogenesis, it is logical that the major therapeutic strategies target VEGF itself (such as bevacizumab) or its receptors (like the inhibitors sunitinib and pazopanib) to inhibit its pathway.

2.4.1 Bevacizumab

The first anti-angiogenic drug targeting VEGF was bevacizumab (Avastin®, Hoffmann-La Roche), since it is well known that VEGF-A is upregulated in many tumor types, including breast cancer (Seddon *et al.*, 2014).

Bevacizumab binds all the major isoforms of VEGF with elevated affinity, preventing their binding to their receptor. Its effects include the reduction of vascular density, through the regression of existing vessels and the inhibition of the proliferation and migration of endothelial cells, which suppresses the development of new vessels. It also normalizes the aberrant characteristics of tumor angiogenesis and interacts with the immune system of the patient by increasing the levels of dendritic cells, T-lymphocytes and NK cells (Koutras *et al.*, 2012).

As it targets angiogenesis, the main adverse effects involve hypertension, proteinuria and hemorrhagic events. Less frequently, serious adverse events can be observed, such as arterial thromboembolism, wound healing complications, gastrointestinal perforation, reversible posterior leukoencephalopathy and congestive heart failure/cardiomyopathy (Koutras *et al.*, 2012).

In the metastatic setting, three phase III clinical trials showed an improvement in the progression-free survival (PFS) and in the objective response rate (ORR) with first-line treatment with bevacizumab in association with chemotherapy, although no effect on overall survival (OS) was observed (Seddon *et al.*, 2014; Trédan *et al.*, 2015).

The improvement in the PFS showed in the E2100 trial, where 722 patients with advanced breast cancer were randomized to receive bevacizumab plus paclitaxel or paclitaxel alone, led to the approval of bevacizumab by FDA for the treatment of HER2-negative metastatic breast cancer in 2008. Further trials failed to prove a significant improvement in OS. They rather showed an increase rate of grade 3-5 adverse reactions (Seddon *et al.*, 2014).

Interestingly, Mikkael Sekeres, a physician at the Cleveland Clinic Taussig Cancer Institute and member of the Oncologic Drugs Advisory Committee to the FDA, wrote in a letter to the New England Journal of Medicine: «Well, I can offer you a drug that will not make you live longer, won't make you feel better, and may have life-

threatening side effects, but it will keep your cancer from worsening by an average of 1-2 months» (Sekeres, 2011).

Given the modest results in advanced breast cancer, the efficacy of bevacizumab was studied in patients with early stage mammary carcinoma, both in adjuvant and neoadjuvant settings. The use of bevacizumab might be beneficial in this context due to the role of VEGF in the initial phase of angiogenesis, that might be more important for carcinogenesis (Koutras *et al.*, 2012).

In HER2-negative early breast cancer in neoadjuvant regimen, a phase III trial showed just modest improvements in the PFS, in the pathological complete response (pCR) and in the ORR. However, the rate of adverse events increased, including cardiotoxicity when bevacizumab was administered in association with cardiotoxic drugs like anthracyclines (Seddon *et al.*, 2014).

Bevacizumab was also tested in patients with HER2-positive breast cancer, combination with trastuzumab. Like the previous studies, a small improvement in PFS and pCR was observed, as well as the adverse effect rate (Seddon *et al.*, 2014).

The approval of bevacizumab for the treatment of metastatic HER2-negative breast cancer was revoked in 2010 by FDA, as efficacy did not counterweight the risks. Nevertheless, EMA (European Medicine Agency) still supports its use in combination with paclitaxel (Koutras *et al.*, 2012).

Bevacizumab is also approved to treat on non-small cell lung cancer (NSCLC), renal cell cancer (RCC) and, as second-line treatment, glioblastoma (Kerbel, 2011).

2.4.2 Sunitinib

Sunitinib (Sutent®, Pfizer) is an oral small-molecule tyrosine kinase inhibitor (TKI) that targets several receptors including VEGFRs, PDGFRs, c-Kit, RET, CSF1R and Flt-3. Nowadays, it is approved for the treatment of renal cell cancer (RCC) and gastrointestinal stromal tumors (GIST).

Several preclinical and clinical studies have investigated the efficacy of sunitinib in breast cancer. Although sunitinib was effective in preclinical xenograft models (Abrams *et al.*, 2003), some clinical studies reported controversial results. A study reported a benefit as second-line treatment in monotherapy, especially in patients with

triple-negative or HER2-positive disease. However, another trial on HER2-negative breast cancer showed a worsening in terms of PFS in patients treated with sunitinib alone in comparison with patients treated with capecitabine. Other studies showed no improvement with the addition of sunitinib to chemotherapy (Koutras *et al.*, 2012).

Two recent clinical trials assessed the efficacy of sunitinib in combination with trastuzumab in patients with advanced HER2-positive breast cancer, showing some anti-tumor activity of the combined therapy. In one study, an objective response was observed in the 73% of the evaluable patients treated with sunitinib plus docetaxel and trastuzumab (Cardoso *et al.*, 2012). In a following study, which involved a higher number of patients, the objective response rate was only 37%, but it was slightly higher in patients that did not receive any other treatment before (Bachelot *et al.*, 2014).

All phase I and II studies with safety as primary endpoint showed manageable adverse effects. These include fatigue, gastrointestinal disorders (diarrhea, nausea, stomatitis, dyspepsia and vomiting), hand-foot syndrome, skin discoloration and anorexia. The most severe adverse events include pulmonary embolism, thrombocytopenia, tumor hemorrhage, febrile neutropenia and hypertension (Nielsen *et al.*, 2010).

2.4.3 Pazopanib

Pazopanib (Votrient®, GlaxoSmithKline) is another oral small-molecule TKI that blocks VEGFR2, PDGFRs and c-Kit, and has also modest activity against FGFRs (fibroblast growth factor receptors) and CSF1R (Schutz *et al.*, 2011). It has been approved for the treatment of advanced or metastatic renal cell cancer and advanced soft-tissue sarcomas.

The efficacy of pazopanib has been evaluated in breast cancer in some preclinical and clinical studies. One phase II trial studied the second- or third-line administration of pazopanib in HER2-negative recurrent or metastatic breast cancer, demonstrating little efficacy (Mackey *et al.*, 2012). A recent phase II single-arm clinical trial studied the combination of pazopanib and paclitaxel after doxorubicin and cyclophosphamide as neoadjuvant therapy in HER2-negative locally advanced disease. A small pCR was observed, but the therapy was discontinued due to toxicity (Tan *et al.*, 2015).

Another phase II study assessed the combination of pazopanib and lapatinib in metastatic HER2-positive mammary carcinoma as first-line therapy, showing a prolongation of the PFS (Mackey *et al.*, 2012). The results on HER2-positive breast cancer seem promising, but still too few patients have been recruited so far. More investigations are needed to study the efficacy of this drug (Amiri-Kordestani *et al.*, 2012).

Phase I clinical trials assessed the safety of pazopanib, demonstrating that it is a well-tolerated drug. The most relevant adverse events include nausea, fatigue, diarrhea, vomiting, rash, anorexia, visual disturbances, alopecia and constipation (Bossung and Harbeck, 2010).

2.4.4 Resistance to anti-angiogenic therapies

The controversial results obtained in several clinical studies question the convenience about using anti-angiogenic agents in breast cancer.

VEGF is one of the main driver of angiogenesis, and targeting the VEGF-dependent angiogenesis seems the most logical approach. However, there is the strong possibility that other alternative pathways are activated to sustain the formation of new blood vessels when VEGF is inhibited. Actually, the more the tumor is advanced, the more there are other proangiogenic factors that are upregulated in breast cancer, such as bFGF. This implies that the selective pressure set by the anti-angiogenic therapies may induce the selection of clones in which redundant pathways are active. In this way, the effect of anti-angiogenic drugs may be only transient (Kerbel, 2011).

The subpopulations that anti-angiogenic therapy may select could be more aggressive, because the increasing hypoxia may upregulate HIF-α-related genes and thus promoting invasion, proliferation and metastatic dissemination. This can explain why only improvements in PFS, and not in OS, were observed in breast cancer (Kerbel, 2011).

Moreover, a preclinical study demonstrated that the therapy with anti-angiogenic drugs causes the metabolic reprogramming towards aerobic glycolysis that leads to resistance to the treatment. Targeting the glycolytic enzymes restores the sensitivity (Wehland *et al.*, 2013).

3. Preclinical mouse models of mammary carcinoma

Transgenic models are animal models that express a homologous or xenogeneic gene that allows the establishment of a pathological condition. They are very useful to better understand the role of the transgene in causing the disease, to study its progression in a complex and alive organism, and to test novel therapeutic approaches (Wagner *et al.*, 1995).

Starting from late '80s, several breast cancer transgenic models were developed. The first one was described by Muller and colleagues in 1988 and was transgenic for the activated form of rat *c-neu* on a FVB background (Muller *et al.*, 1988). This model was followed by several other models, including one murine model that was transgenic for the rat proto-oncogene *neu* (Guy *et al.*, 1992). Another model was transgenic for *neuT* (Lucchini *et al.*, 1992), that was later brought on BALB/c background in the laboratory of Prof. Guido Forni and Prof. Federica Cavallo, in collaboration with the Laboratory of Immunology and Biology of Metastases (Boggio *et al.*, 1998).

3.1 FVBhuHER2 mice

The first transgenic models for human HER2 did not develop autochthonous mammary carcinomas, but lung adenocarcinomas, Harderian gland tumors and B cell lymphomas (Suda *et al.*, 1990). Another model had the transgene expression under the control of the promoter WAP (Whey Activating Protein), which guaranteed the expression of HER2 in the secretory mammary epithelium during pregnancy and lactation but not the development of breast cancer (Piechocki *et al.*, 2003).

The first human HER2-transgenic mouse model that developed mammary carcinomas was described by Finkle and colleagues in 2004. This model was called MMTV.f.huHER2 (but from now on it will be called FVBhuHER2). It was obtained by microinjecting a plasmid containing the cDNA of HER2 in an inbred FVB zygote. The transgene was put under the control of the promoter MMTV (Murine Mammary Tumor Virus), that is active in mammary epithelium by hormonal control. The

embryos that were obtained were implanted in a surrogate mother to generate a HER2-transgenic lineage (Finkle *et al.*, 2004).

The female mice that were born were characterized from the molecular and phenotypic point of view. The transgene was successfully integrated into the genome in a single site on chromosome 6, and the copy number varied from 30 to 50. After 12 weeks of age, the soluble form of HER2 was detectable, indicating the expression of the transgene in the normal mammary epithelium. This expression was confirmed by histological analysis. Moreover, the presence of HER2 was evaluated in other tissues: HER2 was also highly expressed in lungs, uterus, brain, skin, pancreas, adrenal glands, heart, esophagus and salivary glands (Finkle *et al.*, 2004).

The female mice were observed for 52 weeks. At the end of the follow-up, 73% of them had asynchronously developed mammary adenocarcinomas with an average latency of 36 weeks of age. Lung metastases were observed in 40% of the mice that developed tumors (Finkle *et al.*, 2004).

Somatic mutations were found in more than 80% of tumors. The majority was in the juxtamembrane region, whereas rare mutations were in the transmembrane region. About half of the mutations was in-frame. The other mutations, that were much less frequent, were insertions (4%), point mutations (18%) or combinations of deletions and point mutations (6%). The mutations described were not observed in normal mammary epithelium, and were more frequent in the exon 16 (Finkle *et al.*, 2004).

This model was also studied by at the Laboratory of Immunology and Biology of Metastases directed by Prof. Pier-Luigi Lollini at the Department of Experimental, Diagnostic and Specialty Medicine (DIMES), University of Bologna, Italy (De Giovanni *et al.*, 2014; Castagnoli *et al.*, 2014; Palladini *et al.*, 2017). The median latency of this model was around 40 weeks, with the earliest tumors appeared around 30 weeks of age (Picture 8A). The follow-up was longer and Palladini and colleagues determined that tumor incidence could reach 100% after 75 weeks of age. These results reflect what observed by Finkle and his group.

Tumor multiplicity, that is the mean number of tumor per mouse, was not very high in this model. Each FVBhuHER2 mouse developed an average of 1-2 tumors

(Picture 8B). The tumor growth was quite fast, reaching 1 cm^3 after just 5 weeks after onset (picture 8C).

Lung metastases were present in one bearing-tumor mice out of two, and the number of metastases was not high (picture 8D). The higher incidence of lung metastases compared to the one found by Finkle and colleagues can be explained by the longer follow-up of the observational experiment performed by the group at the Laboratory of Immunology and Biology of Metastases, that was well beyond 52 weeks.

The appearance of the tumors was also analyzed. The tumors of FVBhuHER2 female mice were typically reddish and hemorrhagic, with a soft and spongy texture (Balboni, MSc thesis; Palladini *et al.*, 2017).

3.2 Δ16-HER2 mice

The first model that was transgenic for the splicing isoform Δ16 was described by Marchini and colleagues in 2011 (Marchini *et al.*, 2011). It is the result of the collaboration between three Italian laboratories at the Istituto Nazionale dei Tumori in Milan, at the University of Camerino and at the University "G. D'Annunzio" of Chieti.

Like FVBhuHER2 model, the transgene is placed under the control of the promoter MMTV. The plasmid that was used to transfect the FVB zygote also contained the gene of firefly luciferase, to let the visualization of the tumors by chemiluminescence. For this reason, this model was named Δ16-HER2-LUC, but from now on it will be simply called Δ16-HER2.

The transgene resulted to be inserted in the genome in a unique site on chromosome 5, in an intergenic region lacking coding or regulatory sequences. The copy number is 5, and therefore much lower than in FVBhuHER2 model.

Virgin female mice of the second generation were monitored by palpation. All the mice developed an average number of tumors of 4-5 with a mean latency of 15 weeks. Earliest tumors appeared around the 12^{th} week of age and all the mice were positive for the present of mammary carcinomas by 19 weeks of age. Lung metastases were detectable starting from the 25^{th} week of age.

The transgene was exclusively expressed in tumors, and no somatic mutations were detected. The authors proposed that these evidences may suggest that it is not

necessary a second mutational event for tumor onset, unlike in the FVBhuHER2 model (Marchini *et al.*, 2011).

Tumors were analyzed from the molecular point of view, revealing that Δ16 stably homodimerized and the homodimers were constitutively active. Src was also active downstream, leading to the activation of STAT3. Other activated pathways involved Akt and MAPK (Marchini *et al.*, 2011).

This model was also studied at the Laboratory of Immunology and Biology of Metastases. The median latency and the mean tumor multiplicity observed were comparable to the ones observed by Marchini and colleagues (picture 8A and 8B; Castagnoli *et al.*, 2014; Palladini *et al.*, 2017).

Tumor growth was slower that the one of FVBhuHER2. The volume reached after 5 weeks of follow-up was less than 0.5 cm^3 (picture 8C).

However, the metastatic burden to the lungs was similar, both regarding the number and the incidence of metastases (picture 8D).

Macroscopically, Δ16-HER2 tumors looked very different than FVBhuHER2 ones. They were usually pale and solid, with small hemorrhagic areas in rare cases (Balboni, MSc thesis; Palladini *et al.*, 2017). These differences may suggest a possible role of the two isoforms in tumor angiogenesis.

Another mouse model transgenic for Δ16 have been recently developed. Differently from Δ16-HER2 model, the expression of Δ16 is inducible in this model (Turpin *et al.*, 2016). This model has been called ErbB2ΔEx16. Δ16 transgene was placed under the transcriptional control of the tetracycline response element. The FVB animals with these genomic features were crossed with a separate FVB strain expressing the reverse tetracycline transactivator under the transcriptional control of the MMTV promoter. The expression of the transgene was induced by adding doxycycline to the drinking water. The expression of Δ16 was restricted to the mammary and salivary epithelium. The tumors developed on this model showed an earlier onset than FVBhuHER2 mice: the first tumors appeared after 10 and 28 days after treatment with doxycycline in two different founder strains. Differently from HER2-expressing tumors, which have luminal-like features, ErbB2ΔEx16 tumors displayed characteristics that were more similar to basal-like tumors. Even in this model, Src

kinase was more activated than in FVBhuHER2 tumors. Moreover, Δ16 activated Stat3, Smad2 and HIF1α transcription factors. In addition, the metastatic burden to the lungs was higher than in FVBhuHER2 mice. They also proved that the stop of treatment with doxycycline was accompanied by tumor regression, but tumors reappeared after a variable tumor-free period. However, these recurrent tumors did not express Δ16 and displayed EMT features.

3.3 FVBΔ16huHER2 (F1) mice

Murine models that are transgenic for each HER2 isoform were developed, but a preclinical model that mimicked the clinical situation in which both full-length HER2 and Δ16 are co-expressed was lacking.

For this reason, the team of researchers at the Laboratory of Immunology and Biology of Metastases (University of Bologna, Italy) recently obtained a novel mouse model that is transgenic for both isoforms, created by crossing FVBhuHER2 and Δ16-HER2 strains (Palladini *et al.*, 2017). This model has been called F1 HER2/Delta16 (but in this thesis, it will be called simply F1).

Double-transgenic female mice were monitored by palpation. The tumor-free survival curve overlapped the one of Δ16-HER2 mice, showing a median latency of 16 weeks (picture 8A). On the other hand, tumor multiplicity was higher, with a mean number of tumors per mouse of 6-7 (picture 8B). Tumor growth rate was also similar to the one of Δ16-HER2 model (picture 8C), and so the incidence and number of lung metastases (picture 8D).

These evidences suggest a dominant role of Δ16 in determining a faster carcinogenesis. However, HER2 and Δ16 seem to have a role only in the early stages of tumor onset and not in tumor progression, since there was no difference in metastatic spread between the three models.

The appearance of F1 tumors seemed to be more heterogeneous. Both macroscopic characteristics of parental strains were observable, with a prevalence of pale and solid aspect, typical of Δ16-HER2 tumors (Balboni's MSc thesis, 2014).

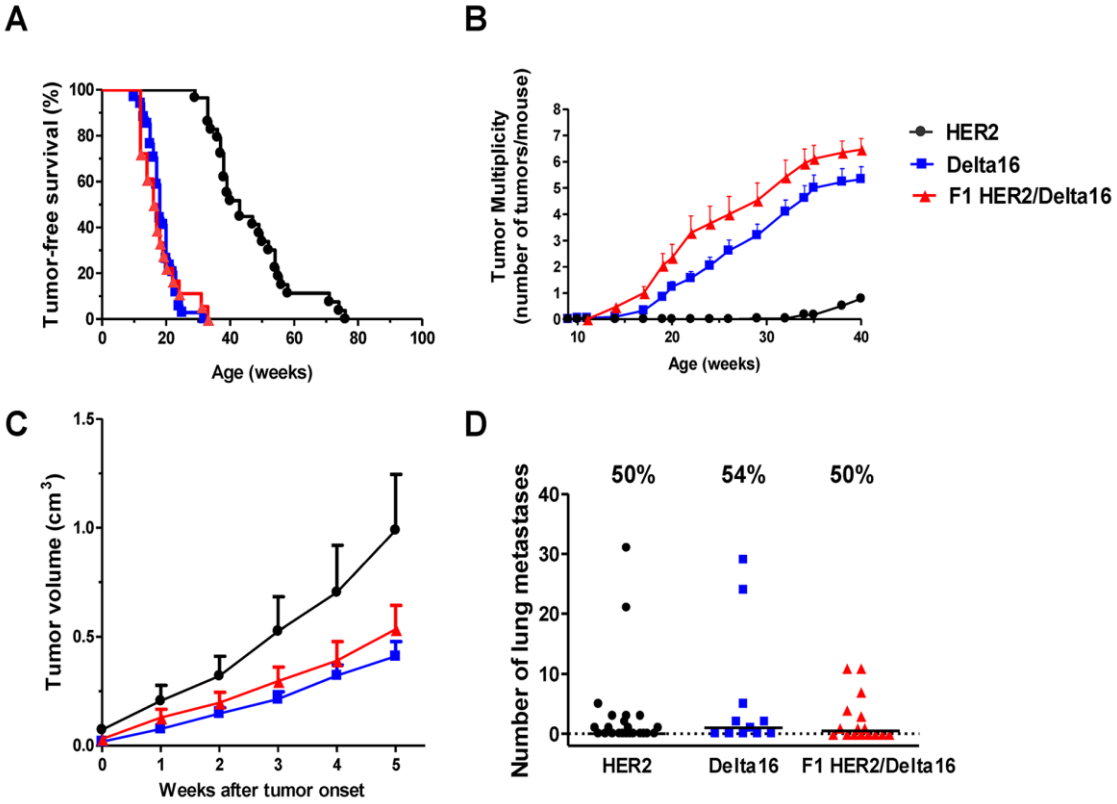

Picture 8. Comparison of spontaneous mammary carcinogenesis in FVBhuHER2 (black), Δ16-HER2 (blue) and F1 (red) mice (Palladini *et al.*, 2017). A: tumor-free survival. B: Tumor multiplicity. C: kinetics of tumor growth of the first tumor. C: number and incidence of lung metastases.

The level of expression of HER2 and Δ16 was evaluated in tumors and in preneoplastic mammary glands. Since no specific antibody for Δ16 is currently available, the expression of the two isoforms has been evaluated by Real Time qPCR. Both isoforms were expressed at intermediate levels in normal mammary tissue, compared to FVBhuHER2 and Δ16-HER2 tumors, but in F1 tumors the expression of the two isoforms were more heterogeneous. Most tumors expressed only Δ16 at high levels, whereas some tumors highly expressed both isoforms and only few had a high expression of the only full-length HER2 (picture 9).

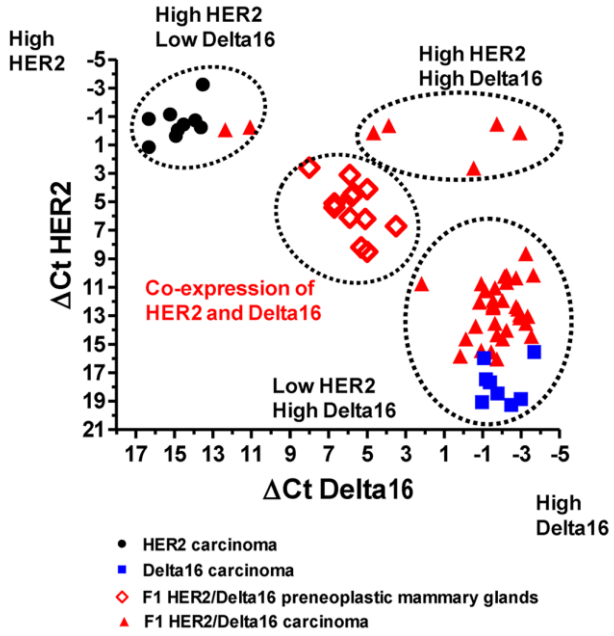

Picture 9. Expression of HER2 and Δ16 transcripts in F1 preneoplastic mammary glands and primary mammary carcinomas of FVBhuHER2 (black), Δ16-HER2 (blue) and F1 (red) mice (Palladini *et al.*, 2017).

Materials and Methods

1. Mice

FVBhuHER2 mice (Finkle *et al.*, 2004) were obtained from Genentech Inc. (South San Francisco, CA, USA). This line carries in heterozygosis the human full-length HER2 cDNA gene under the control of the Murine Mammary Tumor Virus (MMTV) promoter on a FVB background. HER2 gene heterozygosis was maintained by crossing FVBhuHER2 male mice with non-transgenic FVB female mice (purchased from Charles River Laboratories, Calco, Italy).

Δ16-HER2 mice (Marchini *et al.*, 2011) were kindly given by Prof. Augusto Amici (University of Camerino, Italy). This line carries in heterozygosis the human splice variant Δ16 cDNA gene under the control of MMTV promoter on a FVB background. Δ16 gene heterozygosis was maintained as described above for FVBhuHER2 model.

F1 mice, transgenic for both genes, were obtained in the Laboratory of Immunology and Biology of Metastases directed by Prof. Pier-Luigi Lollini (Department of Experimental, Diagnostic and Specialty Medicine, University of Bologna, Italy) by crossing Δ16-HER2 male mice with FVBhuHER2 female mice.

All the above-mentioned animals were bred in the animal facility of the Laboratory of Immunology and Biology of Metastases. Transgenic mice were screened by routine genotyping through PCR analysis (Finkle *et al.*, 2004; Marchini *et al.*, 2011).

All the experiments on FVB, FVBhuHER2, Δ16-HER2 and F1 mice were approved by the institutional review board of the University of Bologna, authorized by the Italian Ministry of Health and done according to Italian and European guidelines.

8-week-old female NOD-SCID mice were purchased from The Jackson Laboratories (Sacramento, CA, USA) and bred in the animal facility of the Instituto de Medicina Molecular (University of Lisbon, Portugal). The experiment performed on these mice was approved by the institutional review board of the Instituto de Medicina Molecular, authorized by the Portuguese National Authority for Animal Health (*Direcção-Geral de Alimentação e Veterinária*, DGAV) and done according to Portuguese and European guidelines.

2. Cell culture

Four murine mammary tumor cell lines were employed in this project: MAMBO89, MAMBO38, MAMBO43 and Mi6.

MAMBO89, MAMBO38 and MAMBO43 cell lines were obtained in the Laboratory of Immunology and Biology of Metastases. MAMBO89 cell line was established from a spontaneous mammary carcinoma of a FVBhuHER2 female mouse. MAMBO43 cell line was derived from a mammary carcinoma grown after the subcutaneous injection in a FVBhuHER2 female mouse of a FVBhuHER2 cell line established from a spontaneous FVBhuHER2 mammary carcinoma. MAMBO38 line was obtained and established *in vitro* from a tumor grown after the subcutaneous injection of MAMBO43.

MAMBO89 and MAMBO43 cell lines were stabilized in Dulbecco's Modified Eagle Medium (DMEM; Life Technologies, Milan) + 20% Fetal Calf Serum (FCS; Life Technologies, Milan, Italy), supplemented with Bovine Pituitary Extract 30 μg/ml (BPE; BD Biosciences, USA) and MITO Serum Extender 1:200 (BD Biosciences). MAMBO38 was stabilized in DMEM + 20% FCS.

Mi6 cell line was established from a spontaneous primary mammary carcinoma arisen in Δ16-HER2 model in the Laboratory of Dr. Elda Tagliabue and Dr. Serenella M. Pupa (Istituto Nazionale dei Tumori, Milan, Italy). Mi6 cell line was stabilized in MammoCult complete medium (StemCell Technologies, Canada) supplemented with 1% FCS (Life Technologies, Milan, Italy).

In the experiments reported in this thesis, MAMBO89 and Mi6 were cultured in MammoCult complete medium (StemCell Technologies, Canada) supplemented with 1% FCS, whereas MAMBO43 and MAMBO38 were cultured in DMEM + 20% FCS, supplemented with BPE 30 μg/ml and MITO Serum Extender 1:200.

Moreover, two humans breast cancer cell lines were employed: SKBr3 and MDA-MB-231. SKBr3 was derived from the pleural effusion of a metastatic HER2-positive mammary adenocarcinoma and was kindly given to the Laboratory of Immunology and Biology of Metastases by Dr. Serenella M. Pupa (Istituto Nazionale dei Tumori,

Milan, Italy). MDA-MB-231 was purchased by ATCC and was derived from the pleural effusion of a metastatic triple-negative mammary adenocarcinoma. Both cell lines were cultured in Roswell Park Memorial Institute (RPMI; Life Technologies, Milan, Italy) + 10% FCS (Life Technologies, Milan, Italy).

MDA-MB-231 for the *in vivo* experiment was kindly given to the Vascular Morphogenesis Lab at the Instituto de Medicina Molecular (Lisbon, Portugal) by Dr. Sérgio De Almeida (Chromatin and Epigenetics Lab, Instituto de Medicina Molecular, Lisbon, Portugal) and cultured in DMEM + 10% FCS supplemented with 1% non-essential amino acids (NEAA, Life Technologies).

All mediums were supplemented with penicillin 100 U/ml and streptomycin 100 μg/ml (Sigma-Aldrich, Milan, Italy). All cell lines were maintained at 37°C in a humidified 5% CO_2 atmosphere.

For the maintenance culture, cells were washed with Phosphate Buffer Saline (PBS; Life Technologies, Milan, Italy) and harvested by trypsin (0.05%)-EDTA (0.002%) treatment (Life Technologies, Milan, Italy). Cell number and viability were determined through erythrosine dye exclusion (Sigma-Aldrich, MO, USA) and cell count with a Neubauer chamber.

2.1 FACS analysis

FACS analysis was performed to evaluate the accumulation of doxorubicin and trastuzumab in tumor masses. After necropsy, tumors were minced with scissors, incubated for 5 minutes with trypsin-EDTA and passed through a 70 μm cell strainer (Becton Dickinson, Bedford, MA, USA) to obtain a homogeneous cell suspension.

Tumors treated or not with doxorubicin were directly analyzed by flow cytometry considering that doxorubicin emits in the red spectrum.

Tumors treated with trastuzumab were processed as described above as well. Before the incubation with the primary antibody, tumor suspensions were incubated with rat anti-mouse CD16/CD32 clone 2.4G2 antibody Fc block (1:100 dilution; BD PharMingen, San Diego, CA). Then, samples were incubated with the FITC-conjugated goat anti-human IgG secondary antibody (1:20 dilution; Invitrogen, CA, USA) or the

anti-human HER2 clone MGR2 primary antibody (1:100 dilution; Alexis Biochemical, Enzo Life Science, Lansen, Switzerland). Then, the samples incubated with MGR2 antibody were incubated with the secondary fluorescein-conjugated mouse monoclonal antibody (IgG AlexaFluor 488, 1:100 dilution; Life Technologies, Milan, Italy). All samples were finally suspended in ethidium bromide 1 μg/ml (Sigma-Aldrich, MO, USA) to stain dead cells.

For the detection of BCSCs, cells were harvested and incubated with a mixture of two conjugated antibodies: anti-mCD24-AF (M1/69) (diluted 1:10; Bio-Legend, San Diego, CA, USA) and anti-mCD44-PE (IM7) (diluted 1:10; Bio-Legend, San Diego, CA, USA).

Fluorescence intensity was determined through flow cytometry (Partec Cyflow Space, Sysmex). Analysis was performed with FCS Express 4 software (De Novo Software, Glendale, California, USA).

2.2 Tube Formation Assay

The Tube Formation Assay (Corning, NY, USA) consists in the seeding of cells on an appropriate scaffold made of Matrigel that allows the formation of vessel-like channels *in vitro*.

Matrigel (Corning, NY, USA) was thawed on ice at 4°C overnight. The day after, it was diluted to 10 mg/ml in cold serum-free DMEM (Life Technologies, Milan, Italy). 289 μl was added to a 24-well plate (Corning Life Sciences, USA) placed on ice, using pre-cooled tips and pipette. Plates were put at 37°C for 30-60 minutes to allow the Matrigel to solidify.

Meanwhile, MAMBO89, MAMBO43, MAMBO38, Mi6, SKBr3 and MDA-MB-231 cells were harvested and counted. 120,000 viable cells of each cell line were seeded in duplicate on Matrigel dropwise and incubated at 37°C in a humidified 5% CO_2 atmosphere.

16-18 hours later, the vascular-like structures formed were counted under the inverted microscope Diavert (Leitz, Milan, Italy) with 2.5x magnification, dividing them according to their dimensions using a graded ocular. Tubes with a diameter

smaller than 0.5 mm were considered as "small"; tubes with a diameter of between 0.5 and 1.5 mm were considered as "medium"; tubes with a diameter bigger than 1.5 mm were considered as "big".

Tubes were also photographed by using the Canon EOS600D camera (ISO200, exposition time 0.8 seconds).

2.2.1 Impact of anti-angiogenic drugs on tube formation

250,000 MDA-MB-231 viable cells and 500,000 MAMBO89 and Mi6 viable cells were seeded in 6-well plates (Corning Life Sciences, USA). The day after the seeding, the medium was replaced with:

- fresh medium
- DMSO 0.05% (Sigma-Aldrich, MO, USA)
- sunitinib at a final concentration of 5 μM (LC Laboratories, MA, USA)
- pazopanib at a final concentration of 5 μM (LC Laboratories, MA, USA)

After 24 hours of treatment, cells were harvested, counted, resuspended in fresh drug-free medium and seeded on Matrigel 10 mg/ml, placed on 24-well plates (Corning Life Sciences, USA) as previously described. 120,000 cells of each cell line for each treatment were seeded in duplicate.

18 hours later, the vascular-like tubes formed were counted dividing them by dimensions and photographed like described above.

2.3 In vitro sensitivity to anti-angiogenic drugs

250,000 MDA-MB-231 viable cells and 500,000 MAMBO89 and Mi6 viable cells were seeded in 6-well plates (Corning Life Sciences, USA). The day after the seeding, the medium was replaced with:

- fresh medium
- DMSO 0.05% (Sigma-Aldrich, MO, USA)
- sunitinib at a final concentration of 5 μM (LC Laboratories, MA, USA)
- pazopanib at a final concentration of 5 μM (LC Laboratories, MA, USA)

24, 48 and 72 hours after treatment, cells were harvested and counted to calculate the total number of cells per well and the percentage of growth over control.

MAMBO38 was tested both in adherent conditions and in 3D-culture. For the experiment in adherent conditions, cells were seeded in a 96-well plate (Corning Life Sciences, USA) at a concentration of 1,000 viable cells per well. The day after, fresh medium containing or not DMSO 0.1%, sunitinib 5 μM or pazopanib 5 μM was added to each well.

After 24 and 48 hours of treatment, WST-1 reagent (Sigma-Aldrich, MO, USA) was added to each well. WST-1 is a compound that is cleaved by mitochondrial dehydrogenases of viable cells into a compound that can be quantified by absorbance measurement. The absorbance was measured at 450 and 620 nm with an ELISA microreader (Tecan Systems) 60 minutes after the adding of WST-1 reagent.

For the 3D-culture experiment, MAMBO38 cells were suspended in DMEM + 20% FCS containing 0.33% agar (overlayer) and layered on a base of DMEM + 20% FCS containing 0.5% agar (underlayer) on a 24-well plate (Corning Life Sciences, USA) at a concentration of 1,000 cells per well. Drugs were added both to underlayer and to overlayer:

- no drugs
- DMSO 0.05% (Sigma-Aldrich, MO, USA)
- sunitinib at a final concentration of 5 μM (LC Laboratories, MA, USA)
- pazopanib at a final concentration of 5 μM (LC Laboratories, MA, USA)

Plates were maintained at 37°C in a humidified 5% CO_2 atmosphere. Colony growth was monitored weekly and determined by counting at 31.25x magnification with Diavert microscope (Leitz, Milan, Italy) after 2 weeks from seeding. Colonies were arbitrary defined as every cell aggregate bigger than 1 mm. The effectiveness of the drugs was assessed as percentage of colonies grown over control.

3. Preclinical models

Virgin female mice were used in this thesis. Experimental animals were monitored weekly by palpation and tumor dimensions were measured with calipers. Masses with a mean diameter exceeding 3 mm were considered tumors.

Mice were euthanized when tumor burden was equivalent to 10% of body mass. Tumor volume was calculated as $(\pi/6)$ $(\sqrt{ab})^3$, where a = maximal tumor diameter and b = maximal tumor diameter perpendicular to a.

At necropsy, tumor masses were collected for molecular and histological analyses.

3.1 Histological analysis

The histological analyses presented in this thesis have been performed in collaboration with Prof. Manuela Iezzi and Dr. Alessia Lamolinara from Aging Research Center, University "G. D'Annunzio" of Chieti, Italy.

Autochthonous tumors from FVBhuHER2, Δ16-HER2 and F1 mice, and from F1 MDI models were analyzed by immunofluorescence and by hematoxylin-eosin staining. Hematoxylin-eosin staining was performed on samples fixed in 10% neutral buffered formalin (Sigma-Aldrich, MO, USA) and embedded into paraffin. 5 μm slides were cut and stained with Hematoxylin (BioOptica, Milan, Italy) and Eosin (BioOptica, Milan, Italy) for histological examination. Immunofluorescence was performed on samples fixed in 4% PFA and frozen in a cryo-embedding medium (OCT, BioOptica, Milan, Italy). 4-6 μm cryostat sections were air-dried, fixed in ice-cold acetone for 10 minutes and incubated with the following primary antibodies: rat monoclonal anti-CD31 (550274, BD Pharmingen, BD Biosciences, San Jose, CA, USA) mixed with rat monoclonal anti-CD105 (550546, BD Pharmingen), and rabbit polyclonal anti-NG2 (ab5320, EMD Millipore, Billerica, MA, USA), followed by secondary antibodies conjugated with Alexa 546 and Alexa 488 (Thermo Fisher Scientific), respectively. Nuclei were stained with DRAQ5 (Alexis, Life Technologies, Monza, Italy). The mixture of antibodies against CD31 and CD105 was used to increase the probability of

staining all the tumor endothelium. The same secondary antibody was used because there was not the need of distinguishing the presence and the quantity of each single protein on cell surface.

Image acquisition was performed using Zeiss LSM 510 META confocal microscope. The number and area of vessels were evaluated on the digital images of 3-5 tumors per group (five fields per tumor at 200x microscope) by two different pathologists, independently and in a blind fashion. Vessels area (in pixels) was evaluated with Adobe Photoshop by selecting vessels with the lasso tool and reporting the number of pixels indicated in the histogram window.

FVBhuHER2 and Δ16-HER2 MDI tumors treated with vehicle or anti-angiogenic drugs were analyzed by immunohistochemistry. Tumors were fixed in 10% neutral buffered formalin (Sigma-Aldrich, MO, USA) and embedded into paraffin. 5 μm slides were cut. The samples were then deparaffinized, serially rehydrated and, after the appropriate antigen retrieval procedure, stained with anti-mouse CD31 (DIA-310, Dianova GmbH, Hamburg, Germany), followed by an appropriate anti-mouse secondary antibody (Jackson ImmunoResearch, West Grove, PA, USA). Immunoreactive antigens were detected using streptavidin peroxidase (Thermo Fisher Scientific, Waltham, MA, USA) and the Vulcan Fast Red Chromogen (Biocare Medical, Concord, CA, USA). After chromogen incubation, slides were counterstained in Hematoxylin (BioOptica) and images were acquired by Leica DMRD optical microscope (Leica, Wetzlar, Germany). The vascularization was analyzed by evaluating CD31-positive endothelial cells on digital images of 4-5 tumors per group, using Adobe Photoshop, by selecting vessels with the Magic Wand tool and reporting the number of pixels indicated in the histogram window with respect to the total area. Tumor necrosis was evaluated with Adobe Photoshop by selecting the necrosis area with the Lasso tool and reporting the number of pixels indicated in the histogram window as percentage of the total tumoral area.

3.2 Mouse-Derived Isografts

Fragments of autochthonous F1 mammary tumors were serially implanted in the fourth left mammary fat pad of 5-17-week-old FVBhuHER2 transgenic female mice. Tumors grown from serial grafts of fragments from two F1 tumors (referred to as MoMo1 and MoMo2 respectively) were harvested for molecular investigation and also immediately implanted into other mice.

Tumors from representative passages have been analyzed from the histological point of view as described before. In particular, passage I and IV of MoMo1, and passage III and V of MoMo2 have been examined. The number and the mean area of the vessels have been also quantified.

3.3 Evaluation of doxorubicin and trastuzumab accumulation

To evaluate drug delivery in tumors, a first experiment was performed exploiting the fluorescent properties of the chemotherapeutic drug doxorubicin. 7-15-week-old female FVB mice were subcutaneously injected with $5x10^6$ viable MAMBO89 cells or with $5x10^6$ viable Mi6 cells, cultured as described above. Tumor growth were monitored weekly and tumor dimensions were measured with a caliper.

When tumors induced by the injection of MAMBO89 and Mi6 cells exceeded 1 cm^3, mice were divided into treated and untreated mice. Treated mice received an intravenous injection of doxorubicin (Accord, Milan, Italy) 16 mg/kg, diluted in PBS.

Later the delivery of trastuzumab was examined. Three FVBhuHER2, bearing one tumor each, and two Δ16-HER2 mice, bearing one and two mammary carcinomas respectively, received an intraperitoneal injection of trastuzumab (Hoffmann-La Roche, Basel, Switzerland) 4 mg/kg, diluted in saline.

In both experiments, mice were euthanized 2 hours after drug injection and tumors were collected to be dissociated mechanically and enzymatically. Tumor cell suspensions were then analyzed by flow cytometry.

3.4 *In vivo* sensitivity to anti-angiogenic and anti-HER2 drugs

For the sensitivity to sunitinib and pazopanib according to HER2 and Δ16, fragments of five FVBhuHER2 or nine Δ16-HER2 autochthonous tumors were injected in 15 6-10-week-old FVB female mice in the fourth left mammary fat pad.

Tumor growth was monitored weekly for all the duration of the experiment. When tumors became palpable, mice were divided into three groups to receive sunitinib 60 mg/kg, pazopanib 100 mg/kg or the vehicle in which the drugs were dissolved (sterile methocel 0.5% + tween80 0.4% in tap water). Drugs were administered for four weeks, five days a week.

For the combined therapy experiment, twenty-five tumor-free FVBhuHER2 female mice were orthotopically injected in the fourth left mammary fat pad with fragments from six autochthonous mammary carcinomas of FVBhuHER2 mice to create a MDI model. Tumor growth was monitored weekly, and when the tumors became palpable, the animals were divided into five experimental groups: vehicle of sunitinib, sunitinib, trastuzumab, sunitinib and then trastuzumab, trastuzumab and then sunitinib.

Sunitinib was administered at a dose of 60 mg/kg in methocel 0.5% + tween80 0.4% in tap water for four weeks, five times a week. Trastuzumab was administered intraperitoneally at a dose of 4 mg/kg in saline, twice a week for four weeks. In the combined setting, four weeks of treatment with a drug were followed by four weeks of treatment with the other drug.

In both experiments, mice were sacrificed one week after the end of the treatment. Necropsy was performed, and tumors were collected for molecular and histological analyses.

4. Gene expression analysis

To explore the molecular differences between the tumor angiogenesis in FVBhuHER2, Δ16-HER2 and F1 models, gene expression analysis was performed on tumors. Spontaneous mammary carcinomas and MDI tumors have been collected and immediately frozen in liquid nitrogen to preserve RNA integrity.

4.1 Real Time qPCR

Frozen tissue samples were first disrupted by using the gentleMACS Octo Dissociator (Miltenyi Biotech GmbH, Bergisch Gladbach, Germany) with the program RNA_02. RNA was extracted according to the TRIzol protocol (Total RNA Isolation Reagent; Life Technologies, Milan, Italy).

The concentration and purity of RNA was determined according to the protocol of the Qubit RNA Assay Kit (Life Technologies, Milan, Italy).

1 μg of total RNA was reverse transcribed using iScript cDNA Synthesis Kit (Bio-Rad Laboratories, CA, USA). The synthetized cDNA was diluted 1:4 with DNase/RNase free water.

10 ng of cDNA was amplified by using Sso Advanced SyBR Green Supermix (Bio-Rad Laboratories, CA, USA) reagents. Gene expression was analyzed by Real Time qPCR using Thermal Cycler CFX96 (Bio-Rad Laboratories, CA, USA).

Evaluated target genes were: human HER2 and Δ16, and mouse KDR, FGF2, MCAM, PECAM1, PTGS2 and VEGF-A. mRNA expression levels were normalized to mouse GAPDH (glyceraldehyde 3-phosphate dehydrogenase) or mouse TBP (TATA box binding protein), as endogenous reference genes.

HER2, Δ16, GAPDH and TBP primers were purchased from Life Technologies (table III for primer sequences) and were used at a final concentration of 200 nM. KDR, FGF2, MCAM, PECAM1, PTGS2 and VEGF-A primers were purchased from Bio-Rad Laboratories and were used at a final dilution of 1X (table IV for primer references).

The steps of amplification for GAPDH were: 95°C for 30 seconds and then 40 cycles including 5 seconds at 95°C and 15 seconds at 60°C. For HER2, Δ16 and TBP, the

steps of amplification were: 95°C for 30 seconds and then 40 cycles including 5 seconds at 95°C and 15 seconds at 65°C. The steps of amplification for angiogenesis-related genes were: 95°C for 30 seconds and then 40 cycles including 5 seconds at 95°C and 30 seconds at 60°C. A default melting curve program was used to obtain the dissociation curve for each gene.

The analysis was performed using Bio-Rad CFX Manager 3.1 software. For relative quantification, ΔCt method was used:

$$\Delta Ct_{\,gene} = Ct_{\,gene} - Ct_{\,housekeeping}$$

Gene	Sequence (5′- 3′)
Full-length human HER2 (Mitra *et al.*, 2009)	For: GTGTGGACCTGGATGACAAGGG Rev: GCTCCACCAGCTCCGTTTCCTG
Human Δ16 (Mitra *et al.*, 2009)	For: CACCCACTCCCCTCTGAC Rev: GCTCCACCAGCTCCGTTTCCTG
Mouse GAPDH	For: GCTCACTGGCATGGCCTTC Rev: CCTTCTTGATGTCATCATACTTGGC
Mouse TBP (Bieche *et al.*, 2014)	For: CCCTTGTACCCTTCACCAATGAC Rev: TCACGGTAGATACAATATTTTGAAGCTG

Table III: primer sequences from Life Technologies, Milan, Italy.

Gene	Reference
FGF2 (b-FGF)	qMmuCED0049098
KDR (VEGFR2)	qMmuCID0005890
PECAM1 (CD31)	qMmuCID0005317
MCAM (CD146)	qMmuCID0023780
PTGS2 (COX-2)	qMmuCED0047314
VEGF-A	qMmuCED0040260

Table IV: primer references from Bio-Rad Laboratories, CA, USA.

4.2 PCR Array

RNA has been extracted, purified and quantified from four FVBhuHER2 mammary tumors and four Δ16-HER2 ones following the protocol of the Aurum Total Fatty and Fibrous Tissue Kit (Bio-Rad Laboratories, CA, USA).

After mRNA quantification and cDNA synthesis as described above, PrimePCR Angiogenesis (SAB target list) Array was used (Bio-Rad Laboratories, CA, USA). This PCR Array analyzes the expression of 82 genes involved in angiogenesis by Real Time qPCR. It consists of a 96-well qPCR plate which includes different specific primers in each well. Therefore, each sample was plated into one PCR Array plate and Real Time qPCR has been performed using Sso Advanced SyBR Green Supermix.

ΔCt was calculated as described before, using as reference the six housekeeping genes included in the PCR Array (actin-β, B2M, GUSB, TBP, HPRT1 and GAPDH). The analysis of the results has been performed to identify all the genes that were up- or down-regulated in FVBhuHER2 tumors in comparison to Δ16-HER2 ones, considering all those genes with a higher fold change than 4, calculated using Bio-Rad CFX Manager 3.1 software.

5. *Protein analysis*

5.1 Tumor lysis and quantification of proteins

Frozen tumor tissues of two FVBhuHER2 tumors and two Δ16-HER2 ones were completely immersed in lysis buffer consisting of Novagen PhosphoSafe Extraction Reagent (EMD Millipore, MA, USA) plus phosphatase and protease inhibitors (Sigma-Aldrich, MO, USA).

Samples were dissociated and homogenized by gentleMACS Octo Dissociator (Miltenyi Biotech GmbH, Bergisch Gladbach, Germany) and then incubated for 10 minutes at room temperature. Nuclei were removed by centrifugation at 12,000 RCF at 4°C for 15 minutes, and protein concentration in the supernatants was determined by

DC Protein Assay (Bio-Rad Laboratories, CA, USA) using bovine serum albumin as standard.

5.2 Antibody Array

The Proteome Profiler Mouse Angiogenesis Array Kit (R&D Systems Inc, MN, USA) is an Antibody Array that consists in the analysis of the amount of 53 specific proteins involved in angiogenesis by using a membrane on which a collection of capture antibodies is spotted in duplicate.

Two FVBhuHER2 tumors and two Δ16-HER2 ones were compared with Antibody Array analysis. To be sure that the samples were homogenous between each other, a Western Blot for actin was previously performed.

For each sample, 200 μg of tumor lysate were mixed with a cocktail of biotinylated detection antibodies. These mixtures were added on the membrane to allow the binding of the proteins to the capture antibodies. Streptavidin-horseradish peroxidase and detection reagents were added to produce a chemiluminescent signal where the proteins were captured by the antibodies, with an intensity that is proportional to its amount in the lysate. This system of chemiluminescent detection of protein presence is therefore similar to a Western blot.

Protein presence was therefore revealed by chemiluminescence reaction and images of the membranes were taken using the ChemiDoc Imaging System (Bio-Rad Laboratories, CA, USA) at the Laboratory of Prof. Gabriella Campadelli-Fiume of the University of Bologna. An exposition time of 630 seconds was used for all membranes.

The calculation of spot volume was performed on the scanned images by using TotalLab gel analysis software (TotalLab Ltd, UK). Percent fold change of FVBhuHER2 proteins compared to Δ16-HER2 ones was calculated as follows:

$$\left(\frac{Spot\ volume_{FVBhuHER2}}{Spot\ volume_{\Delta 16-HER2}} * 100\right) - 100$$

The mean of results of FVBhuHER2 and Δ16-HER2 tumors analyses was calculated. The differences in protein presence between FVBhuHER2 tumors and Δ16-HER2 ones with a percent fold change higher than 25 and/or with a *p* value less than 0.05 were considered.

6. Statistical analysis

Student's *t* test was used to analyze and compare the data presented in this thesis. The comparisons were considered statistically different with a *p* value less than 0.05.

Results

1. HER2 and vascular phenotype

The proto-oncogene HER2 is over-expressed in 15-20% of human breast cancers. In about half of them a splicing isoform lacking exon 16, and therefore called Δ16, is present as well.

Preclinical models that are transgenic for full-length HER2 and/or Δ16 have been developed. These mouse models are characterized by the spontaneous development of multiple mammary carcinomas in female mice. Carcinogenesis occurs earlier in Δ16-HER2 and in double-transgenic (F1) mice than in FVBhuHER2 mice (Castagnoli *et al.*, 2014; Palladini *et al.*, 2017). F1 tumors could express at high levels both isoforms or only one (Palladini *et al.*, 2017).

The autochthonous tumors developed on FVBhuHER2, Δ16-HER2 and F1 mice were macroscopically different. The mammary tumors of FVBhuHER2 mice were often hemorrhagic, reddish and spongy. Tumors of Δ16-HER2 mice were typically whitish and had a solid texture, with rare and small hemorrhagic areas in some cases. The appearance of F1 tumors was more heterogeneous, with a prevalence of Δ16-HER2-like phenotype (Balboni's MSc thesis, 2014; Palladini *et al.*, 2017).

To investigate whether the differences observed did not only concern the macroscopic appearance, tumors from the three mouse models were collected to be analyzed from the histological and molecular point of view.

The effect of modulation of HER2 expression on vascularization was also explored through an *in vivo* model that is characterized by the stable expression of Δ16 and by the fluctuation of the levels of HER2 expression.

Lastly, the vasculogenic ability of HER2- and/or Δ16-expressing tumor cells was studied *in vitro*, following the protocol of the Tube Formation Assay.

1.1 HER2 isoforms and vascular architecture of mammary tumors

The tumors of FVBhHER2, Δ16-HER2 and F1 mice were not only different in the macroscopic appearance, but they also differed microscopically. The histological

analysis of the tumors has been performed in the laboratory of Prof. Manuela Iezzi of the Aging Research Center, "Gabriele D'Annunzio" University, Chieti, Italy.

Hematoxylin-eosin staining evidenced the presence of few large vessels or vascular *lacunae* in tumors of FVBhuHER2 (figure 1A). On the other hand, Δ16-HER2 carcinomas were characterized by numerous small endothelium-lined vessels (figure 1B). In F1 tumors both phenotypes could be found (figure 1C).

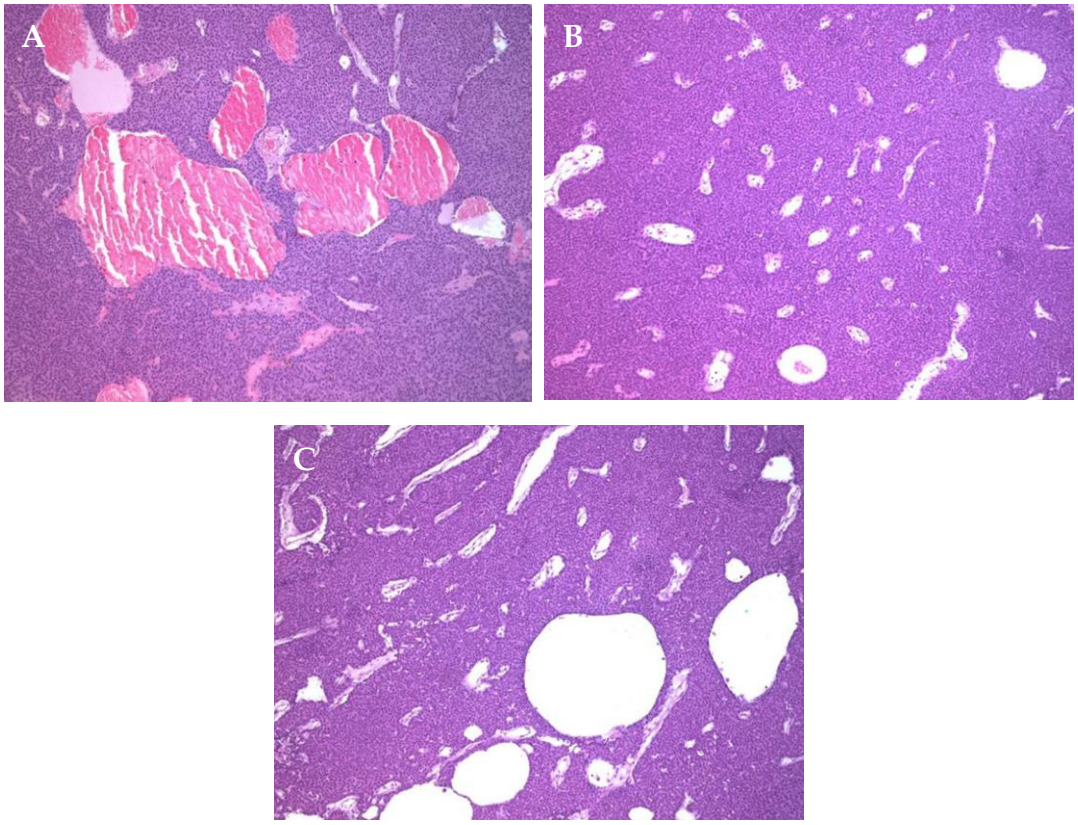

Figure 1. Different vascular patterns in transgenic mammary carcinomas of FVBhuHER2 (A), Δ16-HER2 (B) and F1 (C) mice. Hematoxylin-eosin staining are shown, with a 100x magnification (Palladini *et al.*, 2017).

To better characterize the vascular architecture and the composition of blood vessels, immunostaining of endothelial cells and pericytes has been performed. Endothelium has been labeled by using anti-CD31 and anti-CD105 antibodies. An anti-NG2 antibody was used to label pericytes (figure 2).

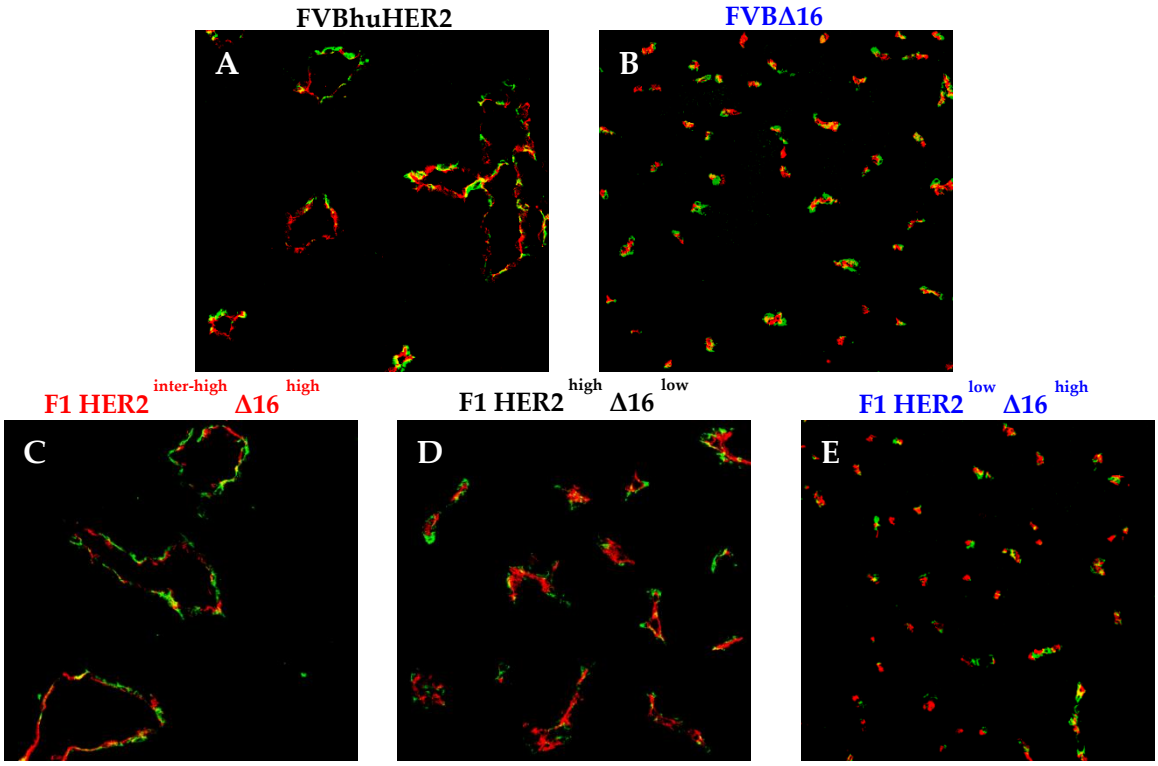

Figure 2. Vascular phenotype of FVBhuHER2 (A), Δ16-HER2 (B) and F1 (C-D-E) tumors. F1 tumors have been divided according to the levels of expression of HER2 and Δ16. Primary anti-CD31 and anti-CD105 antibodies have been used to stain endothelium (in red). Primary anti-NG2 antibody has been used to label pericytes (in green). Images obtained using a confocal microscope. Magnification: 200x.

As it was observable in hematoxylin-eosin stained samples, FVBhuHER2 tumors were characterized by few large vessels (figure 2A). On the contrary, the vascular phenotype of Δ16-HER2 was characterized by many small vessels (figure 2B).

To investigate the role of the two isoforms in determining the vascular pattern, F1 tumors have been examined considering that HER2 and Δ16 can be co-expressed or only one isoform can be highly expressed. Tumors that expressed both isoforms (figure 2C) or that expressed only full-length HER2 at high levels (figure 2D) showed a vascular pattern similar to the one typical of FVBhuHER2 mice, with few large vessels. On the other hand, F1 tumors with high expression of Δ16 and a low expression of HER2 (figure 2E) showed many small vessels, as it is characteristic of Δ16-HER2 tumors.

The quantification of the mean area and the number of vessels has been performed (figure 3). The analysis confirmed that the vessels of FVBhuHER2 tumors

are statistically fewer than the vessels of Δ16-HER2 tumors, but their mean area is bigger.

Analyzing the characteristics of the vessels among the F1 tumors according to their relative expression of HER2 and Δ16, it was confirmed that F1 $HER2^{high}$ $\Delta16^{low}$ and F1 $HER2^{high}$ $\Delta16^{high}$ have larger and fewer vessels than F1 $HER2^{low}$ $\Delta16^{high}$ tumors, therefore resembling the features of FVBhuHER2 and Δ16-HER2 tumor respectively.

Thus, it is possible to conclude that when full-length HER2 is expressed at high levels, regardless of the level of expression of Δ16, the vessels are larger and fewer. When only Δ16 is highly expressed, the vessels are smaller and more numerous. In this sense, the full-length form of HER2 seems to have a dominant role in determining tumor vascularization in comparison to Δ16.

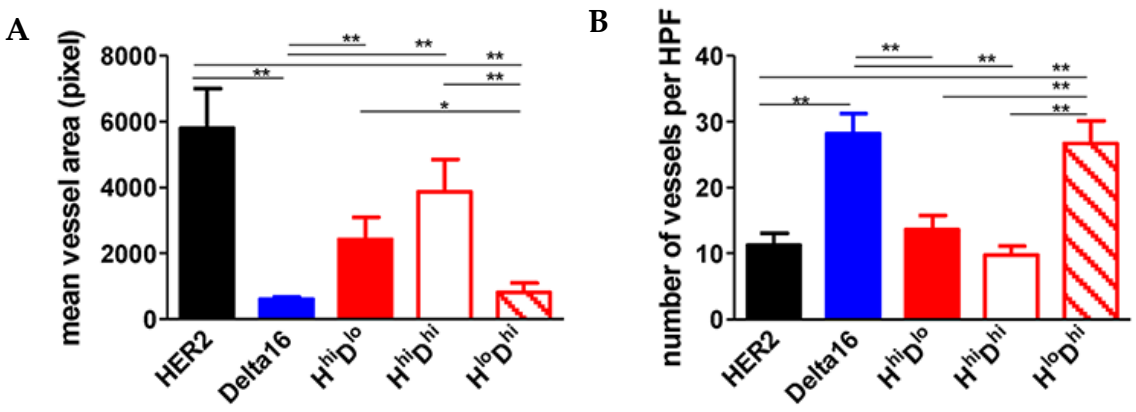

Figure 3. Quantification of the vascular area (A) and number (B) of vessels per high power field (HPF) ×200, in FVBhuHER2 (in black), Δ16-HER2 (in blue) and F1 (in red) tumors. Each bar represents the mean and SEM of five×200 fields for each tumor (n=3-5). Statistical analysis (Student's *t* test): *=$p<0.05$, **=$p<0.01$.

1.2 Modulation of HER2 and vascular phenotype

To better understand the role of HER2 and its splice isoform Δ16 in regulating tumor vascularization, the vascular pattern has been analyzed using an *in vivo* model of modulation of the expression of full-length HER2.

This model has been obtained through serial *in vivo* transplants of two F1 tumors in syngeneic immunocompetent mice. These mouse-derived isograft (MDI) models have been called MoMo1 and MoMo2.

The tumors of these models have been analyzed by Real Time qPCR to determine the kinetics of expression of full-length HER2 and Δ16. In particular, MoMo1 was characterized by a high expression of both isoforms at the first two passages, and then the expression of full-length HER2 decreased. The expression of Δ16 remained stable over serial passages (figure 4A). MoMo2, on the contrary, showed a high expression of Δ16 and a low expression of HER2 at the beginning, and later the levels of the full-length form progressively increased (figure 4B).

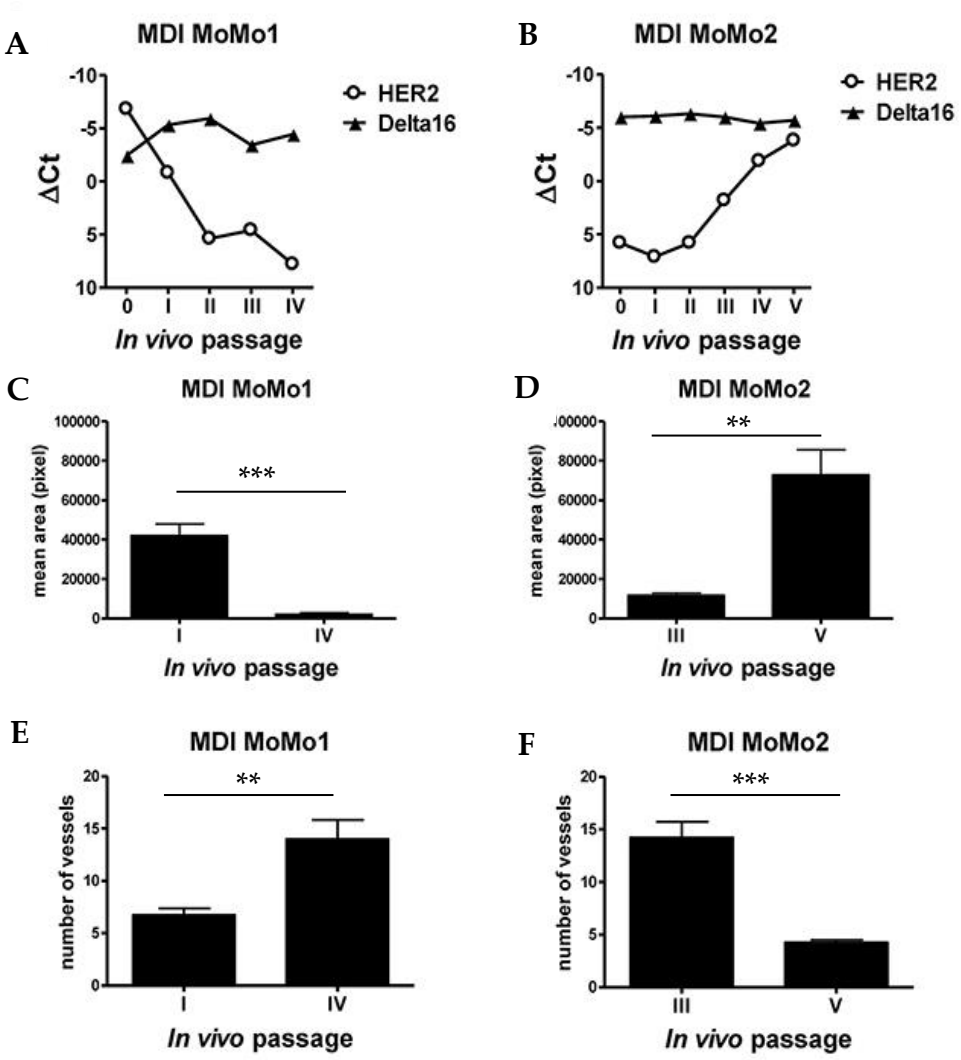

Figure 4. Kinetics of expression of HER2 isoforms and of the vascular phenotype during serial passages of F1 tumors (MDIs). A-C-E: model MoMo1. B-D-F: model MoMo2. A-B: Expression of full-length HER2 (white rounds) and Δ16 (black triangles) obtained by Real Time qPCR. Housekeeping gene: mTBP. C-D and E-F: respectively area and number of the vessels of the tumors of two different *in vivo* passages of MoMo1 and MoMo2 models, measured by CD31 immunostaining; each bar represents the mean and the SEM of four×200 fields for each tumor (n=3-5). Statistical analysis (Student's t test): **=p<0.01; ***=p<0.001.

Similarly to what done for autochthonous mammary carcinomas, the tumors of different passages from both MDIs have been analyzed. The passages were chosen to represent different points of the kinetics of HER2 expression.

In MoMo1 models, high levels of full-length HER2 observed at the first passage was associated with a vascular pattern with few large vessels, as well as FVBhuHER2 tumors. The subsequent loss of HER2 expression observed at the fourth passage, was accompanied by the acquisition of the Δ16-HER2-like phenotype, with an increased number of smaller vessels (figure 4C and 4E).

In model MoMo2, that had a specular kinetics of expression of full-length HER2 in comparison with MoMo1, an opposite trend was observed: at the third passage, when only Δ16 was expressed at high levels, the tumors had many small vessels, but at the fifth passage the higher HER2 levels caused the increase of the mean area of the vessels (figure 4D) and the decrease of their number (figure 4F).

These results confirmed the dominant role of HER2 in affecting tumor vasculature, even in dynamic models such as the MDIs that have been developed. Moreover, the direct responsibility of HER2 on vascularization has been confirmed.

1.3 Expression of angiogenesis-related genes

In order to study the molecular profile associated with the different vascular patterns and the expression of full-length HER2 and Δ16, the autochthonous mammary tumors developed on FVBhuHER2, Δ16-HER2 and F1 mice have been analyzed from the molecular point of view. As done before, F1 tumors have been divided into three subgroups according to their levels of expression of HER2 and Δ16.

As a preliminary test, six angiogenesis-related markers have been taken into consideration (figure 5): VEGFR2 (KDR), FGF2 (bFGF), MCAM (CD146), PECAM1 (CD31), PTGS2 (COX-2) and VEGF-A.

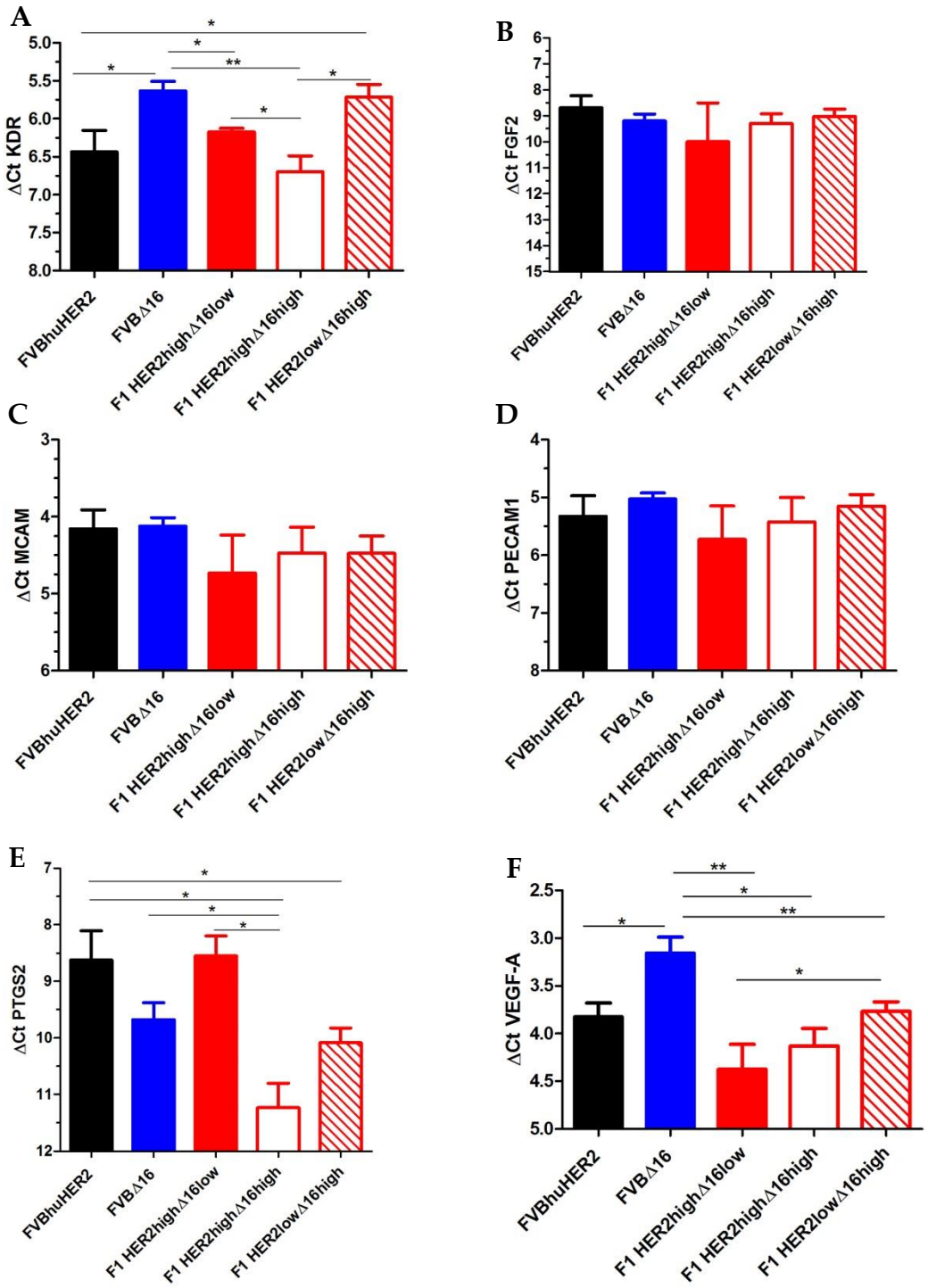

Figure 5. Expression of angiogenesis-related genes by Real Time qPCR in FVBhuHER2 (black bars), Δ16-HER2 (blue bars) and F1 (red bars) tumors. A: KDR (VEGFR2). B: FGF2 (bFGF). C: MCAM (CD146). D: PECAM1 (CD31). E: PTGS2 (COX-2). F: VEGF-A. Each bar represents the mean and the SEM of ΔCt for each tumor (n=3-19). Housekeeping gene: mGAPDH. Statistical analysis (Student's t test): *=p<0.05; **=p<0.01. Borderline statistical comparisons (PTGS2): Δ16 vs. F1 HER2^{high}Δ16^{low} p=0.090; F1 HER2^{high}Δ16^{low} vs. F1 HER2^{low}Δ16^{high} p=0.091.

The expression of VEGFR2 was lower in FVBhuHER2 tumors than in Δ16-HER2 ones. Among F1 tumors, those which highly express HER2 showed a lower expression of VEGFR2 than F1 HER2^{low} Δ16^{high} tumors. The presence of high levels of Δ16 did not seem to influence the expression of VEGFR2, since the bar corresponding to the F1 tumors that co-express the two isoforms is the lowest one (figure 5A).

In general, FGF2 was poorly expressed by all tumors. Moreover, no statistical difference in expression was detected among the different tumors (figure 5B).

MCAM and PECAM1, which are endothelial markers, were more expressed than FGF2 but no difference was found between the levels of expression of the five subgroups of tumors (figure 5C and 5D respectively).

On the contrary, COX-2 expression showed some differences that seem to be negatively correlated with the high expression of Δ16. In particular, Δ16-HER2 tumors showed a higher expression of COX-2 than FVBhuHER2 ones. Among F1 subgroups, in F1 HER2^{high} Δ16^{high} and F1 HER2^{low} Δ16^{high} tumors the expression of COX-2 is lower than in F1 HER2^{high} Δ16^{low} (figure 5E).

VEGF-A is highly expressed by all tumors, but some statistical differences have been detected. The expression of this gene is the highest in Δ16-HER2 tumors, where the expression of HER2 is completely absent. F1 tumors, regardless of the expression of the two isoforms, showed a level of expression comparable to the one of FVBhuHER2 tumors. In this sense, even low levels of HER2 seem to be sufficient to keep lower the expression of VEGF-A (figure 5F).

The analysis of the molecular differences between the vascular patterns sustained by HER2 and its isoform Δ16 has been extended to a higher number of angiogenesis-related markers using tools such as PCR arrays and antibody arrays.

The first technique analyzes the gene expression by Real Time qPCR. It consists of a qPCR plate which contains specific different primers in each well.

Ten genes were found to be more expressed in FVBhuHER2 tumors, three of which reached the statistical significance (i.e. Angiopoietin-1, Csf3 and CXCL5; figure 6A). On the other hand, four genes were more expressed in Δ16-HER2 tumors, but only Leptin reached the statistical significance (figure 6B).

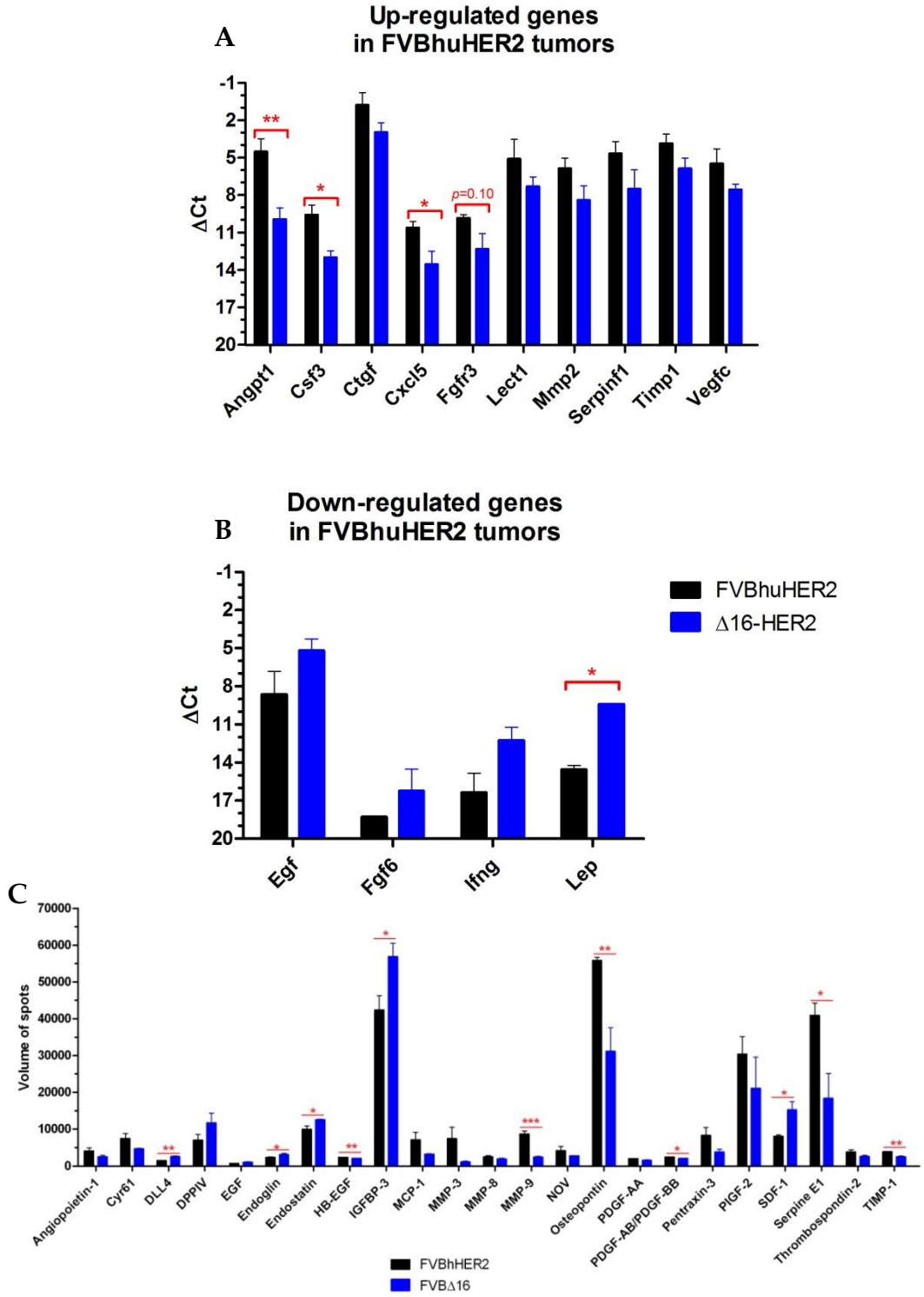

Figure 6. Expression of angiogenesis-related genes in FVBhuHER2 (black bars) and Δ16-HER2 (blue bars) tumors. A and B: up- and down-regulated genes in FVBhuHER2 tumors compared to Δ16-HER2 ones, respectively (cut-off: fold change > 4) obtained by PCR array. Each bar represents the mean and the SEM of the ΔCt of each tumor (n=4 for each group), obtained subtracting the mean Ct of a collection of six housekeeping genes to the Ct of each tumor. C: amount of angiogenesis-related proteins obtained by antibody array (cut-off: fold change > 25 and/or statistical significance reached). Each bar represents the mean and the SEM of the volumes of the two spots for each protein (n=2 for each group). Statistical analysis (Student's t test): *=p<0.05; **=p<0.01; ***=p<0.001.

The second approach consists in the analysis of the amount of specific proteins using a membrane on which a collection of capture antibodies is spotted in duplicate.

Twenty-three proteins were identified with a fold change higher than 25 and/or a statistically significant difference between FVBhuHER2 and Δ16-HER2 tumors. Eleven proteins were statistically different between the two groups of tumors: delta-like ligand 4 (Dll-4), Endoglin, Endostatin, HB-EGF, IGFBP-3, MMP-9, Osteopontin, PDGF-AB/BB, stromal cell-derived factor 1 (SDF-1), Serpine E1 and TIMP-1 (figure 6C).

Comparing the results obtained from these two techniques, three markers were in common: Angiopoietin-1, EGF and TIMP-1. These might be good candidate genes to further explore the differences in vascularization driven by the two isoforms.

1.4 Distribution of drugs

The different patterns of vascularization induced by the two isoforms were analyzed from the functional point of view, in order to explore whether there was a difference in the delivery of therapeutic agents into the tumor mass.

A first approach consisted in the cytofluorimetric analysis of the accumulation of doxorubicin in tumors. Doxorubicin is a chemotherapeutic drug with fluorescent properties that can be detected and measured by flow cytometry.

The two cell lines MAMBO89 and Mi6, derived from an FVBhuHER2 mammary carcinoma and a Δ16-HER2 tumor respectively, were injected subcutaneously in non-transgenic FVB female mice. When the tumors reached a volume higher than 1 cm^3, that was 8 and 5 weeks after injection respectively, the mice were divided into control and treated group, and doxorubicin 16 mg/kg was injected intravenously in the latter. All the mice were euthanized two hours after the treatment and the tumors were collected to obtain cell suspension to be analyzed by flow cytometry.

The analysis of the results has been performed by calculating the fluorescence ratio between the medians of intensity of treated and untreated mice. Δ16-expressing tumors significantly accumulated more doxorubicin than HER2-espressing ones (figure 7A), thus indicating that the different vasculatures sustained by HER2 and Δ16 have a functional impact on drug delivery.

To validate these results, we also evaluated the delivery of the HER2-targeted drug trastuzumab. Since it is a humanized antibody, an anti-human IgG antibody was used to measure the amount of the drug inside the tumors by flow cytometry.

Three FVBhuHER2 mice, bearing one mammary tumor each, and two Δ16-HER2 mice, bearing one and two tumors respectively, were injected with trastuzumab 4 mg/kg intraperitoneally. Like the experiment with doxorubicin, mice were sacrificed after two hours to collect the tumors, and tumor suspensions were analyzed by flow cytometry. The median of fluorescence intensity of each tumor was normalized on the expression of total HER2.

The results obtained with this approach confirmed the outcome of the previous experiment: Δ16-HER2 tumors accumulated more trastuzumab than FVBhuHER2 ones, even if statistical significance was not reached (figure 7B).

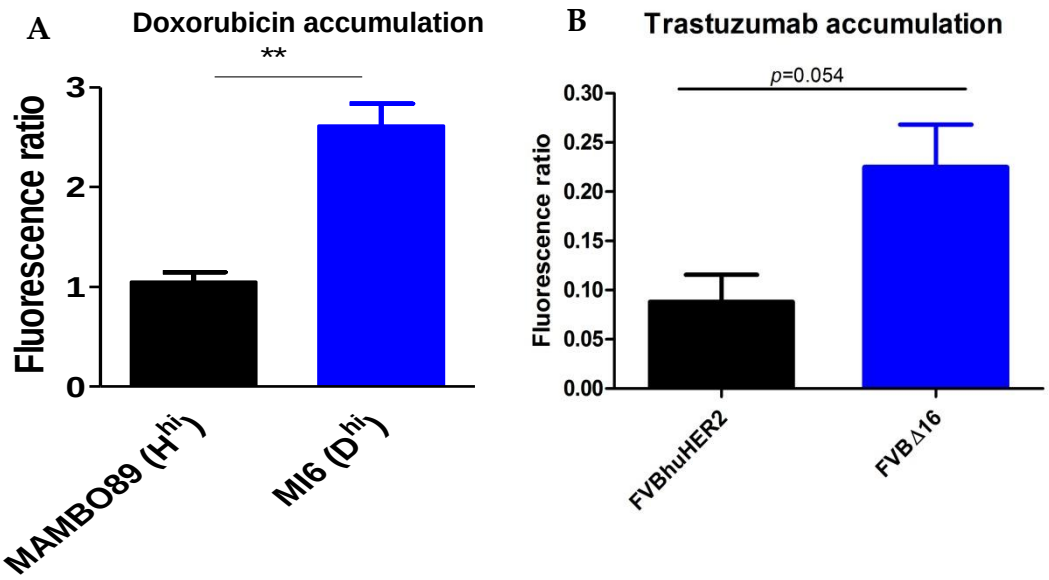

Figure 7. Drug accumulation in FVBhuHER2 (black bars) and Δ16-HER2 (blue bars) tumors detected by flow cytometry. A: accumulation of doxorubicin expressed as fluorescence ratio between the median of fluorescence intensity of tumors of treated and untreated mice. Each bar represents the mean and SEM of 5-6 tumors. B: accumulation of trastuzumab expressed as fluorescence intensity normalized on HER2 expression of each tumor. Each bar represents the mean and the SEM of 3 tumors. Statistical analysis (Student's *t* test): **=$p<0.01$.

1.5 *In vitro* evaluation of tube formation ability of tumor cells

Vascular mimicry (VM) is a type of angiogenic mechanism that consists in the participation of tumor cells in vascular architecture. Tumor cells with stem cell-like features can undergo an epithelial-mesenchymal transition (EMT) that confers an endothelial-like phenotype. VM was found to be present in HER2-positive (Liu *et al.*, 2013) and in triple-negative breast cancers (Plantamura *et al.*, 2014).

VM activity can be detected by using an *in vitro* test that consists in the seeding of tumor cells on Matrigel to test their attitude to form vessel-like structures. This test is called Tube Formation Assay (Maniotis *et al.*, 1999).

To study the capability of forming *lacunae in vitro* conferred by full-length HER2 and Δ16, different human and murine breast cancer cell lines have been used, selected for their different characteristics in terms of expression of the two isoforms.

Four murine cell lines were taken into account: three derived from tumors of FVBhuHER2 mice (MAMBO89, MAMBO43 and MAMBO38) and one derived from a tumor of a Δ16-HER2 mouse (Mi6).

The cell line MAMBO89 has a high and stable expression of full-length HER2, whereas the cell line MAMBO43 has a high expression of HER2, but that is lost after the treatment with drugs or *in vivo* injection.

The cell line MAMBO38 was derived from a tumor induced by the *in vivo* injection of MAMBO43. It is characterized by the loss of HER2 expression and it underwent an epithelial-mesenchymal transition (EMT).

Moreover, two human breast cancer cell lines were considered: MDA-MB-231 (which does not express HER2 because it derives from a triple-negative breast cancer, and it is known to form vessel-like structures on Matrigel) and SKBr3 (which expresses both HER2 and Δ16 and it is known to be unable to form tubes). Therefore, these cell lines were used as positive and negative control respectively (Plantamura *et al.*, 2014).

Tubes that have formed after 16 hours from the seeding have been divided according to their dimensions, using a graded ocular (table 1). Tubes with a diameter smaller than 0.5 mm were considered as “small”; tubes with a diameter of between 0.5

and 1.5 mm were considered as "medium"; tubes with a diameter bigger than 1.5 mm were considered as "big".

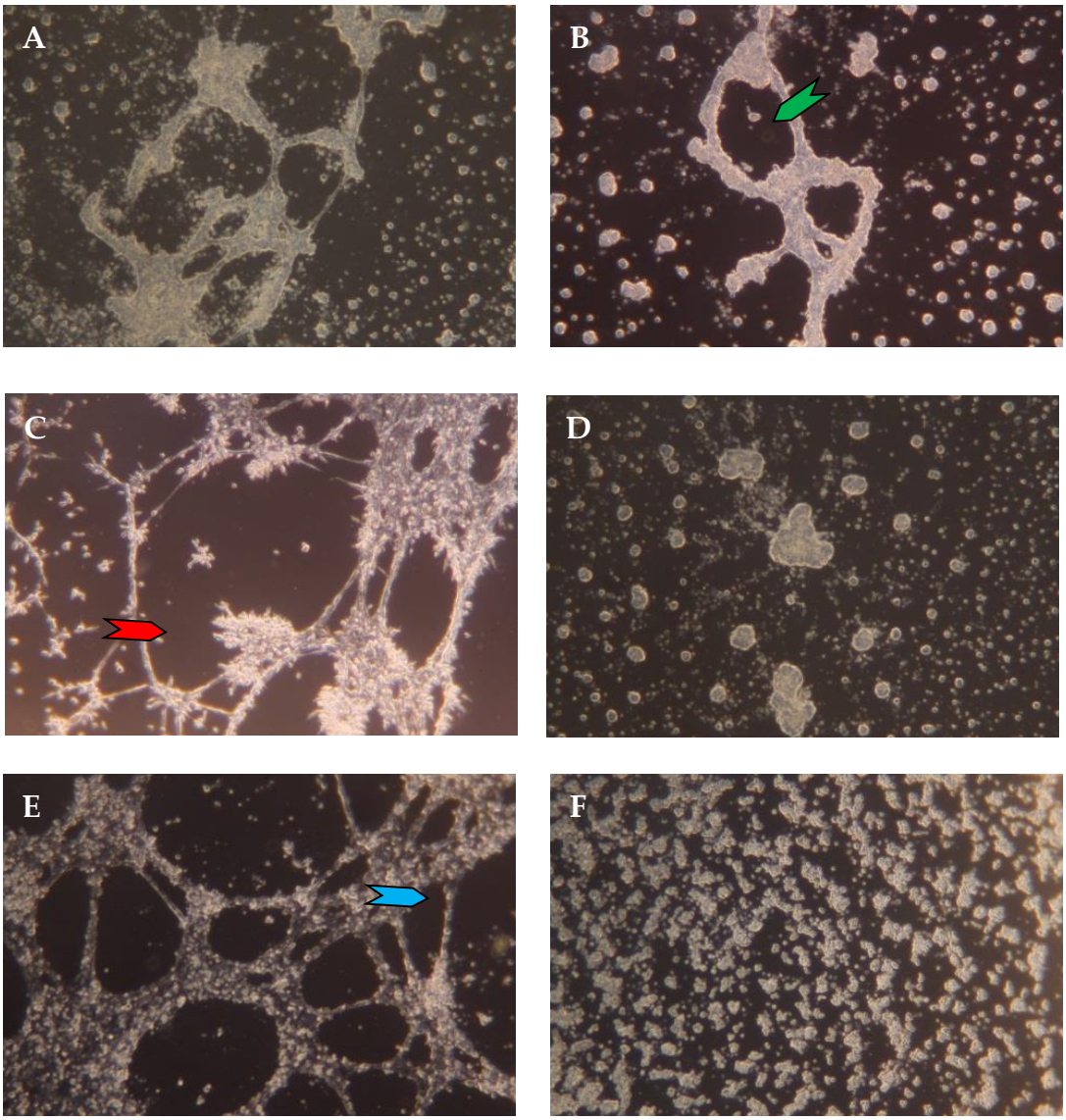

Figure 8. Tube Formation Assay *in vitro* of MAMBO89 (A), MAMBO43 (B), MAMBO38 (C), Mi6 (D), MDA-MB-231 (E) and SKBr3 (F) cell lines. Pictures taken under an inverted microscope with a 2.5x magnification (0.8" of exposure, ISO 200). Red arrow: big tube. Green arrow: medium tube. Blue arrow: small tube.

The two cell lines that express neither HER2 nor Δ16 (MAMBO38 and MDA-MB-231, figure 8C and 8E respectively) showed an elevated ability of forming tubes *in vitro*. Cells placed to form a reticle throughout the well, and they were the only cell lines that were also able to form big tubes. In particular, MAMBO38 was the one that formed

most tubes, with a mean number of tubes formed of 115 ($p<0.05$ vs. MDA-MB-231, $p<0.01$ or $p<0.001$ vs. the other cell lines by the Student's t test).

The cell lines that express only full-length HER2 (MAMBO89 and MAMBO43, figure 8A and 8B respectively) have a limited but present capability of forming vessel-like structures, even of medium dimensions.

As expected, SKBr3 cell line did not form any tubes (figure 8F). Interestingly, the other cell line that expresses Δ16, that is Mi6 (figure 8D), do not seem to be able to form tubes *in vitro*, too.

Cell lines	Small tubes	Medium tubes	Big tubes	Total	Mean
MAMBO89	11	0	0	11	12
	11	1	0	12	
MAMBO43	4	0	0	4	5
	3	2	0	5	
MAMBO38	79	27	10	116	115
	92	14	8	114	
Mi6	0	0	0	0	1
	1	0	0	1	
MDA-MB-231	41	7	8	56	66
	50	18	8	76	
SKBr3	0	0	0	0	0
	0	0	0	0	

Table 1. Number of vessel-like structures (tube) in murine and human breast cancer cell lines by Tube Formation Assay *in vitro*. Small tubes: diameter smaller than 0.5 mm; medium tubes: diameter of between 0.5 and 1.5 mm; big tubes: diameter bigger than 1.5 mm.

1.6 Detection of Breast Cancer Stem Cells

The presence of Breast Cancer Stem Cells (BCSCs) defined as $CD44^{+}$ $CD24^{-/low}$ cells have been evaluated in representative cell lines of FVBhuHER2 and Δ16-HER2 tumors by flow cytometry. Anti-CD44 and anti-CD24 antibodies have been used to evaluate the presence of this specific population of BCSCs in MAMBO89, Mi6 and MAMBO38 cell lines (figure 9).

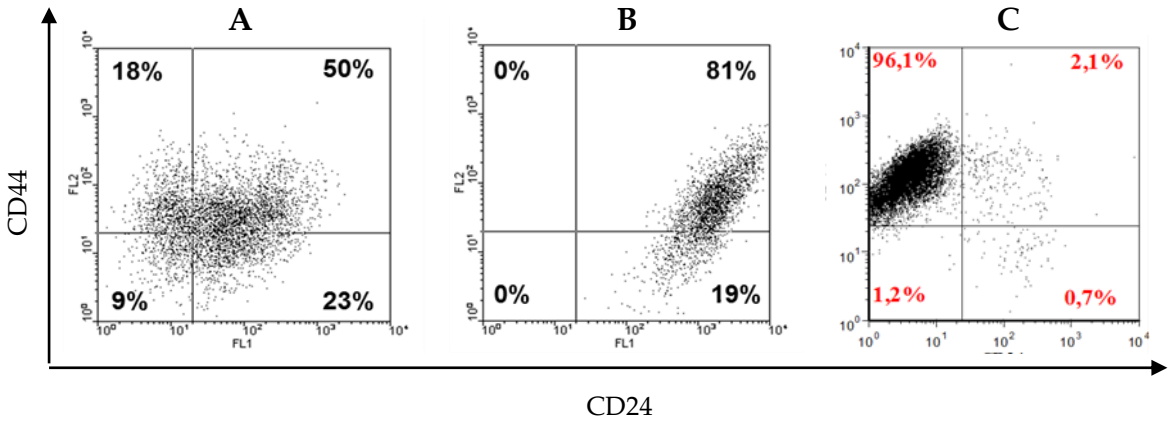

Figure 9. Detection of BCSCs through the evaluation of the expression of CD44 and CD24 by flow cytometry in MAMBO89 (A), Mi6 (B) and MAMBO38 (C) cell lines.

The population of $CD44^{+}$ $CD24^{-/low}$ cells was present in MAMBO89 cell line, representing the 18% of the total population (figure 9A). In Mi6 cells, $CD44^{+}$ $CD24^{-/low}$ cells have not been detected (figure 9B). Interestingly, in MAMBO38 this population represented almost the totality of the total cell population (figure 9C).

2. *Angiogenesis and sensitivity to anti-tumoral drugs in HER2-positive mammary carcinoma*

As it was shown before, the different vascular patterns sustained by HER2 and Δ16 affect the distribution of drugs. This fact may influence the sensitivity to anti-tumoral drugs such as trastuzumab.

The different vascularization may also affect the sensitivity to anti-angiogenic drugs, such as sunitinib and pazopanib. Moreover, according to the Jain's concept (Goel *et al.*, 2011), drugs that target angiogenesis may have a direct effect on the vascular phenotype of tumors, thus potentially affecting the sensitivity of other therapeutic agents.

The sensitivity to anti-angiogenic agents has been first explored *in vivo*, in monotherapy or in association with trastuzumab.

The efficacy of anti-angiogenic therapies was later analyzed *in vitro*, studying the inhibition of tumor cell lines proliferation or the effect on the ability of forming tubes on Matrigel.

2.1 *In vivo* sensitivity to sunitinib and pazopanib

Since FVBhuHER2 tumors and Δ16-HER2 ones show different patterns of angiogenesis that affect drug distribution and have different levels of expression of VEGFR2, the anti-angiogenic drugs sunitinib and pazopanib were tested *in vivo* to explore not only the effect on tumor growth but also the impact on tumor vascularization.

To do that, two Mouse-Derived Isografts (MDI) were created. Fragments of five autochthonous mammary carcinomas from FVBhuHER2 mice were subcutaneously injected in 15 FVB non-transgenic mice. The same was done with the fragments of nine tumors of Δ16-HER2 mice.

Tumor growth was monitored weekly for all the duration of the experiment. When tumors grew and became palpable, mice were divided into three groups to receive sunitinib 60 mg/kg, pazopanib 100 mg/kg or the vehicle in which the drugs were dissolved (sterile methocel 0.5% + tween80 0.4% in tap water). Drugs were administered orally for four weeks, five days a week.

One mouse of each pazopanib group and one mouse of FVBhuHER2 MDI control group were excluded from the analysis, due to premature death of the animals.

All the other mice were euthanized the week after the end of the treatment. Necropsy was performed, and the tumors were collected for histological and molecular analysis.

FVBhuHER2 MDI tumors showed a sensitivity to sunitinib starting from the second week of treatment. At the end of the experiment, tumor growth had an inhibition of 70.3%. No effect was observed upon treatment with pazopanib (figure 10A).

On the other hand, sunitinib was effective on Δ16-HER2 MDI tumors starting from the second week of treatment as well, reaching a tumor growth inhibition of 88.4% at the end of the experiment. Moreover, no tumor growth was observed until the

end of the treatment. Pazopanib was also effective starting from the third week of treatment, with a final tumor growth inhibition of 48.4% (figure 10B).

As a conclusion, sunitinib resulted effective either on FVBhuHER2 MDI tumors or Δ16-HER2 ones, but the effect was bigger on the latter. Pazopanib was effective only on Δ16-HER2 tumors, but the tumor growth inhibition was lower and occurred later than sunitinib.

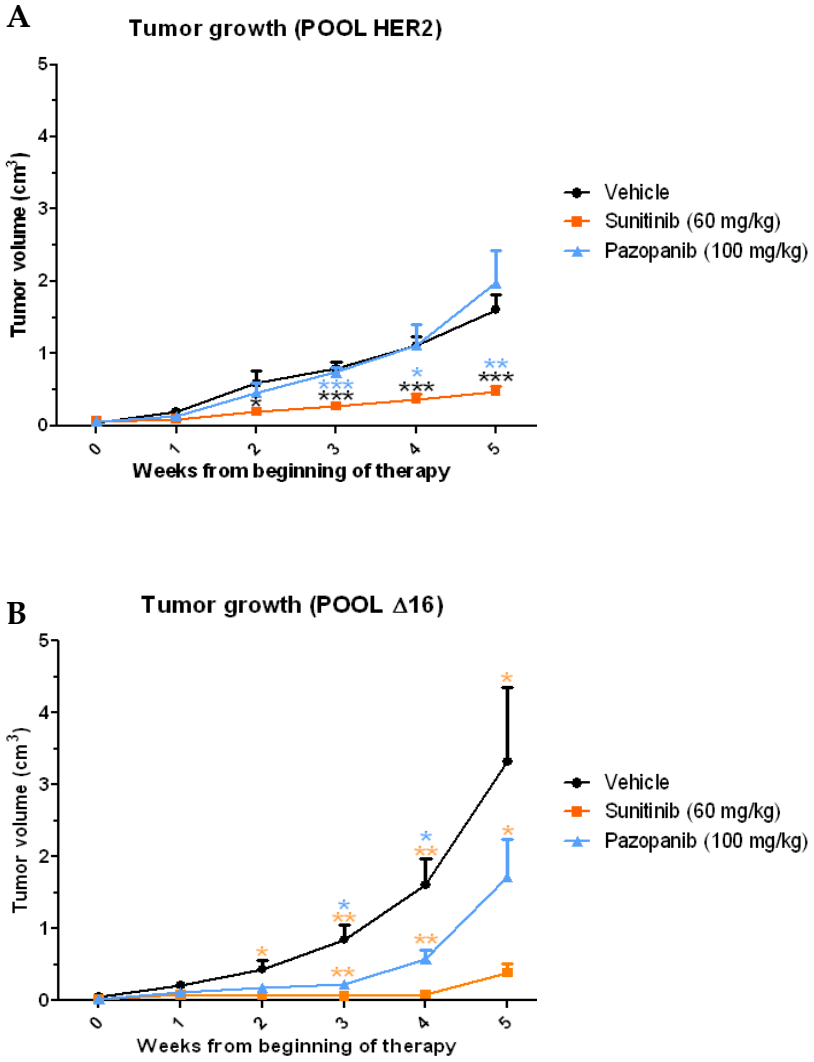

Figure 10. *In vivo* sensitivity to anti-angiogenic drugs on tumors induced by the subcutaneous injection of fragments of FVBhuHER2 (A) and FVBΔ16 (B) autochthonous mammary carcinomas, as kinetics of tumor growth from beginning of therapy. Vehicle: black line. Sunitinib: orange line. Pazopanib: light blue line. Each point represents the mean and the SEM of the volumes of 4-5 tumors. Statistical analysis (Student's *t* test): *=p<0.05; **=p<0.01; ***=p<0.001.

2.1.1 Histology of treated tumors

Tumors of treated mice were compared to untreated ones from the histological point of view. Immunohistochemistry was performed using an antibody against CD31 to detect and quantify the vessels (figure 11).

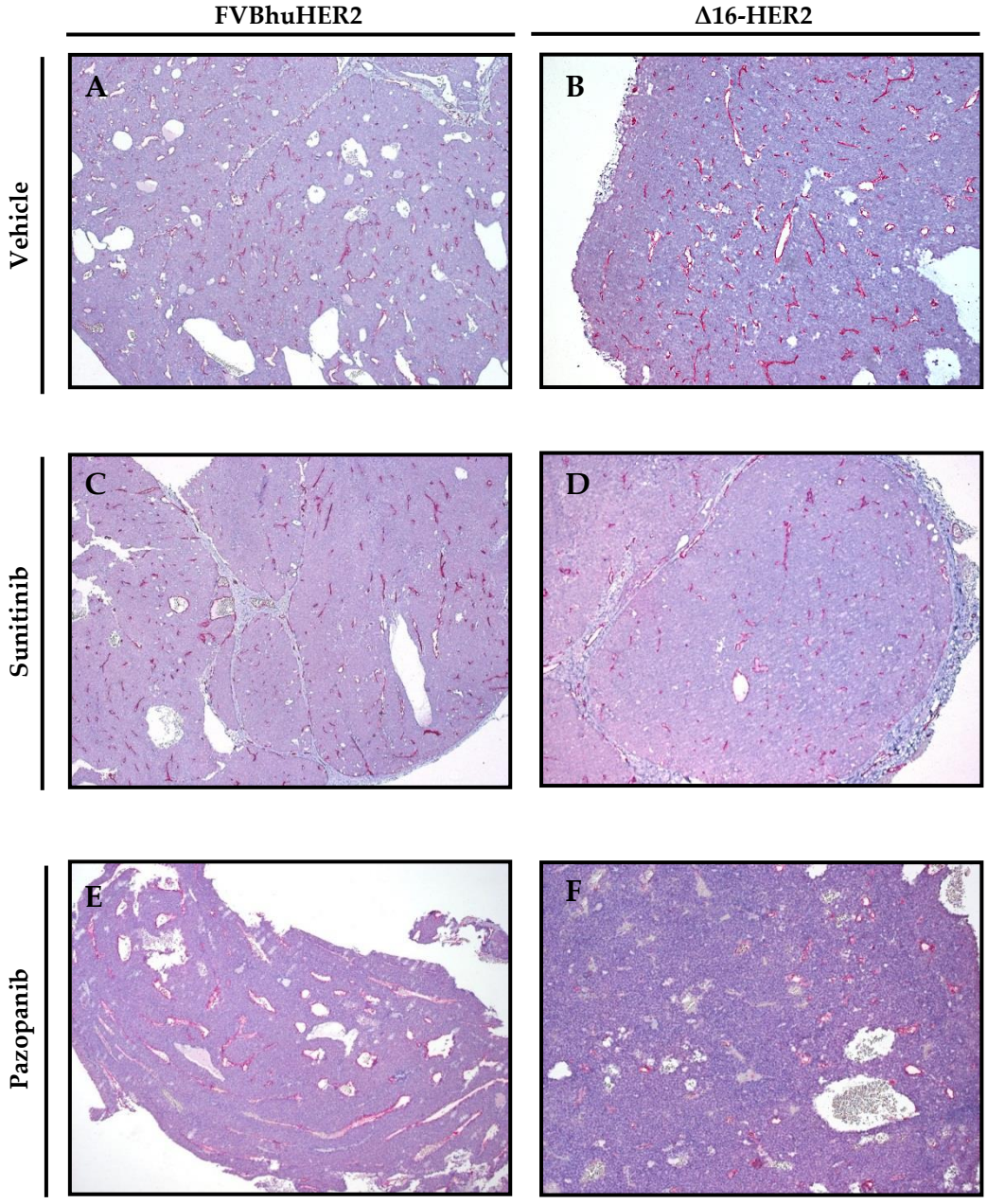

Figure 11. Immunohistochemistry of treated and untreated FVBhuHER2 (A, C and E) or Δ16-HER2 (B, D and F) MDI tumors. A and B: vehicle. C and D: sunitinib. E and F: pazopanib. An anti-CD31 antibody was used to stain in red endothelial cells. Pictures A, C and E were taken with a 5x magnification; pictures B, D and F were taken with a 10x magnification.

No effect on vascularization was observed on FVBhuHER2 MDI tumors upon treatment (figure 12A). The only effect that was noticeable in these tumors was the significant increase of tumor necrosis in sunitinib-treated samples (figure 12B). This effect could explain the sensitivity of these tumors to this drug.

On the contrary, the treatment with sunitinib and pazopanib had a direct effect on vascularization of Δ16-HER2 MDI tumors, significantly reducing the vascular density, that is the number of vessel per tumor area. In particular, vascular density was reduced by the 47.6% by sunitinib, and by the 50.4% by pazopanib (figure 12C).

Therefore, sunitinib and pazopanib were effective both as anti-tumoral and anti-angiogenic agents in Δ16-HER2 MDI tumors, whereas in FVBhuHER2 MDI tumors only sunitinib had an anti-tumoral effect likely by necrosis induction.

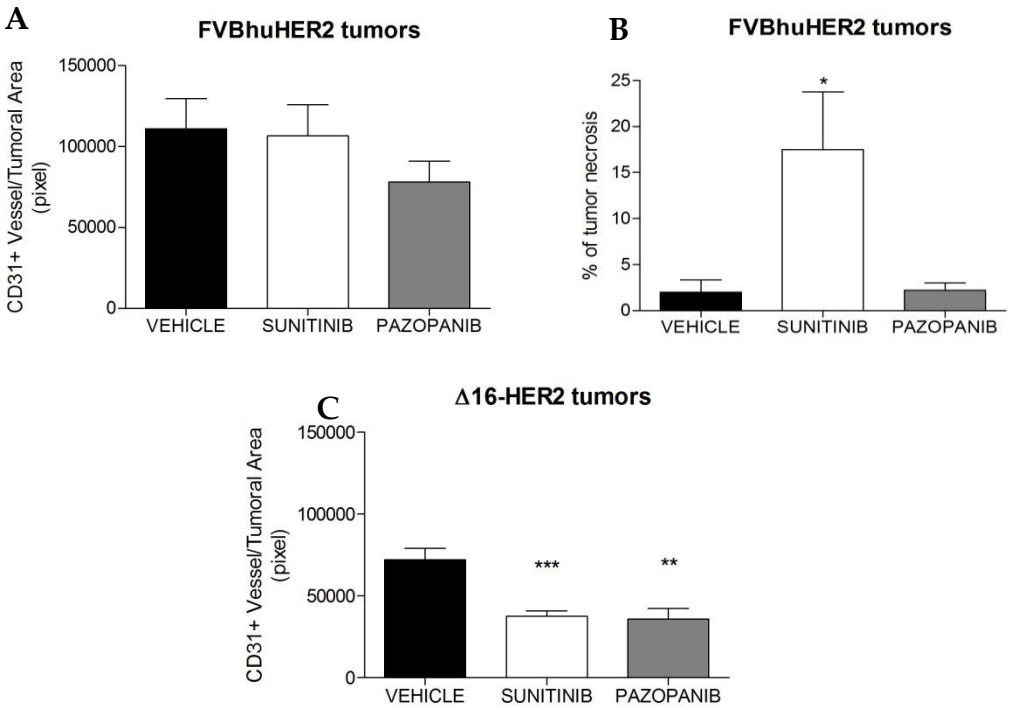

Figure 12. Effect on vascularization of sunitinib (white bars) and pazopanib (grey bars) in FVBhuHER2 (A and B) or Δ16-HER2 (C) tumors, compared to vehicle group (black bars). A and C: quantification of vessels as number of $CD31^+$ pixels per tumoral area. B: percentage of necrotic cells inside the tumors. Each bar represents the mean and the SEM of the analysis of 4-5 tumors. Statistical analysis (Student's *t* test): *=p<0.05; **=p<0.01; ***=p<0.001.

2.1.2 Molecular analysis of treated tumors

The MDI tumors treated with sunitinib or pazopanib were also analyzed from the molecular point of view, in order to detect any variation in the expression of angiogenesis-related markers induced by the treatment with the two anti-angiogenic drugs. The expression of VEGF-A, VEGFR2, COX-2, CD31 and CD146 was evaluated by Real Time qPCR (figure 13).

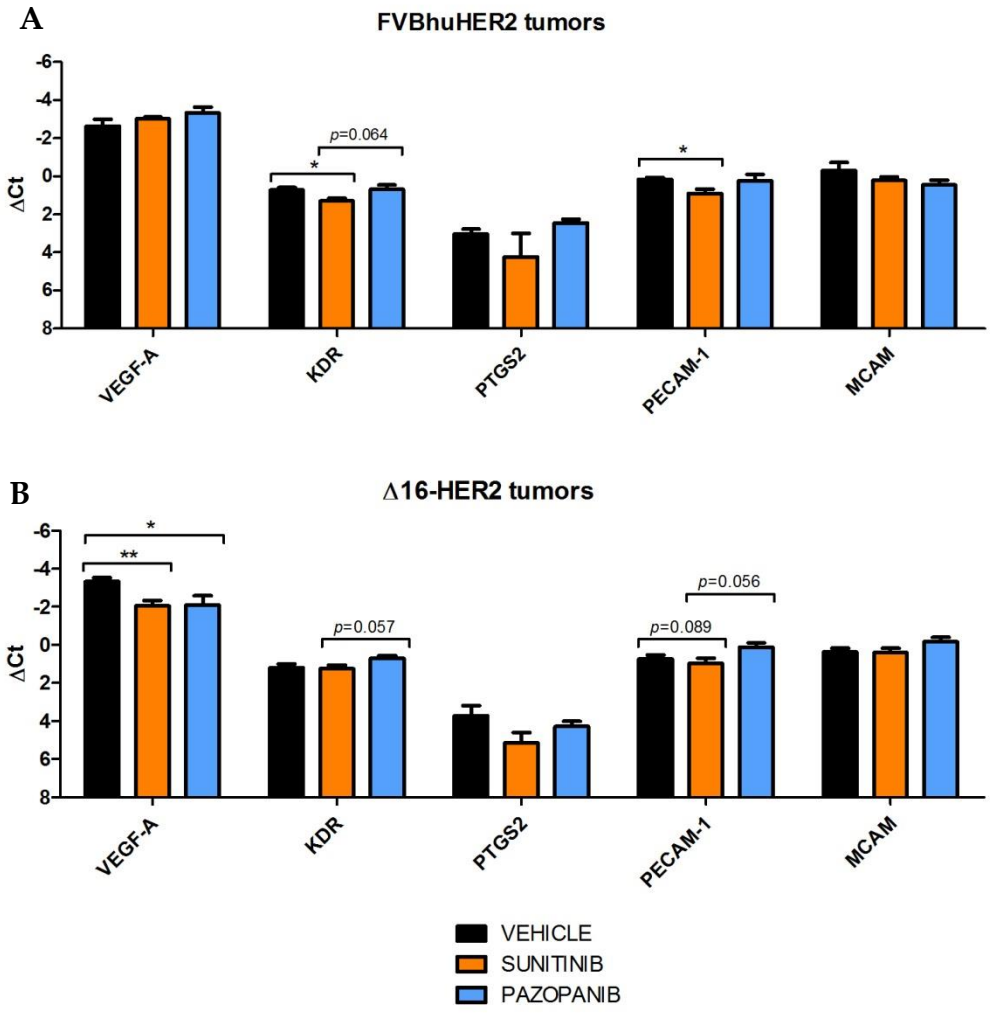

Figure 13. Expression of angiogenesis-related genes by Real Time qPCR in FVBhuHER2 (A) or Δ16-HER2 (B) tumors treated with vehicle (black bars), sunitinib (orange bars) or pazopanib (light blue bars). Each bar represents the mean and the SEM of ΔCt for each tumor (n=4-5). Housekeeping gene: mTBP. Statistical analysis (Student's t test): *=p<0.05; **=p<0.01.

In FVBhuHER2 MDI tumors, the expression of VEGFR2 and PECAM1 was lower in sunitinib-treated tumors. No other significant difference in expression was observed (figure 13A).

On the other hand, VEGF-A expression was lower in treated Δ16-HER2 MDI tumors compared to control ones. Even if statistical significance was not reached, some other tendencies were observed: the slightly higher expression of VEGFR2 in pazopanib-treated samples, and the expression of CD31 that is slightly lower in sunitinib-treated tumors and a little bit higher in pazopanib-treated ones (figure 13B).

2.2 Combined therapy *in vivo*: sunitinib plus trastuzumab

As previously shown, sunitinib was less effective on HER2-expressing tumors than Δ16-expressing ones. Moreover, HER2-expressing cells or tumors are less responsive to trastuzumab (Palladini *et al.*, 2017), either in preventive or therapeutic setting. Therefore, a combined therapy approach including sunitinib and trastuzumab was tested to try to obtain a better pharmacological response in FVBhuHER2 model, since it was less sensitive to anti-angiogenic and anti-HER2 drugs than Δ16-HER2 model.

To do so, twenty-five tumor-free FVBhuHER2 female mice were subcutaneously injected with fragments from six autochthonous mammary carcinomas of FVBhuHER2 mice to create a MDI model. Tumor growth was monitored weekly, and when the tumors became palpable, the animals were divided into five experimental groups: vehicle of sunitinib, sunitinib, trastuzumab, sunitinib and then trastuzumab, trastuzumab and then sunitinib.

Sunitinib was administered at a dose of 60 mg/kg in methocel 0.5% + tween80 0.4% in tap water for four weeks, five times a week. Trastuzumab was administered intraperitoneally at a dose of 4 mg/kg in saline, twice a week for four weeks. In the combined setting, the two drugs were administered in sequence to evaluate whether the order of administration of the drugs were important for the therapeutic result. Therefore, four weeks of treatment with a drug were followed by four weeks of treatment with the other drug.

Tumor dimensions were measured weekly throughout the experiment to monitor the tumor growth inhibition (figure 14).

In the monotherapy setting, both drugs were effective in slowing down tumor growth (figure 14A). Sunitinib reduced tumor volume by 85.7% at the end of the

experiment, whereas trastuzumab had an effect by 58.8% compared to control. Therefore, sunitinib was more effective than trastuzumab.

In the combined therapy setting (figure 14B), the first segment of both treatment lines (that is before the switch of therapy) reflected the slope of their respective line in monotherapy setting. After the change of treatment, the slope of both lines changed and at the end of the follow-up the last points of each line were almost superimposed.

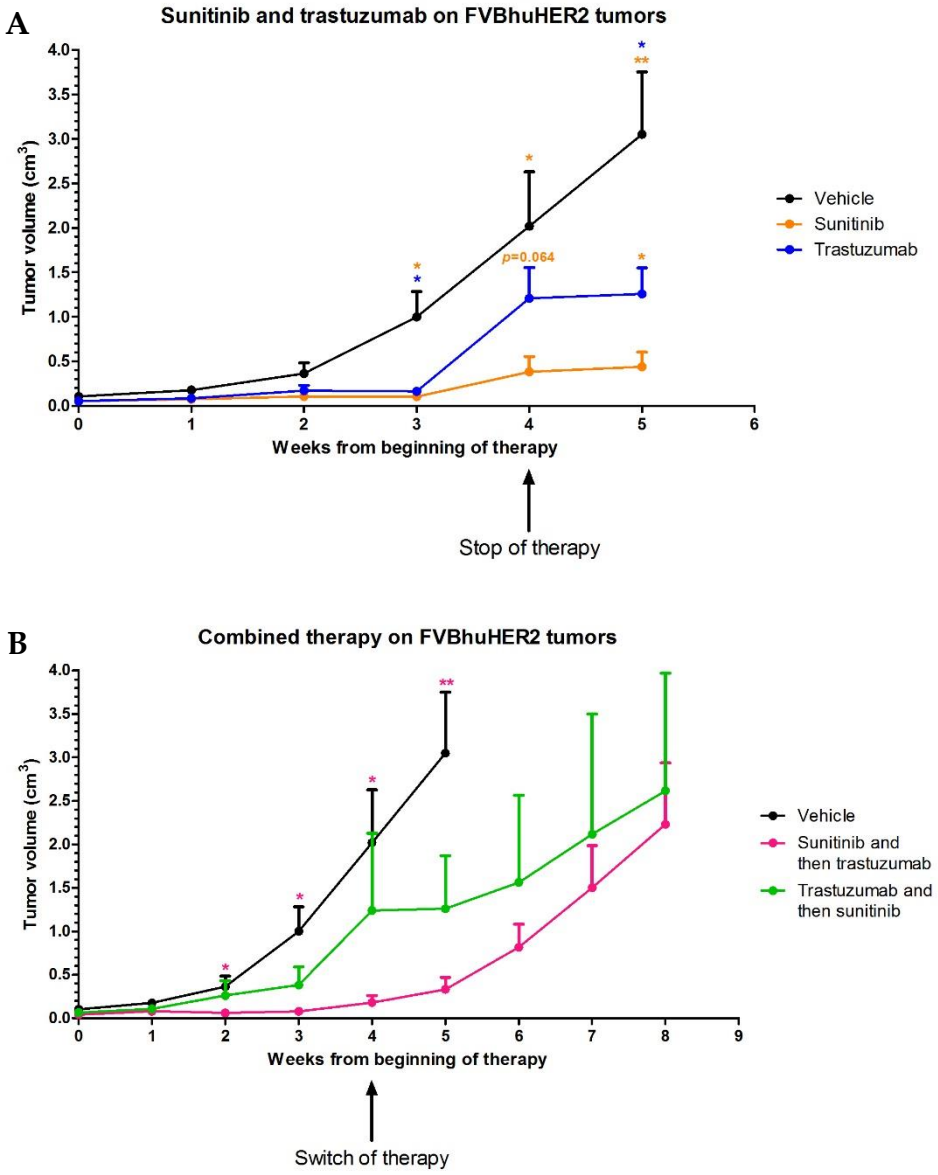

Figure 14. *In vivo* therapy with sunitinib and/or trastuzumab on tumors induced by the subcutaneous injection of fragments of FVBhuHER2 autochthonous mammary carcinomas, as kinetics of tumor growth from beginning of therapy. Each point represents the mean and the SEM of the volumes of 5 tumors. A: therapy with sunitinib (orange line) or trastuzumab (blue line), compared to control group (vehicle, black line). B: combined therapy as sunitinib followed by trastuzumab (pink line) or trastuzumab followed by sunitinib (green line). Statistical analysis (Student's *t* test): *=p<0.05; **=p<0.01.

Because of a great variability among the two groups, the SEM were so big that the difference with the control group was not statistically significant. Anyway, at the end of the experiment there was no difference in terms of benefit in tumor growth rate according to the order of administration of the two drugs.

2.3 *In vitro* sensitivity to sunitinib and pazopanib

The impact on proliferation of anti-angiogenic drugs such as sunitinib and pazopanib has been assessed *in vitro* using cell lines with different levels of expression of the two isoforms of HER2, to evaluate the intrinsic sensitivity of these cell lines to the drugs.

The cell lines that were considered were MAMBO89 (derived from a FVBhuHER2 tumor) and Mi6 (derived from a Δ16-HER2 tumor). Cells were seeded in adherent conditions and drug sensitivity was evaluated after 24, 48 and 72 hours after treatment by cell count.

MAMBO89, which expresses full-length HER2, resulted sensitive only to pazopanib at 72 hours after treatment, with a growth inhibition of 64.6% (figure 15A and 15C).

The Δ16-expressing cell line Mi6 showed sensitivity to both drugs. Sunitinib was already effective in inhibiting cell proliferation after 24 hours of treatment, reaching a growth inhibition of 45.5% after 72 hours. Pazopanib was effective too, but only after 48 and 72 hours of treatment, with a growth inhibition of 18% and 49.9% respectively (figure 15B and 15D).

In conclusion, both drugs were effective in inhibiting cell growth *in vitro*, with some differences. First of all, in Mi6 cell line the effectiveness was evident earlier than in MAMBO89 cells. Moreover, MAMBO89 showed resistance to sunitinib but not to pazopanib, even if the effect of pazopanib was observable only after 72 hours.

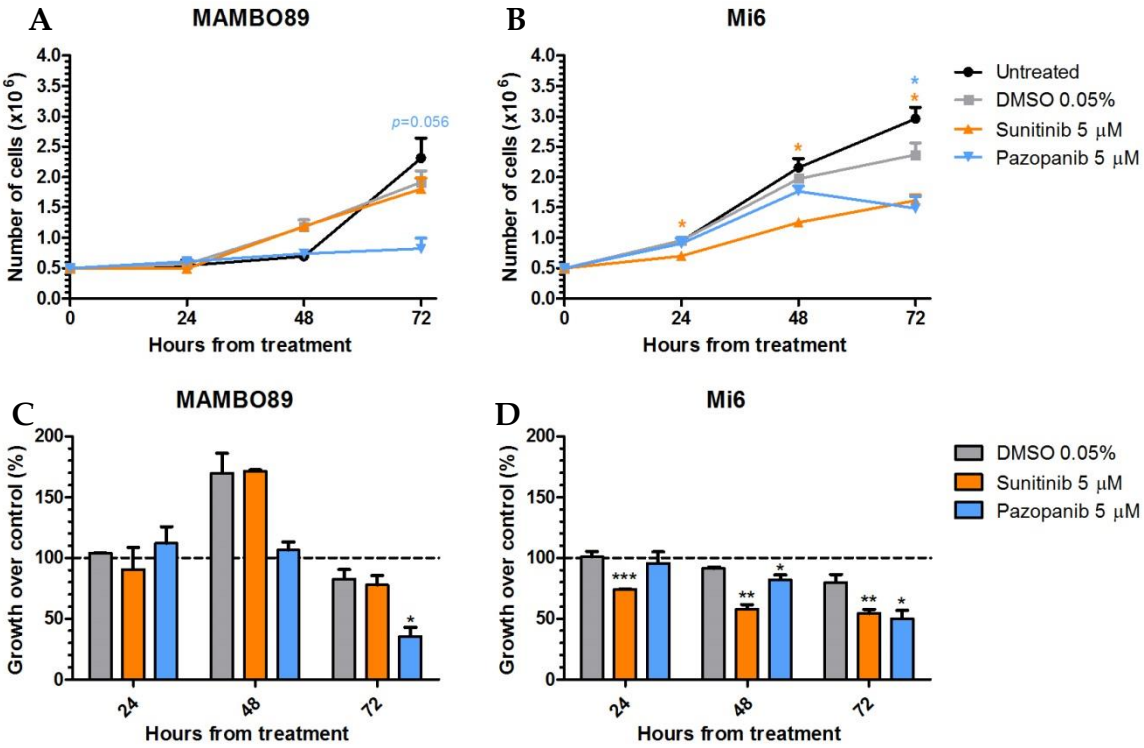

Figure 15. *In vitro* sensitivity to anti-angiogenic drugs of MAMBO89 (A, C) and Mi6 (B, D) cell lines. A and B: total number of cells per well at 24, 48 and 72 hours after treatment with sunitinib 5 μM (orange line) or pazopanib 5 μM (light blue line), compared to untreated cells (black line) and DMSO-treated cells (grey line). Each point represents the mean and the SEM of two replicates. C and D: percentage of growth over control (untreated cells). Each bar represents the mean and the SEM of the ratio between the total number of treated cells and the mean total number of control cells. DMSO 0.05%: grey bars. Sunitinib: orange bars. Pazopanib: light blue bars. Statistical analysis (Student's *t* test): *=p<0.05; **=p<0.01; ***=p<0.001.

2.3.1 Influence of anti-angiogenic drugs on tube formation

Since that FVBhuHER2 cell lines MAMBO89 and MAMBO43 showed a modest capability of forming *lacunae* on Matrigel, whereas this attitude was absent in the Δ16-HER2 cell line Mi6, the effect of anti-angiogenic drugs on this ability has been explored.

MAMBO89 and Mi6 cells were seeded on a 6-well plate. The medium was replaced with drug-containing fresh media the day after. 24 hours after treatment, cells were harvested and seeded on Matrigel, according to the protocol of the Tube Formation Assay. After 18 hours, the *lacunae* formed have been counted, dividing them by dimension as described before.

Mi6 was unable to form any tube in any condition. On the contrary, the treatment with sunitinib reduced the number of tubes compared to the untreated control by almost 4 times in MAMBO89 cell line (table 2).

Treatment	Small tubes	Medium tubes	Big tubes	Total	Average
Untreated	32	4	0	36	27
	15	3	0	18	
DMSO 0.05%	63	14	4	81	75
	61	6	1	68	
Sunitinib 5 μM	8	0	0	8	8
	7	0	0	7	
Pazopanib 5 μM	28	0	1	29	25
	20	0	0	20	

Table 2. Number of vessel-like structures (tube) in MAMBO89 cell line by Tube Formation Assay *in vitro* after treatment with sunitinib 5 μM or pazopanib 5 μM. Small tubes = diameter smaller than 0.5 mm; medium tubes = diameter of between 0.5 and 1.5 mm; big tubes = diameter bigger than 1.5 mm.

Therefore, sunitinib, which was not able to arrest cell growth in adherent cells, was effective in reducing the formation of vessel-like structures on Matrigel of MAMBO89 cell line.

3. Angiogenesis and sensitivity to anti-angiogenic drugs in triple-negative breast cancer

The Tube Formation Assay showed that MAMBO38 and MDA-MB-231, the two HER2-negative cell lines that were used, had a great attitude of forming tubes *in vitro*. The test performed on MAMBO89 cells revealed that sunitinib is able to reduce this ability, that is linked to vasculogenic mimicry (Maniotis *et al.*, 1999).

MDA-MB-231 are known to do mimic endothelial cells *in vivo*, reflecting the ability shown on Matrigel (Plantamura *et al.*, 2014). Therefore, MDA-MB-231 were injected in immunodeficient mice and treated with sunitinib in order to test the

sensitivity to this drug in terms of tumor growth. The sensitivity has been also evaluated *in vitro*.

The sensitivity to anti-angiogenic drugs was also studied on MAMBO38 cell line, both on adherent conditions and in 3D-culture.

3.1 *In vivo* sensitivity to sunitinib in triple-negative breast cancer

To test the efficacy of sunitinib *in vivo* on human HER2-negative breast cancer, MDA-MB-231 cells were injected orthotopically in both flanks of twelve 8-week-old female NOD-SCID mice. The experiment was performed at the Vascular Morphogenesis Lab directed by Dr. Cláudio A. Franco (Instituto de Medicina Molecular, Faculdade de Medicina da Universidade de Lisboa, Lisbon, Portugal).

All the tumors were palpable two weeks after the injection, and six animals were treated with sunitinib 60 mg/kg for twenty consecutive days. The other six mice received the vehicle in which sunitinib was dissolved (sterile methocel 0.5% in tap water). The mice were euthanized to collect the tumors for further analyses one week after the end of the therapy. Due to excessive tumor growth, three mice of the control group had to be euthanized a few days earlier than the other animals.

Tumor growth was monitored throughout the experiment to evaluate the potential inhibition of proliferation after the treatment.

The effect of sunitinib on tumor growth was statistically evident starting from the fourth week after cell injection, that was after two weeks of treatment. The drug was able to reduce the tumor volume by the 43.4% compared to the control group, at the end of the experiment (figure 16).

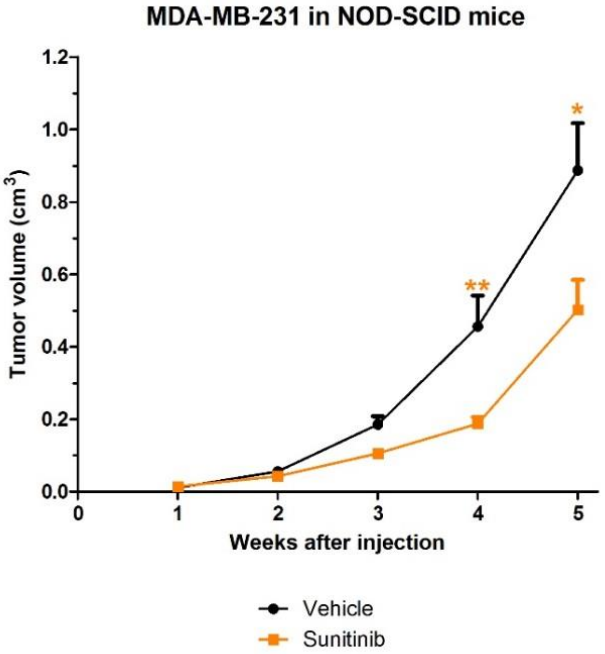

Figure 16. *In vivo* sensitivity to sunitinib on tumors induced by the subcutaneous injection of MDA-MB-231 cells, as kinetics of tumor growth after cell injection. Vehicle: black line. Sunitinib: orange line. Each point represents the mean and the SEM of the volumes of 6-12 tumors (two tumors per mouse). Statistical analysis (Student's *t* test): *=$p<0.05$; **=$p<0.01$.

3.2 *In vitro* sensitivity to sunitinib and pazopanib in HER2-negative cell lines

The impact on proliferation of anti-angiogenic drugs such as sunitinib and pazopanib has been evaluated *in vitro* using cell lines with different levels of expression of the two isoforms of HER2.

The cell lines that were considered were the human triple-negative breast cancer cell line MDA-MB-231, and MAMBO38, which was derived from the tumor induced by the injection of a cell line derived from a FVBhuHER2 tumor and which underwent a EMT and lost HER2 expression.

The sensitivity to sunitinib and pazopanib was first tested on MDA-MB-231 cells, evaluating the cell proliferation at 24, 48 and 72 hours after treatment by cell count (figure 17).

The human triple-negative cell line MDA-MB-231 was sensitive to both drugs after 72 hours of treatment. Sunitinib caused a 40.9% inhibition of cell growth, whereas pazopanib was able to reduce cell proliferation only by 28.3%.

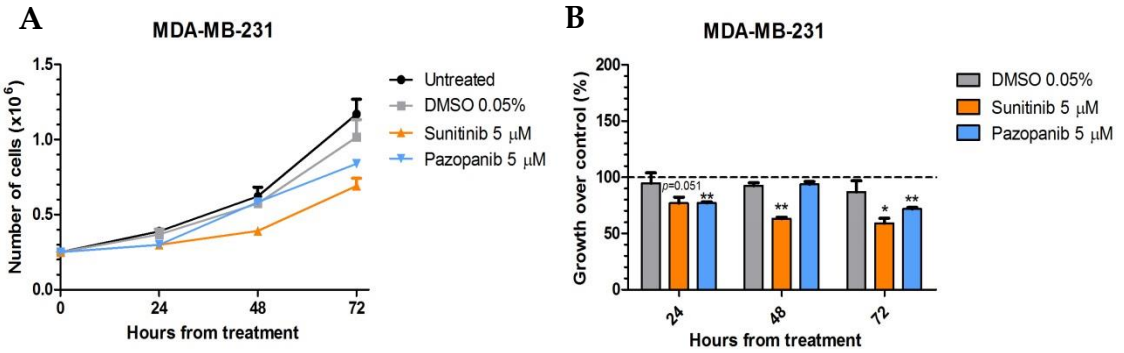

Figure 17. *In vitro* sensitivity to anti-angiogenic drugs of MDA-MB-231 cell lines. A: total number of cells per well at 24, 48 and 72 hours after treatment with sunitinib 5 μM (orange line) or pazopanib 5 μM (light blue line), compared to untreated cells (black line) and DMSO-treated cells (grey line). Each point represents the mean and the SEM of two replicates. B: Percentage of growth over control (untreated cells). Each bar represents the mean and the SEM of the ratio between the total number of treated cells and the mean total number of control cells. DMSO 0.05%: grey bars. Sunitinib: orange bars. Pazopanib: light blue bars. Statistical analysis (Student's *t* test): *=$p<0.05$; **=$p<0.01$.

The sensitivity to sunitinib and pazopanib has been tested in a slightly different way in the cell line MAMBO38. Cell proliferation was evaluated at 24 and 72 hours after treatment through the adding of WST-1 reagent, a compound that is cleaved by mitochondrial dehydrogenases of viable cells into a compound that can be quantified by absorbance measurement.

Sunitinib was effective both at 24 and 72 hours after treatment, with a growth inhibition of 51.3% and 49.3%. Pazopanib was effective only at 72 hours after treatment, inhibiting cell proliferation by 54.7% (figure 18).

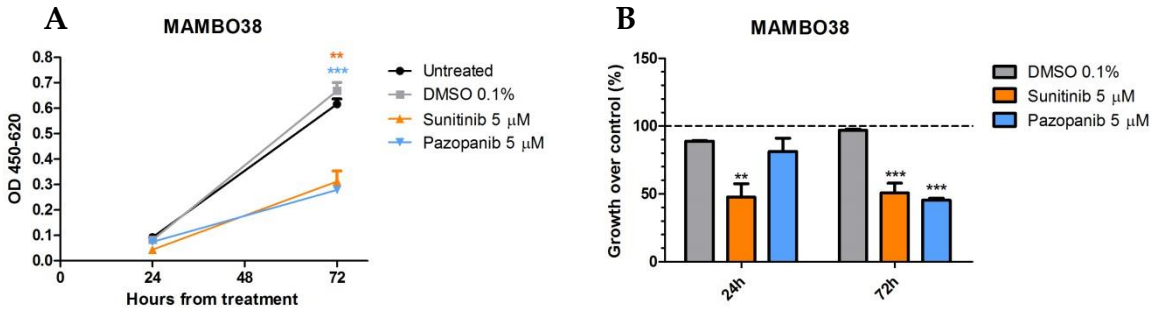

Figure 18. *In vitro* sensitivity to anti-angiogenic drugs of MAMBO38 cell line. A: OD measurement at 24 and 72 hours after treatment with sunitinib 5 μM (orange line) or pazopanib 5 μM (light blue line), compared to untreated cells (black line) and treatment with DMSO 0.1% (grey line). Absorbance was measured one hour after the adding of WST-1 reagent. Each point represents the mean and the SEM of three replicates. B: Percentage of growth over control (untreated cells). Each bar represents the mean and the SEM of the ratio between the mean absorbance of treated cells and of control cells. DMSO 0.1%: grey bars. Sunitinib: orange bars. Pazopanib: light blue bars. Statistical analysis (Student's *t* test): **=$p<0.01$; ***=$p<0.001$.

The influence of anti-angiogenic therapies on MAMBO38 cell line has been also explored in 3D-culture. Cells were seeded in soft agar in a 24-well plate, in presence or not of sunitinib 5 μM or pazopanib 5 μM. After two weeks, colonies were counted under an inverted microscope, arbitrary defined as every cell aggregate bigger than 1 mm.

Both drugs were extremely effective (table 3): no colonies were present at all after 14 days of treatment, whereas 30-40 colonies had formed in control wells (p<0.001 by the Student's t test).

Therefore, MAMBO38 cells were dramatically sensitive to both drugs both in 3D-culture and adherent conditions.

Treatment	**Count replicates**							**Average**
Untreated	29	26	35	25	23	35	40	30
DMSO 0.05%	41	42	44	39	32	41	34	39
Sunitinib 5 μM	0	0	0	0	0	0	0	0
Pazopanib 5 μM	0	0	0	0	0	0	0	0

Table 3. Number of colonies of MAMBO38 cell line by seeding in 3D-culture after treatment with sunitinib 5 μM or pazopanib 5 μM. Aggregates bigger than 1 mm were considered as colonies. Colonies were counted by two different researchers at 7 different times 14 days after seeding.

In conclusion, both sunitinib and pazopanib were effective on HER2-negative cell lines *in vitro* and *in vivo*. The effectiveness of sunitinib was evident earlier than the effect of pazopanib in both MDA-MB-231 and MAMBO38 cells *in vitro* in adherent conditions. Both drugs had an impressive effect on MAMBO38 cell line in 3D-culture.

Discussion

Preclinical models developing human HER2-positive mammary carcinoma have been created to study mammary carcinogenesis. Three mouse models, transgenic for full-length HER2 and/or its splice variant Δ16, have been used in this thesis. The tumors of these three models showed different macroscopic appearance and pattern of vascularization. FVBhuHER2 tumors, that are usually hemorrhagic and have a soft texture, displayed few large vessels. Concordant association between high HER2 expression and atypical vessels was found in human breast cancer: dilated capillaries (called "cavitary" structures) were associated with lymphovascular invasion and higher grade in HER2-positive breast carcinoma (Senchucova *et al.*, 2015). On the other hand, Δ16-HER2 tumors, that usually have a solid and whitish aspect, showed numerous vessels with a smaller diameter. F1 tumors, which derive from a double-transgenic mouse model, could show both characteristics (Palladini *et al.*, 2017).

To better understand the role of HER2 and its splice isoform Δ16 in tuning different vascular phenotypes, vascular architecture of F1 tumors has been analyzed considering that one isoform or both can be expressed. Interestingly, regardless of the level of expression of Δ16, immunostaining of vessels revealed that the F1 tumors which highly express full-length HER2 display the same phenotype of FVBhuHER2 tumors. Only the vascular pattern of F1 tumors with low levels of HER2 and high levels of Δ16 resembles the one of Δ16-HER2 tumors. This evidence is the first proof that full-length HER2 has a dominant and crucial role in influencing the vascularization of the tumor.

The second evidence was obtained through the study of the vascularization in a model of modulation of the expression of HER2. This model is made of two MDIs created through serial transplants of F1 tumors, in which the levels of HER2 decrease or increase while the expression of Δ16 remains high and stable over consecutive passages. Analyzing the vessel density and the mean vascular area of the tumors of different passages, it was clear that a change in expression level of HER2 was always associated with a change in the vascular phenotype. In particular, a gain in HER2 expression conferred the vascular phenotype with few large vessels, but when HER2 expression got lost, the vascular pattern consisted of many small vessels like Δ16-HER2

tumors. In this sense, it is more evident that the presence of a high expression of full-length HER2 strongly influences tumor angiogenesis in a dynamic way.

The different vascularization may impact on functionality of the vascular network of the tumors. In fact, distribution and permeability seemed to be affected, depending on the vascular phenotype. The presence of a smaller number of larger vessels seemed to allow a poorer distribution of drugs, as it has been proved through the analysis of the accumulation of doxorubicin and trastuzumab inside the tumors. A lower permeability may explain why HER2-expressing tumors are less sensitive to targeted drugs *in vivo* (Castagnoli *et al.*, 2014; Palladini *et al.*, 2017). In fact, the reduction of vessel diameter has been associated with higher permeability (Chauhan *et al.*, 2012).

If the vascularization driven by the two isoforms is so different, then HER2 and Δ16 must trigger different pathways. This means that the differences between the two angiogenic patters must also involve different molecular partners. In fact, Δ16-expressing tumors were enriched in VEGF-A and VEGFR2 expression. Several other genes that were differently expressed in FVBhuHER2 and Δ16-HER2 may explain the different phenotypes. For instance, Angiopoietin-1 and TIMP-1 were more expressed in tumors of FVBhuHER2 mice. On the other hand, EGF was more expressed in Δ16-HER2 tumors. Since this growth factor can increase VEGF-A and VEGFR2 expression (van Cruijsen *et al.*, 2005), it could explain what was previously found.

These findings may suggest that the vascular network is less mature in FVBhuHER2 tumors. In fact, numerous angiogenic factors involving sprouting angiogenesis were more expressed in these tumors, and that may imply that the angiogenesis process occurs in a more active manner in these tumors rather than in Δ16-HER2 ones. For example, Angiopoietin-1 and TIMP-1, which were more expressed in FVBhuHER2 tumors, are responsible of the recruitment of endothelial progenitors and of the proliferation of mature endothelial cells respectively (Carmeliet and Jain, 2000; Baker *et al.*, 2002). Metalloproteinases, such as MMP-9 and MMP-3, were also more expressed in FVBhuHER2 tumors. This means that extracellular matrix is more degraded to let the sprouts invade the tissues. Moreover, factors that stimulate

migration and endothelial precursors recruitment were more expressed, such as osteopontin, PAI-1, PlGF-2 and PDGF-AB/BB. Likely, the maturation and remodeling of vessels are somehow inhibited or less activated, leading to a less coordinated process and a less regular vascularization in FVBhuHER2 tumors.

On the other hand, Δ16-HER2 vascularization might be more regular but more developed, in terms of number of branches. Higher permeability and number of vessels can explain a better and more efficient distribution of drugs. Moreover, Angiopoietin-1, which was more expressed in FVBhuHER2 tumors, reduces the permeability of blood vessels: this can also explain why the drugs accumulate less than in Δ16-HER2 tumors.

Another hint about the less regular vascularization in FVBhuHER2 tumors has been given by the Tube Formation Assay, using cell lines derived from FVBhuHER2 and Δ16-HER2 tumors. This technique allows to understand whether tumor cells have the tendency to show vasculogenic mimicry (VM; Maniotis *et al.*, 1999). It emerged that the FVBhuHER2 cell line MAMBO89 was somehow able of forming vessel-like structures, whereas the Δ16-HER2 cell line Mi6 was not.

There can be many possible explanations to that. First, it is known in literature that VM and stemness have a strong link. $CD44^{+}$ $CD24^{-/low}$ Lin^{-} cells were defined as Breast Cancer Stem Cells (BCSCs) and showed stem-like features (Al-Hajj *et al.*, 2003). MDA-MB-231 cells are known to produce a large number of *lacunae* on Matrigel, and are strongly enriched with $CD44^{+}$ $CD24^{-/low}$ cells (An *et al.*, 2015). Interestingly, the HER2-negative cell line MAMBO38 showed the same behavior, and the population of $CD44^{+}$ $CD24^{-/low}$ cells was as present as in MDA-MB-231 cell line. In fact, this population is higher than 96% in both cell lines. In Mi6 cells the $CD44^{+}$ $CD24^{-/low}$ cells were absent, whereas in MAMBO89 cell line they reach the 18% of the total population. This matches with the limited but present capability of MAMBO89 cells to form vessel-like channels *in vitro*.

However, different stem-like populations have been identified in human breast cancer and in mouse models of mammary carcinogenesis. For instance, Castagnoli and colleagues found that a stem cell population, defined as $CD29^{high}/CD24^{+}/Sca\text{-}1^{low}$, is

present in Mi6 cell line. This population conferred greater tumor engraftment in serial dilutions compared to MAMBO89 (Castagnoli *et al.*, 2017). Mi6 has stem-like features but they are not directly linked to BCSCs, defined as $CD44^{+}$ $CD24^{-/low}$ Lin^{-}. It is possible that the stem population found by Castagnoli and his group is mainly linked to tumorigenesis, whereas $CD44^{+}$ $CD24^{-/low}$ Lin^{-} cells can also have an implication in angiogenesis and VM.

VM has also been linked to the expression of COX-2 (Kirschmann *et al.*, 2012). As demonstrated, the expression of Δ16 confers a lower expression of its transcript and this might explain the absent capability to form vascular networks *in vitro*. COX-2 has also been linked to $CD44^{+}$ $CD24^{-/low}$ Lin^{-} cells: the production of prostaglandins sustains the proliferation of this population (Pang *et al.*, 2016). This also supports the hypothesis that HER2-driven angiogenesis is less regular in comparison with Δ16-driven one, and that VM might be present in HER2-expressing tumors.

The capability of forming vessel-like structures was affected after treatment with sunitinib in MAMBO89 cell line. Sunitinib has been found to reduce CSCs in many tumor types, such as renal, breast (Brossa *et al.*, 2015; Czarnecka *et al.*, 2016) and prostate cancer (Diaz *et al.*, 2015). It is possible that the reduced ability of forming tubes showed by MAMBO89 on Matrigel is due to this specific action of sunitinib.

Therefore, the irregular angiogenesis of HER2-expressing tumors might involve VM and other structures such as vascular *lacunae*, which are sustained by a higher presence of a $CD44^{+}$ $CD24^{-/low}$ population and a greater expression of COX-2.

The sensitivity to sunitinib and pazopanib was studied in triple-negative breast cancer. Two cell lines were used: the human MDA-MB-231 and the murine MAMBO38. In both cell lines the $CD44^{+}$ $CD24^{-}$ population is present at a very high percentage.

First of all, MDA-MB-231 cells were injected in NOD-SCID mice to test the effectiveness of sunitinib. Tumor volume was significantly reduced at the end of the experiment, thus indicating a sensitivity to this drug that has been confirmed *in vitro*. Since MDA-MB-231 are known to form VM channels both *in vitro* and *in vivo* (Plantamura *et al.*, 2014), sunitinib might have had a dual effect: on one hand, it could

have affected the formation of vessels and of VM vessel-like tubes; on the other hand, it could have had a direct impact on cell proliferation.

The sensitivity to sunitinib and pazopanib was also tested *in vitro* on MAMBO38 cells. In adherent conditions, both drugs were effective after 72 hours of treatment, but a small effect in sunitinib-treated cells was evident just after 24 hours. Later, the sensitivity to sunitinib and pazopanib was tested in 3D-culture, to better analyze the effect of the drugs in a condition that better resembles the *in vivo* situation. The effect of the drugs was dramatic, since no colonies had grown after 14 days of treatment, compared to the control wells in which 30-40 colonies were present. This proves that sunitinib has an anti-proliferative effect on triple-negative breast cancer.

The sensitivity to sunitinib and to pazopanib in relation to HER2 and Δ16 has been evaluated both *in vitro* and *in vivo*. *In vivo*, Δ16-HER2 tumors were sensitive to both drugs. Differently from FVBhuHER2 tumors, vascularization was affected, in terms of reduction of vessel density. This effect of sunitinib and pazopanib has been reported in renal cell carcinoma (Vasudev *et al.*, 2013) and in breast cancer (Young *et al.*, 2010). The drugs had not only an anti-tumoral effect, therefore causing the decrease of tumor growth, but also showed an anti-angiogenic action through the significant reduction of vessel density.

There can be several possible explanations to this different sensitivity between the two types of tumors. For example, Δ16-HER2 tumors express more VEGFR2 than FVBhuHER2, that is one of the targets of the drugs. The more the target is present, the more the effect is evident. Moreover, the higher perfusion of Δ16-HER2 drugs may distribute the drugs in a more efficient way, leading to an increased effect.

Interestingly, the anti-tumoral effect of sunitinib was higher than the effect of pazopanib in Δ16-HER2 tumors. This can be explained taking into account that sunitinib can block a higher number of targets than pazopanib. In fact, sunitinib inhibits VEGFRs, PDGFRs, c-Kit, RET, CSF1R and Flt-3, whereas pazopanib inhibits only VEGFR2, PDGFRs and c-Kit.

For instance, RET is a tyrosine kinase receptor that is involved in many cancer types. Gain-of-function somatic mutations have been identified in papillary thyroid

carcinoma, lung adenocarcinoma and chronic myelomonocytic leukemia. Wild-type RET has a role also in other tumor types, such as mammary carcinoma, pancreatic cancer, acute myeloid leukemia and colon carcinoma, increasing aggressiveness, invasivity, tumor cell proliferation and drug resistance (Mulligan, 2014). The expression of RET has not been evaluated in this thesis, but it is possible that its presence has a role in increasing the sensitivity of Δ16-HER2 tumors to sunitinib.

In Δ16-HER2 tumors, no effect in tumor necrosis has been found. On the contrary, sunitinib increased tumor necrosis in FVBhuHER2 tumors. In fact, the percentage of necrotic cells in pazopanib-treated tumors was the same as in the tumors of the control group, and no effect on tumor growth was observed after the treatment with this drug. This could explain the sensitivity to this drug, especially in the light of the fact that sunitinib is known to induce tumor necrosis (Verhoest *et al.*, 2014).

The treatment with the two anti-angiogenic drugs have led to modifications of the level of expression of angiogenic-related proteins. The most relevant alteration that has been found is the significant decrease in VEGF-A expression in treated Δ16-HER2 MDI tumors compared to control ones. This might be due to the block of angiogenesis and the reduction of tumor dimensions.

Since a lesser effect was observed in FVBhuHER2 MDI tumors in terms of sensitivity to sunitinib, a combined therapy approach involving sunitinib and trastuzumab was tested to try to obtain a better outcome on these tumors.

The tumor necrosis observed upon treatment with sunitinib likely recruited immune cells, which may mediate the immunological mechanisms of effectiveness of trastuzumab, such as ADCC. A higher presence of immune cells might induce a higher trastuzumab-mediated anti-tumoral response. Since there is no normalization of the vasculature according to the Jain's concept, it was logical to hypothesize that the only opportunity to get a better effect in placing sunitinib before trastuzumab would have been due to the recruitment of immune cells after tumor necrosis induction. For this reason, trastuzumab was administered after sunitinib and not at the same time. This approach was compared with the control group, the groups treated in monotherapy

with sunitinib or trastuzumab and the group that received trastuzumab followed by sunitinib.

In the monotherapy setting, both drugs were effective in reducing tumor growth but the effect of sunitinib was greater. Trastuzumab, in fact, was less effective on HER2-expressing cell line MAMBO89 compared to the Δ16-expressing cell line Mi6, both *in vitro* and *in vivo* (Castagnoli *et al.*, 2014; Palladini *et al.*, 2017), thus indicating an intrinsic less sensitivity of the full-length isoform.

In the combined therapy setting, no difference was found regardless the order of drug administration. Therefore, unlike the initial hypothesis, there is no advantage in administering sunitinib and then trastuzumab, or the other way around.

To better analyze the sensitivity to sunitinib and pazopanib, the effect of the two drugs has been evaluated on cell proliferation *in vitro*, according to the expression of full-length HER2 and Δ16. MAMBO89 cell line showed no sensitivity to sunitinib and some sensitivity to pazopanib *in vitro*. The opposite observation between the treatments *in vitro* and *in vivo* can be explained with the effect on tumors: sunitinib caused an increase of tumor necrosis, that limited tumor growth and likely recruited immune cells that contributed to the decline of tumor cell proliferation. Pazopanib was slightly able to slow down cell proliferation *in vitro*, but no effect was detected *in vivo*, probably because of the lack of induction of tumor necrosis. Moreover, the approach *in vitro* in adherent conditions is less close to the *in vivo* situation: this can also explain the discrepancy between the different studies.

Regarding Δ16, Mi6 cell line showed sensitivity to both sunitinib and pazopanib *in vitro*. The sensitivity to sunitinib was evident after only 24 hours, whereas the effect of pazopanib was observable later. These data confirmed the results of the treatment *in vivo*, showing sensitivity to both drugs. This probably means that the anti-tumoral effect of sunitinib and pazopanib is due to the inhibition of cell proliferation.

In conclusion, for the first time the angiogenesis sustained by full-length HER2 and its splice variant Δ16 has been extensively explored, revealing differences from the phenotypic, functional, molecular and therapeutic point of view. In particular, the vascularization with few large vessels typical of HER2-expressing tumors is less

permeable to drugs and less sensitive to anti-angiogenic drugs such as sunitinib and pazopanib than Δ16-HER2 tumors, where a vascular pattern with numerous small vessels and a higher expression of VEGF-A and VEGFR2 are present. HER2 seemed to have a dominant role in determining these molecular and phenotypic aspect of vascularization in tumors. A less regular angiogenesis, likely with VM channels, may explain these characteristics in FVBhuHER2 tumors, which is affected by sunitinib *in vitro* through the decrease of VM activity. $CD44^{+}$ $CD24^{-/low}$ cells might have a role in HER2-driven angiogenesis, likely inducing abnormal structures. Sunitinib was also effective on triple-negative breast cancer, both *in vitro* and *in vivo*.

These findings suggest the importance of better study angiogenesis in cancer, in order to find new potential targets and improve pharmacological response. Moreover, additional analyses can be done to further study the impact of the two isoforms on vascularization and the differently expressed genes such as Angiopoietin-1, in order to better understand the relation between cancer, angiogenesis and drug response.

The implication of HER2- or Δ16-driven angiogenesis can be studied in other therapeutic contexts, such as innovative immunological approaches. For instance, the relationship between vascularization and leukocytes distribution could be investigated in relation to the response of a novel anti-HER2 vaccine based on virus-like particles (VLP), which very recently showed a great effectiveness in FVBhuHER2 and Δ16-HER2 models both in prophylactic and therapeutic settings (Palladini *et al.*, 2017).

References

Abrams TJ, Murray LJ, Pesenti E, Holway VW, Colombo T, Lee LB, Cherrington JM, Pryer NK (2003*) Preclinical evaluation of the tyrosine kinase inhibitor SU11248 as a single agent and in combination with "standard of care" therapeutic agents for the treatment of breast cancer.* Mol Cancer Ther; 2:1011-1021.

Adair TH, Montani JP (2010) *Angiogenesis* (Chapter 1, "Overview of Angiogenesis"). San Rafael (CA): Morgan & Claypool Life Sciences. Available from: https://www.ncbi.nlm.nih.gov/books/NBK53238/?report=classic

Alajati A, Sausgruber N, Aceto N, Duss S, Sarret S, Voshol H, Bonenfant D, Bentires-Alj M (2013) *Mammary tumor formation and metastasis evoked by a HER2 splice variant.* Cancer Res; 73:5320-5327.

Alameddine RS, Otrock ZK, Awada A, Shamseddine A (2013) *Crosstalk between HER2 signaling and angiogenesis in breast cancer: molecular basis, clinical applications and challenges.* Curr Opin Oncol; 25:313-24.

Al-Hajj M, Wicha MS, Benito-Hernandez A, Morrison SJ, Clarke MF (2003) *Prospective identification of tumorigenic breast cancer cells.* Proc Natl Acad Sci U S A; 100:3983-3988.

Amiri-Kordestani L, Tan AR, Swain SM (2012) *Pazopanib for the treatment of breast cancer.* Expert Opin Investig Drugs; 21:217-225.

An H, Kim JY, Oh E, Lee N, Cho Y, Seo JH (2015) *Salinomycin promotes anoikis and decreases the CD44+/CD24- stem-like population via inhibition of STAT3 activation in MDA-MB-231 cells.* PLoS One; 10:e0141919.

Andrechek ER, White D, Muller WJ (2005) *Targeted disruption of ErbB2/Neu in the mammary epithelium results in impaired ductal outgrowth.* Oncogene; 24:932-937.

Aranda V, Haire T, Nolan ME, Calarco JP, Rosenberg AZ, Fawcett JP, Pawson T, Muthuswamy SK (2006) *Par6-aPKC uncouples ErbB2 induced disruption of polarized epithelial organization from proliferation control.* Nat Cell Biol; 8:1235-1245.

Arigoni M, Barutello G, Riccardo F, Ercole E, Cantarella D, Orso F, Conti L, Lanzardo S, Taverna D, Merighi I, Calogero RA, Cavallo F, Quaglino E (2013) *miR-135b coordinates progression of ErbB2-driven mammary carcinomas through suppression of MID1 and MTCH2.* Am J Pathol; 182:2058-2070.

Arribas J, Baselga J, Pedersen K, Parra-Palau JL (2011) *p95HER2 and breast cancer*. Cancer Res; 71:1515-1519.

Arteaga CL, Sliwkowski MX, Osborne CK, Perez EA, Puglisi F, Gianni L (2011) *Treatment of HER2-positive breast cancer: current status and future perspectives.* Nat Rev Clin Oncol; 9:16-32.

Associazione Italiana di Oncologia Medica (2017) *I numeri del cancro in Italia 2017.* Il Pensiero Scientifico Editore. Available from: http://www.aiom.it/fondazione-aiom/+aiom-airtum-numeri-cancro-2017/1,3021,0,

Bachelot T, Garcia-Saenz JA, Verma S, Gutierrez M, Pivot X, Kozloff MF, Prady C, Huang X, Khosravan R, Wang Z, Cesari R, Tassell V, Kern KA, Blay JY, Lluch A (2014) *Sunitinib in combination with trastuzumab for the treatment of advanced breast cancer: activity and safety results from a phase II study.* BMC Cancer; 14:166-175.

Balboni T's MSc thesis (2014) *HER2 e isoforma Δ16-HER2: ruolo nella cancerogenesi mammaria e nella risposta alle terapie anti-HER2.* Supervisor: Prof. Lollini PL; co-supervisor: Dr. Palladini A.

Baker AH, Edwards DR, Murphy G (2002) *Metalloproteinase inhibitors: biological actions and therapeutic opportunities.* J Cell Sci; 115:3719-3727.

Baselga J, Albanell J, Molina MA, Arribas J (2001) *Mechanism of action of trastuzumab and scientific update.* Semin Oncol; 28:4-11.

Berger MB, Mendrola JM, Lemmon MA (2004) *ErbB3/HER3 does not homodimerize upon neuregulin binding at the cell surface.* FEBS Lett; 569:332-336.

Bergers G, Benjamin LE (2003) *Tumorigenesis and the angiogenic switch.* Nature Rev Cancer; 3:401-410.

Bianchini G, Gianni L (2014) *The immune system and response to HER2-targeted treatment in breast cancer.* Lancet Oncol; 15:e58-68.

Bieche I, Vacher S, Vallerand D, Richon S, Hatem R, De Plater L, Dahmani A, Némati F, Angevin E, Marangoni E, Roman-Roman S, Decaudin D, Dangles-Marie V (2014) *Vasculature analysis of patient derived tumor xenografts using species-specific PCR assays: evidence of tumor endothelial cells and atypical VEGFA-VEGFR1/2 signalings.* BMC Cancer; 14:178-189.

Boggio K, Nicoletti G, Di Carlo E, Cavallo F, Landuzzi L, Melani C, Giovarelli M, Rossi I, Nanni P, De Giovanni C, Bouchard P, Wolf S, Modesti A, Musiani P, Lollini PL, Colombo MP, Forni G (1998) *Interleukin 12-mediated prevention of spontaneous mammary adenocarcinomas in two lines of Her-2/neu transgenic mice.* J Exp Med; 188:589-596.

Boku N (2014) *HER2-positive gastric cancer.* Gastric Cancer; 17:1-12.

Bossung V, Harbeck N (2010) *Angiogenesis inhibitors in the management of breast cancer.* Curr Opin Obstet Gynecol; 22:79-86.

Bouck N, Stellmach V, Hsu SC (1996) *How tumors become angiogenic.* Adv Cancer Res; 69:135-174.

Brossa A, Grange C, Mancuso L, Annaratone L, Satolli MA, Mazzone M, Camussi G, Bussolati B (2015) *Sunitinib but not VEGF blockade inhibits cancer stem cell endothelial differentiation.* Oncotarget; 6:11295-11309.

Burgess AW, Cho HS, Eigenbrot C, Ferguson KM, Garrett TP, Leahy DJ, Lemmon MA, Sliwkowski MX, Ward CW, Yokoyama S (2003) *An open-and-shut case? Recent insights into the activation of EGF/ErbB receptors.* Mol Cell; 12:544-552.

Cardoso F, Canon JL, Amadori D, Aldrighetti D, Machiels JP, Bouko Y, Verkh L, Usari T, Kern KA, Giorgetti C, Dirix L (2012) *An exploratory study of sunitinib in combination with docetaxel and trastuzumab as first-line therapy for HER2-positive metastatic breast cancer.* Breast; 21:716-723.

Carmeliet P (2003) *Angiogenesis in health and disease.* Nat Med; 9:653-660.

Carmeliet P, De Smet F, Loges S, Mazzone M (2009) *Branching morphogenesis and antiangiogenesis candidates: tip cells lead the way*. Nat Rev Clin Oncol; 6:315-326.

Carmeliet P, Jain RK (2000) *Angiogenesis in cancer and other diseases.* Nature; 407:249-257.

Carmeliet P, Jain RK (2011) *Molecular mechanisms and clinical applications of angiogenesis.* Nature; 473:298-307.

Carmeliet P, Jain RK (2011) *Principles and mechanisms of vessel normalization for cancer and other angiogenic diseases.* Nat Rev Drug Discov; 10:417-427.

Castagnoli L, Iezzi M, Ghedini GC, Ciravolo V, Marzano G, Lamolinara A, Zappasodi R, Gasparini P, Campiglio M, Amici A, Chiodoni C, Palladini A, Lollini PL, Triulzi T, Menard S, Nanni P, Tagliabue E, Pupa SM (2014) *Activated d16HER2 homodimers and SRC kinase mediate optimal efficacy for trastuzumab.* Cancer Res; 74:6248-6259.

Castagnoli L, Ghedini GC, Koschorke A, Triulzi T, Dugo M, Gasparini P, Casalini P, Palladini A, Iezzi M, Lamolinara A, Lollini PL, Nanni P, Chiodoni C, Tagliabue E, Pupa SM (2017) *Pathobiological implications of the d16HER2 splice variant for stemness and aggressiveness of HER2-positive breast cancer.* Oncogene; 36:1721-1732.

Castiglioni F, Tagliabue E, Campiglio M, Pupa SM, Balsari A, Ménard S (2006) *Role of exon-16-deleted HER2 in breast carcinomas.* Endocr Relat Cancer; 13:221-232.

Chauhan VP, Stylianopoulos T, Martin JD, Popović Z, Chen O, Kamoun WS, Bawendi MG, Fukumura D, Jain RK (2012) *Normalization of tumour blood vessels improves the delivery of nanomedicines in a size-dependent manner.* Nat Nanotechnol; 7:383-388.

Cheng N, Brantley D, Fang WB, Liu H, Fanslow W, Cerretti DP, Bussell KN, Reith A, Jackson D, Chen J (2003) *Inhibition of VEGF-dependent multistage carcinogenesis by soluble EphA receptors.* Neoplasia; 5:445-456.

Cho HS, Mason K, Ramyar KX, Stanley AM, Gabelli SB, Denney DW Jr, Leahy DJ (2003) *Structure of the extracellular region of HER2 alone and in complex with the Herceptin Fab*. Nature; 421:756-760.

Citri A, Skaria KB, Yarden Y (2003) *The deaf and the dumb: the biology of ErbB-2 and ErbB-3.* Exp Cell Res; 284:54-65.

Coussens L, Yang-Feng TL, Liao YC, Chen E, Gray A, McGrath J, Seeburg PH, Libermann TA, Schlessinger J, Francke U, Levinson A, Ullrich A (1985) *Tyrosine kinase receptor with extensive homology to EGF receptor shares chromosomal location with neu oncogene.* Science; 230:1132-1139.

Czarnecka AM, Solarek W, Kornakiewicz A, Szczylik C (2016) *Tyrosine kinase inhibitors target cancer stem cells in renal cell cancer.* Oncol Rep; 35:1433-1442.

Dako Hercep Test: A Manual for Interpretation. Carpinteria, CA, USA. Dako Corp, 1999.

Dawson SJ, Rueda OM, Aparicio S, Caldas C (2013) *A new genome-driven integrated classification of breast cancer and its implications.* EMBO J; 32:617-628.

De Giovanni C, Nicoletti G, Quaglino E, Landuzzi L, Palladini A, Ianzano ML, Dall'Ora M, Grosso V, Ranieri D, Laranga R, Croci S, Amici A, Penichet ML, Iezzi M, Cavallo F, Nanni P, Lollini PL (2014) *Vaccines against human HER2 prevent mammary carcinoma in mice transgenic for human HER-2.* Breast Cancer Res; 16:R10.

Diaz R, Nguewa PA, Redrado M, Manrique I, Calvo A (2015) *Sunitinib reduces tumor hypoxia and angiogenesis, and radiosensitizes prostate cancer stem-like cells.* Prostate; 75:1137-1149.

Diver EJ, Foster R, Rueda BR, Growdon WB (2015) *The therapeutic challenge of targeting HER2 in endometrial cancer.* Oncologist; 20:1058-1068.

Drecoll E, Nitsche U, Bauer K, Berezowska S, Slotta-Huspenina J, Rosenberg R, Langer R (2014) *Expression analysis of heat shock protein 90 (HSP90) and Her2 in colon carcinoma.* Int J Colorectal Dis; 29:663-671.

Ellis P (2003) *WHO Classification of tumours. Pathology and genetics of tumours of the breast and female genital organs.* Lyon Press: Lyon; 13-59.

Ettl T, Stiegler C, Zeitler K, Agaimy A, Zenk J, Reichert TE, Gosau M, Kühnel T, Brockhoff G, Schwarz S (2012) *EGFR, HER2, survivin, and loss of pSTAT3 characterize high-grade malignancy in salivary gland cancer with impact on prognosis.* Hum Pathol; 43:921-931.

Farnie G, Clarke RB, Spence K, Pinnock N, Brennan K, Anderson NG, Bundred NJ (2007) *Novel cell culture technique for primary ductal carcinoma in situ: role of Notch and epidermal growth factor receptor signaling pathways.* J Natl Cancer Inst; 99:616-627.

Finkle D, Quan ZR, Asghari V, Kloss J, Ghaboosi N, Mai E, Wong WL, Hollingshead P, Schwall R, Koeppen H, Erickson S (2004) *HER2-targeted therapy reduces incidence and progression of midlife mammary tumors in female murine mammary tumor virus huHER2-transgenic mice*. Clin Cancer Res; 10:2499-2511.

Folberg R, Hendrix MJC, Maniotis AJ (2000) *Vascular mimicry and tumor angiogenesis.* Am J Pathol; 156:361-381.

Folkman J (1971) *Tumor angiogenesis: therapeutic implications.* N Eng J Med; 285:1182-1186.

Franco CA, Jones ML, Bernabeu MO, Geudens I, Mathivet T, Rosa A, Lopes FM, Lima AP, Ragab A, Collins RT, Phng L-K, Coveney PV, Gerhardt H (2015) *Dynamic endothelial cell rearrangements drive developmental vessel regression.* PLOS Biology; 13:e1002125.

Franco CA, Jones ML, Bernabeu MO, Vion AC, Barbacena P, Fan J, Mathivet T, Fonseca CG, Ragab A, Yamaguchi TP, Coveney PV, Lang RA, Gerhardt H (2016) *Non-canonical Wnt signalling modulates the endothelial shear stress flow sensor in vascular remodelling.* eLife; 5:e07727.

Gately S (2000) *The contributions of cyclooxygenase-2 to tumor angiogenesis.* Cancer Metastasis Rev; 19:19-27.

Gelao L, Criscitiello C, Fumagalli L, Locatelli M, Manunta S, Esposito A, Minchella I, Goldhirsch A, Curigliano G (2013) *Tumour dormancy and clinical implications in breast cancer.* Ecancermedicalscience; 7:320-334.

Ghedini GC, Ciravolo V, Castagnoli L, Tagliabue E, Pupa SM (2014) *Delta16HER2 splice variant, its role in HER2-overexpressing breast cancer.* Atlas Genet Cytogenet Oncol Haematol; 18:526-531.

Goel S, Duda DG, Xu L, Munn LL, Boucher Y, Fukumura D, Jain RK (2011) *Normalization of the vasculature for treatment of cancer and other diseases.* Physiol Rev; 91:1071-1121.

Goldmann E (1907) *The growth of malignant disease in man and the lower animals with special reference to the vascular system.* Lancet; 2:1236-1240.

Gu G, Dustin D, Fuqua SA (2016) *Targeted therapy for breast cancer and molecular mechanisms of resistance to treatment.* Curr Opin Pharmacol; 31:97-103.

Guy CT, Webster MA, Schaller M, Parsons TJ, Cardiff RD, Muller WJ (1992) *Expression of the neu protooncogene in the mammary epithelium of transgenic mice induces metastatic disease.* Proc Natl Acad Sci; 89:10578-10582.

Hanahan D, Weinberg RA (2011) *Hallmarks of cancer: the next generation.* Cell; 144:646-674.

Hodeib M, Serna-Gallegos T, Tewari KS (2015) *A review of HER2-targeted therapy in breast and ovarian cancer: lessons from antiquity – CLEOPATRA and PENELOPE.* Future Oncol; 11:3113-3131.

Ithimakin S, Day KC, Malik F, Zen Q, Dawsey SJ, Bersano-Begey TF, Quraishi AA, Ignatoski KW, Daignault S, Davis A, Hall CL, Palanisamy N, Heath AN, Tawakkol N, Luther TK, Clouthier SG, Chadwick WA, Day ML, Kleer CG, Thomas DG, Hayes DF, Korkaya H, Wicha MS (2013) *HER2 drives luminal breast cancer stem cells in the absence of HER2 amplification: implications for efficacy of adjuvant trastuzumab.* Cancer Res; 73:1635-1646.

Izumi Y, Xu L, di Tomaso E, Fukumura D, Jain RK (2002) *Herceptin acts as an anti-angiogenic cocktail.* Nature; 280:279-280.

Jain RK, Koenig GC, Dellian M, Fukumura D, Munn LL, Melder RJ (1996) *Leukocyte-endothelial adhesion and angiogenesis in tumors.* Cancer Metastasis Rev; 15:195-204.

Kerbel RS (2011) *Reappraising antiangiogenic therapy for breast cancer***.** Breast; 20:S56-60.

Kirschmann DA, Seftor EA, Hardy KM, Seftor RE, Hendrix MJ (2012) *Molecular pathways: vasculogenic mimicry in tumor cells: diagnostic and therapeutic implications.* Clin Cancer Res; 18:2726-2732.

Klos KS, Wyszomierski SL, Sun M, Tan M, Zhou X, Li P, Yang W, Yin G, Hittelman WN, Yu D (2006) *ErbB2 increases Vascular Endothelial Growth Factor protein synthesis via activation of Mammalian Target of Rapamycin/p70S6K leading to increased angiogenesis and spontaneous metastasis of human breast cancer cells*. Cancer Res; 66:2028-2037.

Kohrt HE, Houot R, Marabelle A, Cho HJ, Osman K, Goldstein M, Levy R, Brody J (2012) *Combination strategies to enhance antitumor ADCC.* Immunotherapy; 4:511-527.

Konecny GE, Meng YG, Untch M, Wang HJ, Bauerfeind I, Epstein M, Stieber P, Vernes JM, Gutierrez J, Hong K, Beryt M, Hepp H, Slamon DJ, Pegram MD (2004) *Association between HER-2/neu and vascular endothelial growth factor expression predicts clinical outcome in primary breast cancer patients.* Clin Cancer Res; 10:1706-1716.

Korkaya H, Paulson A, Charafe-Jauffret E, Ginestier C, Brown M, Dutcher J, Clouthier SG, Wicha MS (2009) *Regulation of mammary stem/progenitor cells by PTEN/Akt/beta-catenin signaling.* PLoS Biol; 7:e1000121.

Korkaya H, Wicha MS (2013) *HER2 and Breast Cancer Stem Cells: more than meets the eye*. Cancer Res; 73:3489-3493.

Koutras AK, Starakis I, Lymperatou D, Kalofonos HP (2012) *Angiogenesis as a therapeutic target in breast cancer.* Mini Rev Med Chem; 12:1230-1238.

Kwong KY, Hung MC (1998) *A novel splice variant of HER2 with increased transformation activity.* Mol Carcinog; 23:62-68.

Langenkamp E, Molema G (2009) *Microvascular endothelial cell heterogeneity: general concepts and pharmacological consequences for anti-angiogenic therapy of cancer.* Cell Tissue Res; 335:205-222.

Lee KF, Simon H, Chen H, Bates B, Hung MC, Hauser C (1995) *Requirement for neuregulin receptor erbB2 in neural and cardiac development.* Nature; 378:394-398.

Li X, Lewis MT, Huang J, Gutierrez C, Osborne CK, Wu MF, Hilsenbeck SG, Pavlick A, Zhang X, Chamness GC, Wong H, Rosen J, Chang JC (2008) *Intrinsic resistance of tumorigenic breast cancer cells to chemotherapy.* J Natl Cancer Inst; 100:672-679.

Liu Q, Qiao L, Liang N, Xie J, Zhang J, Deng G, Luo H, Zhang J (2016) *The relationship between vasculogenic mimicry and epithelial-mesenchymal transitions.* J Cell Mol Med; 20:1761-1769.

Liu T, Sun B, Zhao X, Gu Q, Dong X, Yao Z, Zhao N, Chi J, Liu N, Sun R, Ma Y (2013). *HER2/neu expression correlates with vasculogenic mimicry in invasive breast carcinoma.* J Cell Mol Med; 17:116-122.

Lucchini F, Sacco MG, Hu N, Villa A, Brown J, Cesano L, Mangiarini L, Rindi G, Kindl S, Sessa F, Vezzoni P, Clerici L (1992) *Early and multifocal tumors in breast, salivary, harderian and epididymal tissues developed in MMTY-Neu transgenic mice*. Cancer Lett; 64:203-209.

Mackey JR, Kerbel RS, Gelmon KA, McLeod DM, Chia SK, Rayson D, Verma S, Collins LL, Paterson AH, Robidoux A, Pritchard KI (2012) *Controlling angiogenesis in breast cancer: a systematic review of anti-angiogenic trials.* Cancer Treat Rev; 38:673-688.

Maniotis AJ, Folberg R, Hess A, Seftor EA, Gardner LM, Pe'er J, Trent JM, Meltzer PS, Hendrix MJ (1999) *Vascular channel formation by human melanoma cells in vivo and in vitro: vasculogenic mimicry.* Am J Pathol; 155:739-752.

Mar N, Vrendenburgh JJ, Wasser JS (2015) *Targeting HER2 in the treatment of non-small cell lung cancer.* Lung Cancer; 87:220-225.

Marchini C, Gabrielli F, Iezzi M, Zenobi S, Montani M, Pietrella L, Kalogris C, Rossini A, Ciravolo V, Castagnoli L, Tagliabue E, Pupa SM, Musiani P, Monaci P, Menard S, Amici A (2011) *The human splice variant Delta16HER2 induces rapid tumor onset in a reporter transgenic mouse*. PLoS One; 6:e18727.

Mittendorf EA, Wu Y, Scaltriti M, Meric-Bernstam F, Hunt KK, Dawood S, Esteva FJ, Buzdar AU, Chen H, Eksambi S, Hortobagyi GN, Baselga J, Gonzalez-Angulo AM (2009) *Loss of HER2 amplification following trastuzumab-based neoadjuvant systemic therapy and survival outcome.* Clin Cancer Res; 15:7381-7388.

Mitra D, Brumilk MJ, Okamgba SU, Zhu Y, Duplessis TT, Parvani JG, Lesko SM, Brogi E, Jones FE (2009) *An oncogenic isoform of HER2 associated with locally disseminated breast cancer and trastuzumab resistance.* Mol Cancer Ther; 8:2152-2162.

Mentzer SJ, Konerding MA (2014) *Intussusceptive angiogenesis: expansion and remodeling of microvascular networks.* Angiogenesis; 17:499-509.

Moasser MM (2007) *The oncogene HER2: its signaling and transforming functions and its role in human cancer pathogenesis.* Oncogene; 26:6469-6487.

Muller WJ, Sinn E, Pattengale PK, Wallace R, Leder P (1988) *Single-step induction of mammary adenocarcinoma in transgenic mice bearing the activated c-neu oncogene.* Cell; 54:105-115.

Mulligan LM (2014) *RET revisited: expanding the oncogenic portfolio.* Nat Rev Cancer; 14:173-186.

Nagy JA, Chang SH, Shih SC, Dvorak AM, Dvorak HF (2010) *Heterogeneity of the tumor vasculature.* Semin Thromb Hemost; 36:321-331.

Nagy JA, Dvorak HF (2012) *Heterogeneity of the tumor vasculature: the need for new tumor blood vessel type-specific targets.* Clin Exp Metastasis; 29:657-662.

Nielsen DL, Andersson M, Andersen JL, Kamby C (2010) *Antiangiogenic therapy for breast cancer.* Breast Cancer Research; 12:209-224.

Palladini A, Nicoletti G, Lamolinara A, Dall'Ora M, Balboni T, Ianzano ML, Laranga R, Landuzzi L, Giusti V, Ceccarelli C, Santini D, Taffurelli M, Di Oto E, Asioli S, Amici A, Pupa SM, De Giovanni C, Tagliabue E, Iezzi M, Nanni P, Lollini PL (2017) *HER2 isoforms co-expression differently tunes mammary tumor phenotypes affecting onset, vasculature and therapeutic response.* Oncotarget; 8:54444-54458.

Palladini A, Thrane S, Janitzek CM, Pihl J, Clemmensen SB, De Jongh WA, Clausen TM, Nicoletti G, Landuzzi L, Penichet ML, Balboni T, Ianzano ML, Giusti V, Theander TG, Nielsen MA, Salanti A, Lollini PL, Nanni P, Sander AF. *Virus-like particle display of HER2 induces potent anticancer responses.* OncoImmunology; published online on 29/11/2017.

Pang LY, Hurst EA, Argyle DJ (2016) *Cyclooxygenase-2: a role in cancer stem cell survival and repopulation of cancer cells during therapy.* Stem Cells Int; 2016:2048731.

Parakh S, Gan HK, Parslow AC, Burvenich IJG, Burgess AW, Scott AM (2017) *Evolution of anti-HER2 therapies for cancer treatment.* Cancer Treat Rev; 59:1-21.

Pedersen K, Angelini PD, Laos S, Bach-Faig A, Cunningham MP, Ferrer-Ramon C, Luque-García A, García-Castillo J, Parra-Palau JL, Scaltriti M, Ramón y Cajal S, Baselga J, Arribas J (2009) *A naturally occurring HER2 carboxy-terminal fragment promotes mammary tumor growth and metastasis.* Mol Cell Biol; 29:3319-3331.

Piechocki MP, Ho YS, Pilon S, Wei WZ (2003) *Human ErbB-2 (Her-2) transgenic mice: a model system for testing Her-2 based vaccines.* J Immunol; 171:5787-5794.

Plantamura I, Casalini P, Dugnani E, Sasso M, D'Ippolito E, Tortoreto M, Cacciatore M, Guarnotta C, Ghirelli C, Barajon I, Bianchi F, Triulzi T, Agresti R, Balsari A, Campiglio M, Tripodo C, Iorio MV, Tagliabue E (2014) *PDGFRβ and FGFR2 mediate endothelial cell differentiation capability of triple negative breast carcinoma cells*. Mol Oncol; 8:968-981.

Prat A, Pineda E, Adamo B, Galván P, Fernández A, Gaba L, Díez M, Viladot M, Arance A, Muñoz M (2015) *Clinical implications of the intrinsic molecular subtypes of breast cancer.* Breast; 24 Suppl 2:S26-35.

Puglisi F, Minisini AM, De Angelis C, Arpino G (2012) *Overcoming treatment resistance in HER2-positive breast cancer: potential strategies.* Drugs; 72:1175-1193.

Qiao L, Liang N, Zhang J, Xie J, Liu F, Xu D, Yu X, Tian Y (2015) *Advanced research on vasculogenic mimicry in cancer.* J Cell Mol Med; 19:315-326.

Rexer BN, Arteaga CL (2012) *Intrinsic and acquired resistance to HER2-targeted therapies in HER2 gene-amplified breast cancer: mechanisms and clinical implications.* Crit Rev Oncog; 17:1-16.

Rimawi MF, Schiff R, Osborne CK (2015) *Targeting HER2 for the treatment of breast cancer.* Annu Rev Med; 66:111-128.

Risau W (1997) *Mechanisms of angiogenesis.* Nature; 386:671-674.

Risau W, Flamme I (1995) *Vasculogenesis*. Annual Annu Rev Cell Dev Biol; 11:73-91.

Schechter AL, Stern DF, Vaidyanathan L, Decker SJ, Drebin JA, Greene MI, Weinberg RA (1984) *The neu oncogene: an erb-B-related gene encoding a 185,000-Mr tumour antigen.* Nature; 312:513-516.

Schutz FA, Choueiri TK, Sternberg CN (2011) *Pazopanib: clinical development of a potent anti-angiogenic drug.* Crit Rev Oncol Hematol; 77:163-171.

Seddon AN, Cuellar S, Haaf CM (2014) *The life, death, and attempted rebirth of bevacizumab in breast cancer.* J Oncol Pharm Pract; 20:433-444.

Sekeres MA (2011) *The Avastin story.* N Engl J Med; 365:1454-1455.

Senchukova MA, Nikitenko NV, Tomchuk ON, Zaitsev NV, Stadnikov AA (2015) *Different types of tumor vessels in breast cancer: morphology and clinical value.* Springerplus; 4:512-522.

Siegel PM, Ryan ED, Cardiff RD, Muller WJ (1999) *Elevated expression of activated forms of Neu/ErbB-2 and ErbB-3 are involved in the induction of mammary tumors in transgenic mice: implications for human breast cancer.* EMBO J; 18:2149-2164.

Slamon DJ, Godolphin W, Jones LA, Holt JA, Wong SG, Keith DE, Levin WJ, Stuart SG, Udove J, Ullrich A, Press MF (1989) *Studies of the HER-2/neu protooncogene in human breast and ovarian cancer.* Science; 244:707-712.

Spector NL, Blackwell KL (2009) *Understanding the mechanisms behind trastuzumab therapy for human epidermal growth factor receptor 2-positive breast cancer.* J Clin Oncol; 27:5838-5847.

Suda Y, Aizawa S, Furura Y, Yagi T, Ikawa Y, Saitoh K, Yamada Y, Toyoshima K, Yamamoto T (1990) *Induction of a variety of tumors by c-erbB2 and clonal nature of lymphomas even with the mutated gene (Val^{659}-Glu^{659}).* EMBO J; 9:181-190.

Tagliabue E, Campiglio M, Pupa SM, Balsari A, Ménard S (2011) *The HER2 world: better treatment selection for better outcome*. J Natl Cancer Inst Monogr; 2011:82-85.

Tan AR, Johannes H, Rastogi P, Jacobs SA, Robidoux A, Flynn PJ, Thirlwell MP, Fehrenbacher L, Stella PJ, Goel R, Julian TB, Provencher L, Bury MJ, Bhatt K, Geyer CE Jr, Swain SM, Mamounas EP, Wolmark N (2015) *Weekly paclitaxel and concurrent pazopanib following doxorubicin and cyclophosphamide as neoadjuvant therapy for HER-negative locally advanced breast cancer: NSABP Foundation FB-6, a phase II study.* Breast Cancer Res Treat; 149:163-169.

Tang Y, Wang Y, Kiani MF, Wang B (2016) *Classification, treatment strategy and associated drug resistance in breast cancer.* Clin Breast Cancer; 16:335-343.

Tilio M, Gambini V, Wang J, Garulli C, Kalogris C, Andreani C, Bartolacci C, Elexpuru Zabaleta M, Pietrella L, Hysi A, Iezzi M, Belletti B, Orlando F, Provinciali M, Galeazzi R, Marchini C, Amici A (2016) *Irreversible inhibition of Δ16HER2 is necessary to suppress Δ16HER2-positive breast carcinomas resistant to lapatinib.* Cancer Lett; 381:76-84.

Trédan O, Lacroix-Triki M, Guiu S, Mouret-Reynier MA, Barrière J, Bidard FC, Braccini AL, Mir O, Villanueva C, Barthélémy P (2015) *Angiogenesis and tumor microenvironment: bevacizumab in the breast cancer model.* Target Oncol; 10:189-198.

Turpin J, Ling C, Crosby EJ, Hartman ZC, Simond AM, Chodosh LA, Rennhack JP, Andrechek ER, Ozcelik J, Hallett M, Mills GB, Cardiff RD, Gray JW, Griffith OL, Muller WJ (2016) *The ErbB2ΔEx16 splice variant is a major oncogenic driver in breast cancer that promotes a pro-metastatic tumor microenvironment.* Oncogene; 35:6053-6064.

Valabrega G, Capellero S, Cavalloni G, Zaccarello G, Petrelli A, Migliardi G, Milani A, Peraldo-Neia C, Gammaitoni L, Sapino A, Pecchioni C, Moggio A, Giordano S, Aglietta M, Montemurro F (2011) *HER2-positive breast cancer cells resistant to trastuzumab and lapatinib lose reliance upon HER2 and are sensitive to the multitargeted kinase inhibitor sorafenib.* Breast Cancer Res Treat; 130:29-40.

van Cruijsen H, Giaccone G, Hoekman K (2005) *Epidermal growth factor receptor and angiogenesis: Opportunities for combined anticancer strategies.* Int J Cancer; 117:883-888.

Verhoest G, Dolley-Hitze T, Jouan F, Belaud-Rotureau MA, Oger E, Lavenu A, Bensalah K, Arlot-Bonnemains Y, Collet N, Rioux-Leclercq N, Vigneau C (2014) *Sunitinib combined with angiotensin-2 type-1 receptor antagonists induces more necrosis: a murine xenograft model of renal cell carcinoma.* Biomed Res Int; 2014:901371.

Vasudev NS, Goh V, Juttla JK, Thompson VL, Larkin JM, Gore M, Nathan PD, Reynolds AR (2013) *Changes in tumour vessel density upon treatment with anti-angiogenic agents: relationship with response and resistance to therapy.* Br J Cancer; 109:1230-1242.

Wagner J, Thiele F, Ganten D (1995) *Transgenic animals as models for human disease.* Clin Exp Hypertens; 17:593-605.

Wehland M, Bauer J, Magnusson NE, Infanger M, Grimm D (2013) *Biomarkers for anti-angiogenic therapy in cancer.* Int J Mol Sci; 14:9338-9364.

Welti J, Loges S, Dimmeler S, Carmeliet P (2013) *Recent molecular discoveries in angiogenesis and antiangiogenic therapies in cancer.* J Clin Invest; 123:3190-3200.

Willett CG, Boucher Y, di Tomaso E, Duda DG, Munn LL, Tong RT, Chung DC, Sahani DV, Kalva SP, Kozin SV, Mino M, Cohen KS, Scadden DT, Hartford AC, Fischman AJ, Clark JW, Ryan DP, Zhu AX, Blaszkowsky LS, Chen HX, Shellito PC, Lauwers GY, Jain RK (2004) *Direct evidence that the VEGF-specific antibody bevacizumab has antivascular effects in human rectal cancer.* Nat Med; 10:145-147.

Wolff AC, Hammond MEH, Hicks DG, Dowsett M, McShane LM, Allison KH, Allred DC, Bartlett JMS, Bilous M, Fitzgibbons P, Hanna W, Jenkins RB, Mangu PB, Paik S, Perez EA, Press MF, Spears PA, Vance GH, Viale G, Hayes DF (2013) *Recommendations for Human Epidermal Growth Factor Receptor 2 Testing in Breast Cancer: American Society of Clinical Oncology/College of American Pathologists Clinical Practice Guideline Update*. J Clin Oncol; 31:3997-4013.

Yancopoulos GD, Davis S, Gale NW, Rudge JS, Wiegand SJ, Holash J (2000) *Vascular-specific growth factors and blood vessel formation.* Nature; 407:242-248.

Yersal O, Barutca S (2014) *Biological subtypes of breast cancer: prognostic and therapeutic implications.* World J Clin Oncol; 5:412-424.

Young E, Miele L, Tucker KB, Huang M, Wells J, Gu JW (2010) *SU11248, a selective tyrosine kinases inhibitor suppresses breast tumor angiogenesis and growth via targeting both tumor vasculature and breast cancer cells.* Cancer Biol Ther; 10:703-711.

Zhang L, Ma J, Han Y, Liu J, Zhou W, Hong L, Fan D (2016) *Targeted therapy in esophageal cancer.* Expert Rev Gastroenterol Hepatol; 10:595-604.

Zhang S, Huang WC, Li P, Guo H, Poh SB, Brady SW, Xiong Y, Tseng LM, Li SH, Ding Z, Sahin AA, Esteva FJ, Hortobagyi GN, Yu D (2011) *Combating trastuzumab resistance by targeting SRC, a common node downstream of multiple resistance pathways.* Nature Med; 17:461-467.

Zhao J, Xu W, Zhang Z, Song R, Zeng S, Sun Y, Xu C (2015) *Prognostic role of HER2 expression in bladder cancer: a systematic review and meta-analysis.* Int Urol Nephrol; 47:87-94.